How volcanoes work: A 25 year perspective

Katharine V. Cashman[†] **and R. Stephen J. Sparks**
School of Earth Sciences, University of Bristol, Bristol BS81RJ, UK

INVITED REVIEW

ABSTRACT

Over the past 25 years, our understanding of the physical processes that drive volcanic eruptions has increased enormously thanks to major advances in computational and analytical facilities, instrumentation, and collection of comprehensive observational, geophysical, geochemical, and petrological data sets associated with recent volcanic activity. Much of this work has been motivated by the recognition that human exposure to volcanic hazard is increasing with both expanding populations and increasing reliance on infrastructure (as illustrated by the disruption to air traffic caused by the 2010 eruption of Eyjafjallajökull volcano in Iceland). Reducing vulnerability to volcanic eruptions requires a thorough understanding of the processes that govern eruptive activity. Here, we provide an overview of our current understanding of how volcanoes work. We focus particularly on the physical processes that modulate magma accumulation in the upper crust, transport magma to the surface, and control eruptive activity.

INTRODUCTION

Volcanic eruptions are a spectacular manifestation of a dynamic Earth. They not only link deep Earth (the geosphere) to the hydrosphere, atmosphere, and biosphere but also affect human populations: ~600 million people live close enough to an active volcano to be affected by eruptions, and civilization itself could be threatened by the largest explosive eruptions that have occurred in Earth history. The core questions of volcanology focus on how volcanoes work, that is, how magma forms and moves to the surface, and how the specific properties of the magma, and the lithosphere through which it moves, control eruptive activity. Here, we review progress that has been made on this core topic over the past quarter century. To provide a context, we start by reviewing volcanic landforms and associated styles of eruptive activity. We then describe our current understanding of magma storage regions (magma chambers) and eruption triggers. Finally, we look at eruptions themselves, from the ascent of magma through the crust to the physical controls on eruption styles and generation of eruptive products. We recognize that it is impossible to do justice to all of these topics—or all of the scientists who have contributed to the contemporary understanding of volcanism—in a single article. In this regard, we note that a thorough review of the field was completed in 2000 with the publication of the *Encyclopedia of Volcanoes* (Sigurdsson et al., 2000).

[†]E-mail: cashman@uoregon.edu

VOLCANIC ERUPTIONS—AN OVERVIEW

Volcanoes vary greatly in morphology, evolution, eruptive styles, and behaviors as a consequence of the wide variety of tectonic settings, melt production rates, magma compositions, and eruption conditions that they represent. Here, we introduce common volcanic landforms, together with the eruption styles responsible for their formation. Because magma composition is an important control on eruptive style, we separate discussions of mafic and intermediate/silicic volcanism.

Mafic Volcanoes

Mafic volcanoes vary greatly in scale and construction style. The iconic basaltic landform is a shield volcano, such as those that comprise the Hawaiian Islands, United States (Fig. 1A). Shield volcanoes are constructed primarily by successive lava flows and are commonly characterized by relatively low slopes. Other mafic volcano morphologies include the "inverted soup bowl" shape of Galapagos volcanoes; steep-sided cones, like Pico volcano in the Azores and Kluchevskoi in Kamchatka; fissure volcanoes in tectonic rifts such as Iceland, where they may be associated with a central subsidence caldera; tuja volcanoes erupted under ice or in shallow-marine environments; mid-ocean ridges with morphologies that reflect spreading rate; and fields of monogenetic volcanoes, each related to a single eruptive episode. These landforms reflect a range in eruptive styles, the most common of which are reviewed next (see also Francis et al., 1990).

Hawaiian volcanism is associated with the eponymous Hawaiian eruptive style, which is dominated by fluid lava flows. Lava flows often emerge directly from dike-fed fissure systems; for this reason, shield volcanoes tend to be elongated along the fissure direction. Hawaiian shield volcanoes are built of stacks of these flows; their low slopes reflect both the fluidity of the initial lava and the tendency for lava flows to thicken (because of cooling, crystallization, and associated increases in viscosity) with transport distance from rift zone vents (e.g., Katz and Cashman, 2003). An unprecedented look at the structure of Hawaiian volcanoes has been provided by a 15-yr-long drilling project that recovered core from Hawaii's Mauna Loa volcano to a depth of ~3500 m, which represents an ~700 k.y. history of the Hawaiian plume (Stolper et al., 2009). Not surprisingly, given the proximity of the drilling site to the current shoreline, subaerial lavas represent only a small fraction of the core samples, with most of the volcanic sequence represented by subaqueous hyaloclastites and pillow basalts.

From a hazards perspective, an important discovery about Hawaiian volcanism has been the recognition that Kilauea volcano has experienced periods of highly explosive activity in addition to the effusive eruptions of the past few centuries (Fiske et al., 2009). Episodes of explosive activity are particularly frequent during times immediately following summit caldera formation (Swanson, 2008; Swanson et al., 2012). Summit calderas in mafic shield volcanoes form by rapid drainage of magma from summit storage regions to flank vents (e.g., Gudmundsson, 1987). In Hawaii, this drainage allows access of groundwater to the magmatic system, which may fuel the high explosivity observed in postcaldera periods.

Stromboli volcano, Italy (Fig. 1B), is the type location for the Strombolian eruption style, which is characterized by frequent (often several per hour) small explosions that have been attributed to the rise and bursting of large individual gas bubbles (e.g., Vergniolle and Jaupart, 1986). Stromboli thus represents an "open-system" volcano, that is, a volcano where gases can move freely through the system. In fact, Stromboli typically produces ~10^5 times more gas

GSA Bulletin; May/June 2013; v. 125; no. 5/6; p. 664–690; doi: 10.1130/B30720.1; 18 figures.

For permission to copy, contact editing@geosociety.org
© 2013 Geological Society of America

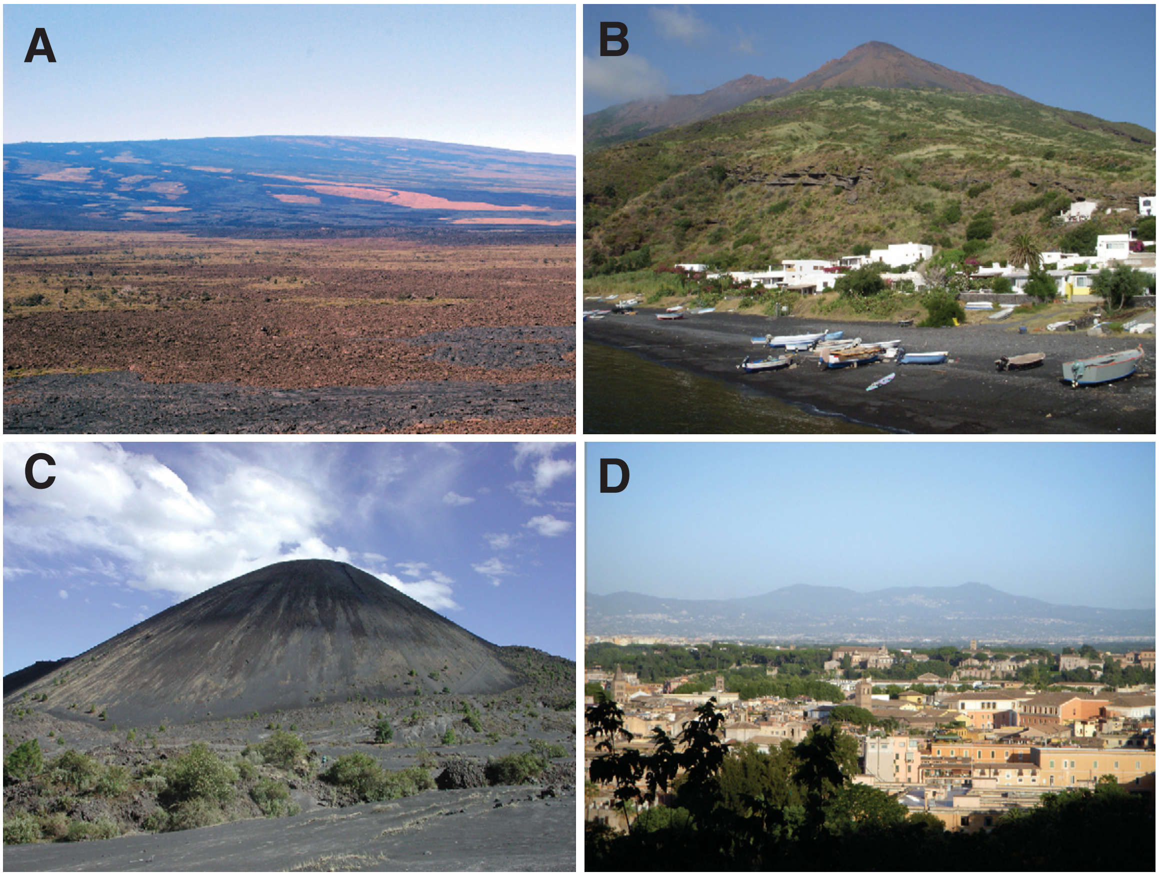

Figure 1. Photographs of mafic volcanic landforms. (A) Mauna Loa shield volcano, United States; (B) Stromboli stratovolcano, Italy; (C) Paricutin cinder cone, Mexico; (D) Colli Albani mafic caldera complex, Italy, viewed from Rome.

than can be accounted for by the magma ejected beyond the vent (e.g., Harris and Ripepe, 2007). However, Stromboli can also produce lava flows and "paroxysmal" eruptions, as demonstrated in 2002–2003 and 2007 (e.g., Ripepe et al., 2005; Calvari et al., 2008; Scandone et al., 2009). This variability in eruption style derives from the complex structure of the magma storage and transport system, and the resulting alternation between near-surface and deep controls on eruptive activity.

Cinder cone fields characterize regions of active extension and transtension (Fig. 1C). Here, ascent and eruption of small mafic magma batches produce a spectrum of eruptive styles from fissure-fed Hawaiian lava flows to Strombolian bubble bursts to explosive gas-charged violent Strombolian eruptions to passive lava effusion. Hawaiian-style eruptions are dominated by lava flows, Strombolian-style eruptions produce small scoria cones and/or lava flows, and violent Strombolian eruptions produce substantial tephra sheets. Other features that are important in the spectrum of small mafic volcanoes are maars and diatremes, which have craters that have excavated well below the pre-eruptive surface; whether this characteristic requires interaction with external water sources remains a matter of debate (e.g., White and Ross, 2011). Improving our understanding of small mafic eruptions is important because cities such as Auckland, New Zealand, Bend, Oregon, and Mexico City, Mexico, are constructed within active cinder cone fields.

More important for hazards, and more puzzling from the perspective of physical volcanology, is the recent documentation of highly explosive eruptions from mafic volcanic centers. Widespread tephra deposits from mafic volcanoes were first recognized from eruptions of Masaya, Nicaragua (Williams, 1983; Bice, 1985). Interest in mafic Plinian eruptions revived with documentation of a mafic Plinian eruption from Etna volcano in 122 B.C. (Coltelli et al., 1998) and has led to numerous detailed fields studies of mafic explosive volcanism (for example, Cas and Giordano, 2006; Pérez and Freundt, 2006; Costantini et al., 2010). Most surprising, however, has been the recognition of very large (tens of cubic kilometers) mafic ignimbrites from Colli Albani volcano, Italy (Fig. 1D; Funiciello and Giordano, 2010). The generation of large mafic ignimbrite deposits is curious from several perspectives, including the mechanisms by which large volumes of mafic (and very low viscosity) magma accumulate in the upper crust (rather than rise to the surface in small batches) and maintain sustained explosive activity (rather than losing volatiles and changing to effusive eruption styles).

Another exciting advance in mafic volcanism over the past few decades has come from the oceans. Studies of submarine volcanism increased with the advent of the RIDGE program of the 1980s and 1990s, which greatly enhanced our understanding of processes occurring in mid-ocean-ridge environments. Mid-ocean ridges are sites of frequent volcanic activity that is typically manifested as fissure-generated lava flow eruptions of varying intensities (e.g., Rubin et al., 2012). These eruptions can be monitored where ocean-based hydrophone networks are sufficiently dense to record T-phase seismicity associated with magma migration to the surface (e.g., Slack et al., 1999). Axial volcano on the Juan de Fuca Ridge (NE Pacific) also hosts a submarine monitoring network of seismic, pressure, and deformation sensors that has now recorded multiple eruptions (e.g., Fox et al., 2001; Nooner and Chadwick, 2009; Caress et al., 2012; Chadwick et al., 2012; Dziak et al., 2012; Mitchell, 2012). Additionally, recent remotely operated vehicle (ROV) cruises to the western Pacific have identified several mafic submarine arc volcanoes that are either commonly or persistently active (e.g., Embley et al., 2006). One of these, NW Rota-1, lies ~100 km north of Guam in the Marianas, has been erupting since at least 2004, and has produced eruptions that range from effusive to mildly explosive (e.g., Chadwick et al., 2008; Fig. 2). Studies of these systems provide important insight into processes that form both oceanic crust and the island-arc component of continents.

Intermediate/Silicic Volcanoes

Stratovolcanoes are perhaps the best-known (and most iconic) volcano type (Fig. 3A). They are steep-sided cones constructed from stacked lavas and pyroclastic deposits (Fig. 3B). Central cones are often surrounded by gently dipping flanks composed of lavas and pyroclastic and volcaniclastic (particularly volcanic mudflow) material. Although not always intermediate in composition (Etna, Italy, Fuji, Japan, and Villarica, Chile, are basaltic examples), this geomorphic form typifies volcanoes constructed from viscous (often intermediate/silicic) magmas that erupt explosively as well as effusively.

Explosive eruptions of stratovolcanoes are classified as Plinian if they are large (with eruption column heights in excess of 20–25 km and dense rock volumes >1 km^3), sustained, and produce widespread tephra deposits (Newhall and Self, 1982). This term derives from the 79 A.D. (Pompeii) eruption of Vesuvius, Italy, and can be applied to sustained eruptions of Mount St. Helens, United States, in 1980 and Pinatubo, Philippines, in 1991. Eruptions with smaller volumes (0.1–1 km^3), lower eruption columns (<20–25 km), and more local tephra deposits are termed subplinian. Short-lived (typically tens of seconds) but intense explosions characterize Vulcanian eruptions, which are most common in volcanoes of intermediate (andesitic to dacitic) compositions. The type locality—Vulcano—is rhyolitic, but also erupts latite and trachyte magmas. The continuum from sustained Plinian through pulsatory subplinian to Vulcanian activity derives from variations in magma kinetics and dynamics during ascent (e.g., Cashman, 2004; Mason et al., 2006).

Stratovolcanoes are prone to failure either by sector collapse, as illustrated by the 1980 eruption of Mount St. Helens (Lipman and Mullineaux, 1981), or by caldera formation, as occurred at Mount Pinatubo in 1991 (Newhall and Punongbayan, 1996). Sector collapse is commonly accompanied by explosive activity; particularly lethal are resulting laterally directed blasts, which occur when the edifice (or dome) fails because of intruding magma (e.g., Druitt, 1992; Hoblitt, 2000; Voight et al., 2002). Caldera collapse follows withdrawal of large volumes of magma. Famous caldera-forming

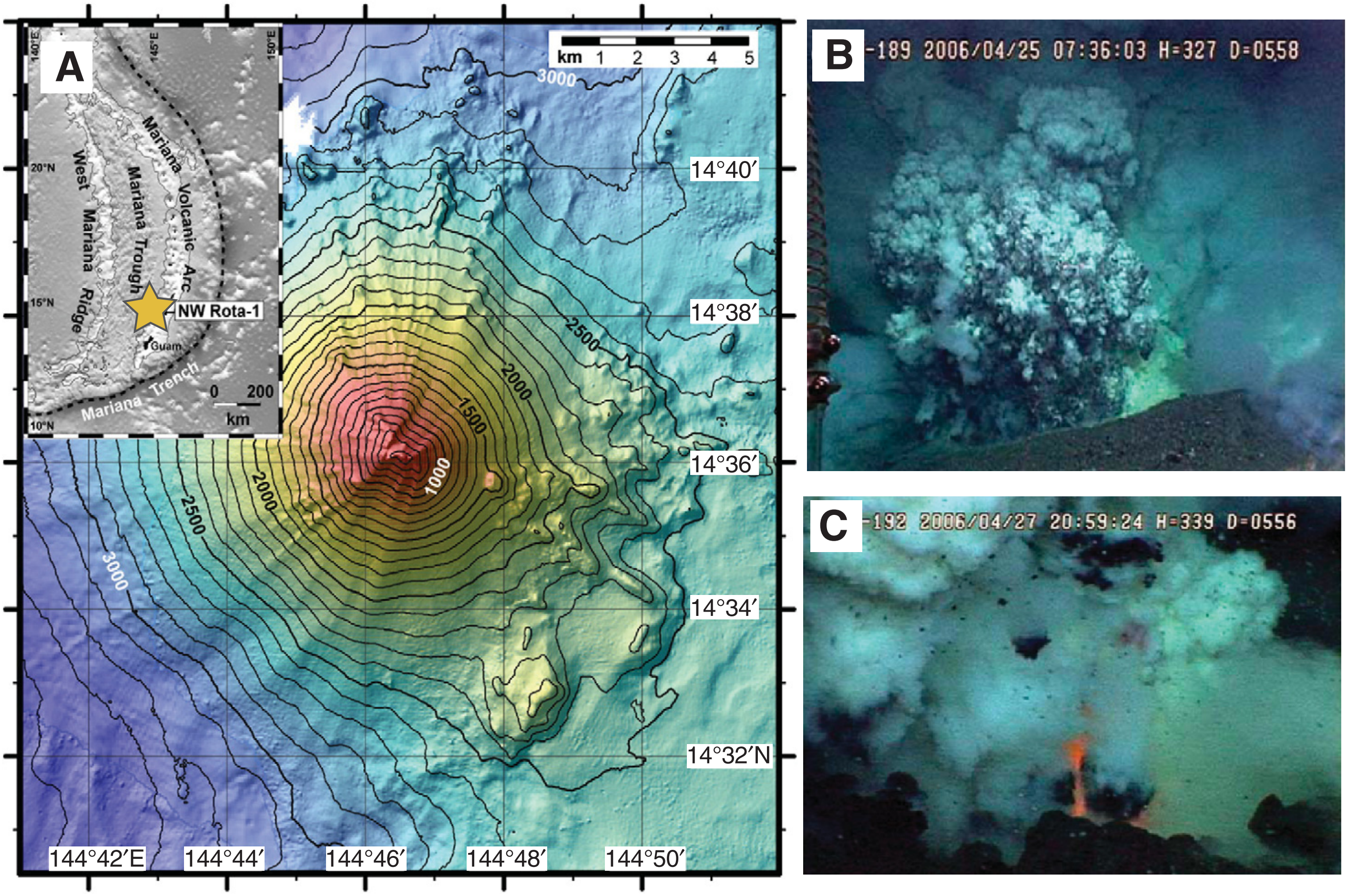

Figure 2. NW Rota-1 submarine volcano. (A) Bathymetry and location map; (B) explosion showing quench fragmentation within the plume; (C) red lava explosion (modified from Chadwick et al., 2008; Deardorff et al., 2011).

Figure 3. (A) Villarica stratovolcano, Chile. (B) Crater walls of Santorini volcano, Greece, showing interlayered lava flows and pyroclastic deposits. (C) Temple of Serapis, Pozzuoli, Italy. This site lies within the Campi Flegrei caldera and has experienced repeated uplift and subsidence, with the most recent uplift in the mid-1980s. (D) Lava spine from the 2004–2008 eruption of Mount St. Helens, Washington (U.S. Geological Survey photograph).

eruptions include the ca. 7700 yr B.P. eruption of Crater Lake, Oregon (Bacon, 1983; Bacon et al., 2002), the ca. 3600 yr B.P. eruption of Santorini, Greece (Druitt et al., 1989), and the more recent eruptions of the Indonesian volcanoes Tambora (A.D. 1815; Oppenheimer, 2003) and Krakatau (A.D. 1883; Simkin and Fiske, 1983; Self, 1992). Exploration of the western Pacific has shown that caldera formation is not confined to subaerial environments, but that silicic submarine calderas are also common in submarine arc volcanoes (e.g., Wright and Gamble, 1999; Fiske et al., 2001; Tani et al., 2008). Moreover, silicic submarine calderas are often associated with extensive Kuroko-type mineralization (e.g., Iizasa et al., 1999).

Very large caldera-forming eruptions create inverse volcanoes, or central collapse depressions surrounded by widespread pyroclastic fans, such as the Taupo volcano, New Zealand (Wilson, 1985). Large caldera systems are commonly termed "supervolcanoes," as they represent an extreme end member of volcanic activity. Caldera formation in these systems is attributed to subsidence related to rapid withdrawal of very large volumes of magma (tens to a few thousand km^3) in single events; subsidence causes large pressure changes, failure of the roof rocks, and collapse (e.g., Gudmundsson, 1988; Lipman, 1997). The central depressions often host thick sequences of caldera fill. After caldera formation, these intracaldera ignimbrites can be lifted up to form resurgent domes at the center of the original depression (e.g., Acocella et al., 2000). Eruptions of these types are rare (Mason et al., 2004); thus recent advances derive from new field studies, analytical techniques, analogue experiments, and numerical models rather than direct observation of eruptive activity (e.g., Wilson and Hildreth, 1997; Jellinek and de Paolo, 2003; Acocella, 2007; Cashman and Cas, 2011). Fascination with these events derives in part from the recognition that large caldera-forming eruptions may have played a role in the development of human history, such as the 39,000 yr B.P. eruption of Campi Flegrei, Italy (e.g., Fedele et al., 2008) and the 75,000 yr B.P. eruption of Toba, Indonesia (e.g., Ambrose, 1998, 2003). These large systems are commonly restless (e.g., Fig. 3C) and thus pose a major monitoring challenge.

Another end member is represented by effusive eruptions of very viscous intermediate to silicic magmas that create high-aspect-ratio lava flows, domes, and spines (Fig. 3D). Although effusive, these eruptions pose unique hazards related to pressurization and collapse of dense lava plugs. Recent well-observed dome eruptions of Mount St. Helens (1980–1986 and 2004–2008; Swanson and Holcomb, 1990; Sherrod et al., 2008); Unzen, Japan (1991–1995; Nakada et al., 1999), and Soufrière Hills volcano, Montserrat (1995–present; e.g., Sparks and Young, 2002) have provided a wealth of observational data about this eruption style, and show that growing domes (or cryptodomes) can generate (1) lateral volcanic blasts and sector collapse with debris avalanches, (2) subplinian and Vulcanian explosive eruptions, and (3) (sometimes lethal) pyroclastic flows from collapse of active flow fronts. A key factor for hazard assessment has been the recognition of not only the longevity of some dome-forming activity but also the rapid transitions from effusive to explosive activity that characterize eruptions of this type (e.g., Sparks, 1997).

DEVELOPMENT OF SHALLOW MAGMA STORAGE SYSTEMS

A critical control on eruption style is the pre-eruptive history of shallow magma storage in magma chambers. Magmatic systems are commonly envisaged as interconnected crystal-melt mush zones and melt-dominated regions, or magma chambers (Hildreth, 2006; Annen et al., 2006), where the distinction between mush and magma is that of noneruptible and eruptible material. The threshold itself depends on factors like crystal size, shape, and strain rate (e.g., Kerr and Lister, 1991; Cimarelli et al., 2011). Below a critical melt fraction, the system can be viewed rheologically as partially molten rock, while above the threshold, the system is magma. The focus by the volcanological community on (instantaneously) *eruptible* magma has produced a different view of magmatic systems than that derived from those who study (noneruptible) plutons, where the entire history of the magmatic system is preserved.

Our knowledge of magma storage systems has improved enormously over the past 25 yr thanks to developments in observational, analytical, experimental, and numerical techniques. Geophysical techniques for imaging magma reservoirs have evolved from earthquake location (e.g., Scandone and Malone, 1985; Ryan, 1987) to sophisticated tomographic and deformation inversion techniques (e.g., Koulakov et al., 2011; Ofeigsson et al., 2011; Paulatto et al., 2012). New analytical techniques for measuring the volatile contents of phenocryst-hosted melt inclusions (reviewed in Métrich and Wallace, 2008; Blundy and Cashman, 2008) and crystal zoning profiles (reviewed in Costa and Morgan, 2010) provide detailed constraints on magma storage conditions that lead to volcanic eruptions. Additionally, experimental constraints on magma storage (reviewed in Pichavant et al., 2007) and the kinetics of phase transformations (reviewed in Hammer, 2008; Hamada et al., 2010) can be linked to geophysical and geochemical observations to provide a detailed and coherent picture of well-studied volcanic systems (e.g., Blundy et al., 2008). Finally, integration of geophysical information with numerical models is providing new views into the evolution of magma storage regions (Pearse and Fialko, 2010; Paulatto et al., 2012). Taken as a whole, the growing convergence of geophysical and petrological evidence for the location and geometry of magma storage regions is encouraging, particularly with regard to understanding links between magma storage conditions and volcanic eruptions.

Magma Chamber Formation

It is important to note that most magma never makes it to the surface. Estimates of the proportion of intruded to extruded magma range from 3 to 10 (e.g., Newhall and Dzurisin, 1989; White et al., 2006). From this perspective, intrusions can be viewed as failed eruptions (or, from another perspective, eruptions may be viewed as failed intrusions). In either case, understanding the causes of, and interpreting the signs of, magma arrest has become an important focus of volcanological studies (e.g., Moran et al., 2011; Bell and Kilburn, 2012).

Rising magma can stall for a variety of mechanical reasons (Taisne and Tait, 2009). Dikes may not reach the surface if the driving pressure is insufficient (e.g., Lister and Kerr, 1991), if the magma density is too high (Ryan, 1987), or because the volcanic edifice itself creates regions of high stress below (Pinel and Jaupart, 2004). Dikes can suffer thermal death because of cooling (Taisne and Tait, 2011) or viscous death by decompression-induced crystallization (Annen et al., 2006). Sills form where magma moves laterally; this can occur when rising magma encounters a rigidity or density barrier (Kavanagh et al., 2006; Taisne and Jaupart, 2009), or where the minimum principal stress is vertical. Sheeted sills probably constitute much of the crust formed at mid-ocean ridges (e.g., Fialko, 2001). Dike-sill complexes may also amalgamate to form magma reservoirs (e.g., Hildreth, 2006; Menand, 2011; Fig. 4). Magma accumulation sufficient for amalgamation requires heat to be advected into the upper crust faster than heat can be conducted away or lost by hydrothermal circulation. Modeling by Annen (2009) suggests that magma intrusion rates must exceed 10^{-3} km^3/yr to allow magma chambers to form.

Geophysical Evidence for Magma Chambers

Locations of active magma intrusion can be identified from geophysical data and constrained by surface phenomena such as invigorated fumaroles or phreatic explosions. A particularly exciting development in the past decade has been the increasing use of interferometric synthetic aperture radar (InSAR) to identify and monitor intrusion sites (e.g., Pritchard and Simons, 2004; Biggs et al., 2009; Fournier et al., 2010; Riddick and Schmidt, 2011). Regions of melt accumulation can also be imaged geophysically using both active and passive seismic techniques. Passive source techniques, such as location of earthquakes adjacent to magma bodies (Ryan, 1987),

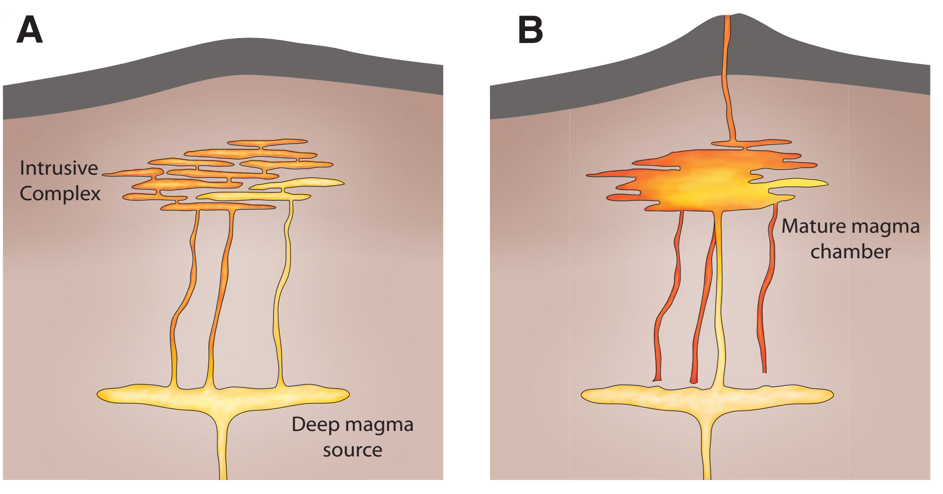

Figure 4. Proposed development of a magma chamber at Soufrière Hills volcano, Montserrat (after Zellmer et al., 2003). (A) Repeated intrusion of magma from the deeper crust creates a network of partially solidified dikes and sills. (B) Continued intrusions reheat, remobilize, and amalgamate melt pockets into a magma chamber; additional influx of deep mafic magma triggers an eruption.

are the most common. Passive source seismology has improved dramatically through use of broadband and three-component seismometers; new data have also raised new questions about the source of volcano-related seismicity (e.g., Neuberg et al., 2006; Harrington and Brodsky, 2007; Waite et al., 2008; Moran et al., 2008). At the same time, improvements to data inversion techniques are providing increasingly detailed three-dimensional views of active magmatic systems (e.g., Chaput et al., 2012).

During the 1990s, geophysical experiments in mid-ocean-ridge environments showed that melt storage along fast-spreading ridges is typically shallow (2–3 km) and confined primarily to thin along-axis sills (e.g., Singh et al., 2006). A similar picture is emerging from recent activity in Iceland, where deformation and seismic signals related to the 2010 eruption of Eyjafjallajökull volcano, Iceland, suggest that this eruption was fed by a complex network of sill-like magma bodies that may have extended to the base of the crust (e.g., Sigmundsson et al., 2010; Tarasewicz et al., 2012). In contrast, magma beneath stratovolcanoes is apparently stored in narrow and vertically elongated regions that may segregate into small melt pockets (e.g., Lees, 1992; Waite and Moran, 2009; Paulatto et al., 2012; Fig. 5). Upper-crustal magma chambers beneath stratovolcanoes are probably fed from larger magma accumulations at depth. An example is provided by Vesuvius, Italy. Here, a small shallow magma body (4–5 km depth) is underlain by a main magmatic system at 10–15 km depth, while the melt-bearing region extends to ≤30 km depth (Di Stefano and Chiarabba, 2002). More generally, zones of plate convergence often show midcrustal anomalies that may be associated with melt accumulation (Brown et al., 1996; Zandt et al., 2003).

Taken together, these studies show that magmatic systems beneath many volcanoes and volcanic regions consist of localized magma chambers (zones of melt accumulation) concentrated at the top of much thicker regions of crystal-melt mush. Importantly, large bodies of melt are rarely detected, which suggests that most persistent magma chambers are small and that the accumulation of very large bodies of magma required to feed large ignimbrite eruptions is rare. This in turn suggests that melt is generated and stored as partial melt within the deeper crust for long periods of time prior to being transferred rapidly to shallow levels (Annen et al., 2006). Support for rapid magma transfer can be found in a recent petrological study of magma accumulation prior to the Bronze Age eruption of Santorini (Druitt et al., 2012) and in a zircon chronology study of the Taupo volcanic system, New Zealand (Wilson and Charlier, 2009).

Petrologic Constraints on Magma Storage and Eruption Triggers

Petrology has long been used to study the evolution of magmatic systems. Over the past few decades, petrologic techniques have been increasingly applied to questions of pre-eruption magma storage, particularly those that may lead to eruptions. Here, we briefly review insight about magma storage conditions that has been acquired from petrologic studies. We then look at petrologic constraints on triggers of eruptive activity.

Petrologic Constraints on Magma Storage

Once a magma chamber has formed, it determines both the nature of magmas that can erupt and the fate of new melt inputs. Magma accumulation retards the ascent of new magma, and thus extends the time of magma residence in the upper crust prior to eruption. For this reason, identical magmas rising beneath, or outside of, central magma storage regions may have the same composition but different temperatures, crystallinities, and eruption styles (e.g., Frey and Lange, 2011). Processes active within central (and open) magma chambers can be complex, including magma mingling/mixing, compositional stratification, disruption of cumulates, and assimilation of wall rock. Additionally, several recent studies document the presence of diverse and intimately mixed individual crystals with very different origins. These processes are illustrated schematically in Figure 6, which shows both the magma storage and transport system of Shiveluch volcano, Kamchatka, and the consequent diverse histories of individual phenocrysts reconstructed from petrological studies. Importantly, these observations require physical mechanisms of incorporating, and homogenizing, crystal cargo from very different parts of the magma storage systems. How this occurs remains an important question.

Constraints on the temperature, pressure, volatile partial pressures, and oxidation state in magma chambers can be obtained using geothermometers, geobarometers, melt inclusion studies, and comparison of natural mineral assemblages with those produced in experiments (reviewed in Pichavant et al., 2007; Blundy and Cashman, 2008; Putirka, 2008; Métrich and Wallace, 2008). Experimental studies of subduction-zone volcanoes suggest that magma is commonly stored at 100–200 MPa under volatile-saturated conditions. These experiments also show that exsolution of H_2O accompanying magma ascent changes the stability of some crystal phases, most notably plagioclase. Thus, the preserved phase assemblage (phases, phase proportions, and phase compositions) often provides tight constraints on storage conditions just prior to eruption (Fig. 7A). Information on pre-eruptive magma storage can also be derived from analysis of phenocryst-hosted melt inclusions. The preserved volatile content of melt inclusions, in particular, can be used to infer the pressure (depth) of crystal formation and thus the nature of magma storage systems characteristic of different volcano types (Fig. 7B). Early-erupted samples from large (ignimbrite-producing) rhyolitic eruptions typically preserve melt inclusions that are H_2O-rich but have lost much of their CO_2, suggesting protracted storage at (often) 150–200 MPa (open circles, Fig. 7B). Later-erupted samples from the same eruptions have melt inclusions that are more enriched in CO_2, and often encompass a wider range in pressure than early-erupted

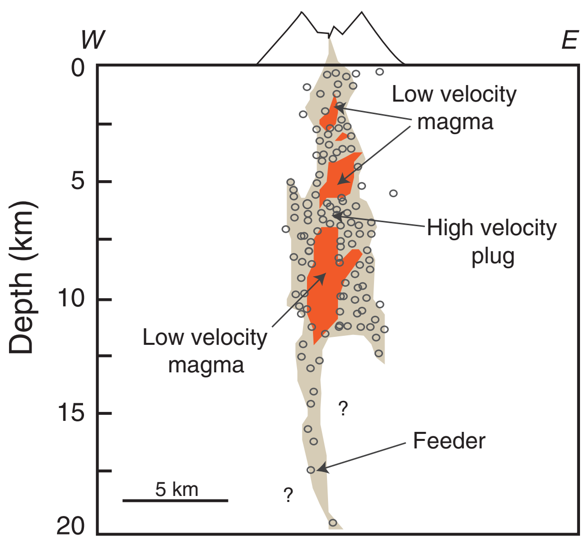

Figure 5. Schematic illustration of the magma storage system beneath Mount St. Helens showing earthquake locations (open circles) in country rock (high velocity) surrounding earthquake-free zones of magma storage (low velocity). Modified from Lees (1992).

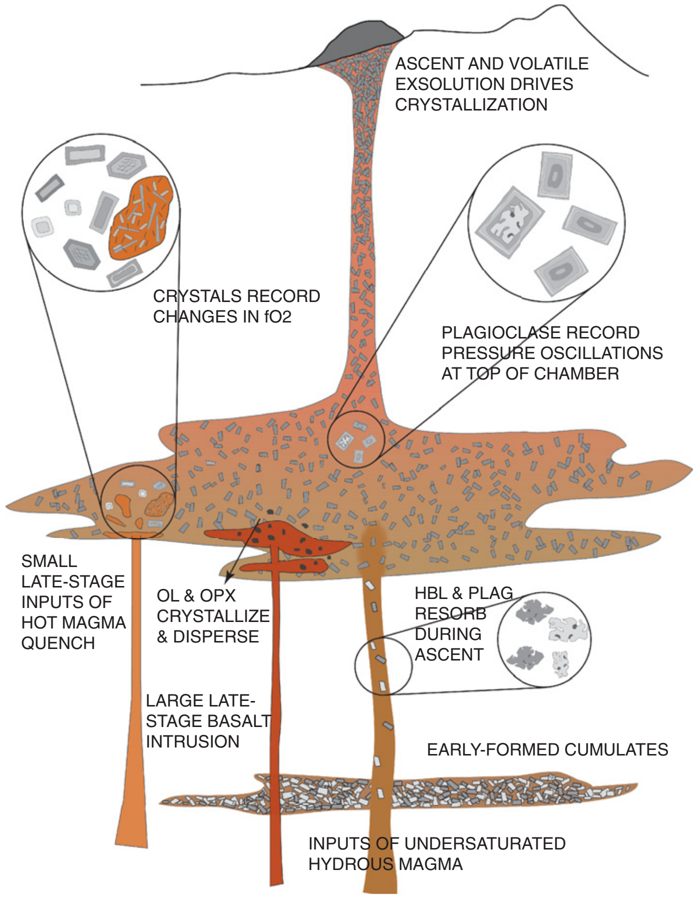

Figure 6. Schematic diagram showing reconstruction of the processes taking place in the open-system magma chamber of Shiveluch volcano, Kamchatka, before and during eruption, based on petrological studies. Phenocryst zoning patterns provide evidence of multiple episodes of magma intrusion, crystallization, and resorption at varying pressures and oxygen fugacities, as well as late-stage crystallization driven by magma ascent and volatile exsolution. Figure is after Humphreys et al. (2006).

samples (filled circles in Fig. 7B), suggesting complex patterns of magma withdrawal during later stages of caldera-forming eruptions. In contrast, open-system andesitic volcanoes, such as Popocatepetl, Mexico, preserve phenocryst-hosted melt inclusions that suggest that magma was supplied from a large pressure range despite small eruptive volumes (filled diamonds in Fig. 7B). These data can be correlated with seismic and gas geochemistry data when the samples are well constrained (i.e., both timing and eruption conditions are known; e.g., Blundy et al., 2008; Saunders et al., 2012). Additionally, discrepancies between petrologic and geophysical monitoring data may provide critical information on late-stage processes (those that occur just prior to eruption) such as magma rise (Blundy and Cashman, 2001), flushing of volatiles through the magma chamber (Hammer and Rutherford, 2003), and arrival of recharge magma into the shallow system (Murphy et al., 2000).

The past decade has also seen rapid improvements in microanalytical techniques that are providing new insight into the details of magma storage conditions. Time scales of magmatic activity are constrained by isotopic (particularly U-series isotopes) and diffusion studies. U-series studies place constraints on phenocryst residence times within magma storage regions (e.g., Zellmer et al., 2003; Cooper and Reid, 2008). These studies reflect the integrated age of the crystal population and commonly yield time scales of thousands of years. In contrast, diffusion studies take advantage of chemical zoning profiles in phenocrysts caused by magma recharge or depressurization. This approach is more likely to reflect events responsible for triggering eruptive activity, and commonly yields time scales of months to decades (e.g., Hawkesworth et al., 2004; Costa and Morgan, 2010). Similar time scales are recorded by U-series studies of magma degassing (e.g., Condomines et al., 2003; Berlo et al., 2004).

Triggering Eruptions

Two end-member models have emerged for eruption triggering. First, there is clear evidence that melt recharge events may trigger eruptions by mobilizing stored and partially crystalline magma (e.g., Murphy et al., 2000; Ruprecht and Cooper, 2012). Second, evolved melt may be rapidly and efficiently extracted from mush zones and transported to shallow storage regions. These two mechanisms are not mutually exclusive, and they may act in tandem to fuel some eruptions. Other triggering mechanisms include buildup of pressure in crystallizing, water-supersaturated magma (Tait et al., 1989) and tectonic triggering (e.g., Gravley et al., 2007).

Mafic recharge can trigger eruptions when hot, low-viscosity, crystal-poor melt batches interact with cooler stored magma that is typically more evolved and more crystalline. The (semirigid) mush zone serves to both stabilize the magma and to act as a trap, or rheological barrier, to eruption of either the evolved crystalline melt or the low-viscosity recharge magma (e.g., Kent et al., 2010). The recharge magma may disrupt the crystal network by fluxing gases (Bachmann and Bergantz, 2006), by heating to cause convective self-mixing (e.g., Couch et al., 2001), or by fracturing (Wright et al., 2011). Although the recharge magma is commonly mafic, cryptic recharge of (hotter and less viscous) silicic magma may also serve as an eruptive trigger (e.g., Smith et al., 2009).

There is also growing evidence of efficient segregation and upward migration of rhyolitic melt from midcrustal "mush" zones. First suggested by Eichelberger et al. (2000), rhyolite melt segregation has been particularly well documented by zircon dating of the products of Taupo volcano, New Zealand. Here, melt segregation appears to have been both efficient and rapid, such that large (~500 km^3) volumes of melt may have accumulated in hundreds to a few thousands of years (e.g., Charlier et al., 2005). Rapid melt segregation and shallow accumulation of rhyolitic melt prior to large caldera-forming eruptions are consistent with melt inclusion evidence for sill-like geometries (e.g., Blundy and Cashman, 2008), field and theoretical evidence for the inherent instability of such melt accumulations (e.g., Jellinek and DePaolo, 2003; De Silva et al., 2006), thermal models (Annen, 2009), and lack of geophysical evidence for large melt accumulations in most magmatic settings.

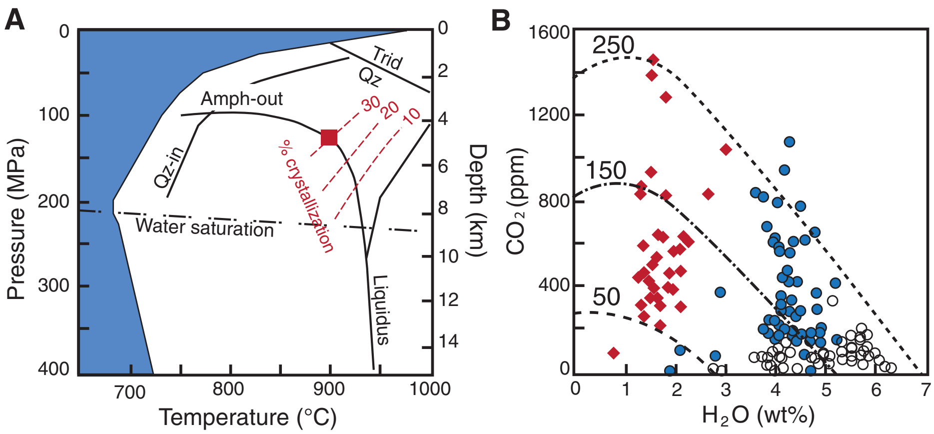

Figure 7. Magma storage conditions determined from (A) phase equilibria experiments and (B) phenocryst-hosted melt inclusions. Phase equilibria data are for magma erupted from Mount St. Helens in 1980; solid square shows location of last magma storage as determined from the phenocryst assemblage and Fe-Ti–oxide thermometry (modified from Blundy and Cashman, 2001). Melt inclusion data are from early (open circles) and late (filled circles) phases of the Bishop Tuff (Wallace et al., 1999) and Oruanui (Liu et al., 2006) ignimbrites and Popocatepetl stratovolcano (solid diamonds; Atlas et al., 2006). Note that early phases of ignimbrite eruptions have melt inclusions that are H_2O-rich and CO_2-poor, suggesting long residence times within upper crust. In contrast, both late-stage ignimbrites and open-system volcano Popocatepetl preserve melt inclusions with a wide range in CO_2 (pressure) for a limited range of H_2O. Figure is modified from Blundy and Cashman (2008).

VOLCANIC CONDUITS

Prior to the mid-1980s, the vigor of eruptive activity was linked directly to the extent to which stored magma was saturated, or undersaturated, with volatile components. The 1990s saw a change in emphasis to conditions of magma transport from magma storage regions to the surface (that is, the role of conduits). This shift was largely the result of detailed observations of effusive eruptions of Mount St. Helens, United States, and Unzen volcano, Japan, coupled with recognition of the extent to which the physical properties of magma could change during transport because of decompression-driven volatile exsolution (e.g., Dingwell et al., 1996) and crystallization (e.g., Cashman, 1992). These rheological changes set up complex feedbacks between conditions of magma ascent and resulting styles of eruptive behavior (e.g., Melnik and Sparks, 1999).

Conduit Construction and Evolution

With the exception of open-system volcanoes such as Stromboli, Italy, and Villarica, Chile, magma storage regions are not connected to the surface; it is this isolation that allows them to develop sufficient overpressure to generate eruptive activity. Thus, magma must construct a pathway (conduit) to the surface. Conduit construction is not well understood, although it is commonly assumed that magma ascends via dike propagation, at least until it reaches shallow levels. The speed of dike propagation depends principally on magma viscosity (Kerr and Lister, 1991) and can be fast for basaltic magmas (decimeters to meters per second; e.g., Linde et al., 1993). Dike width is controlled by magma pressure through elastic deformation of the wall rock, with magma flow rate proportional to the product of the cube of the dike width and the length. For this reason, dike-fed eruptions show strong interactions between eruption rate and magma pressure (e.g., Costa et al., 2006). Dike closure may cause eruptions to end (or vents to shift) if the pressure becomes too low to drive continued magma flow or if magma cools and solidifies on the dike walls. These scenarios can be distinguished if there are good temporal constraints on mass flux. For example, documentation of a linear decrease in magma supply to the Kūpaianaha vent of Kilauea volcano, Hawaii, between April and November of 1991 provided evidence of a gradual loss of driving pressure with time (Kauahikaua et al., 1996). Alternatively, dikes may fail to close completely when cooling at the thin edges is combined with inelastic deformation (Daniels et al., 2012).

Eruptions of viscous silicic magma are also dike-fed (e.g., Mastin and Pollard, 1988; Roman and Cashman, 2006), although silicic dikes ascend sufficiently slowly that arrival of magma at Earth's surface may take weeks, months, or even years. For example, about eight weeks of precursory activity (seismicity, deformation, and explosions) preceded climactic eruptions of both the 1980 eruption of Mount St. Helens, United States, and the 1991 eruption of Pinatubo volcano, Philippines. Both of these precursory sequences involved movement of magma to shallow levels, as evidenced by the growth of a cryptodome (Mount St. Helens) or dome (Pinatubo). However, a time delay of hours (Mount St. Helens) to a few days (Pinatubo) between eruption initiation and full development of climactic activity suggests that the conduit did not develop full connectivity until after the main eruptive phase had commenced (Scandone et al., 2007).

Once formed, conduit geometry can evolve in space and time as the result of mechanical and/or thermal erosion, magma solidification, and changing stress conditions. Conduit evolution is particularly apparent in basaltic eruptions, which typically initiate with a "curtain of fire" as magma-transporting dikes intersect the surface, but rapidly focus into one (or a few) localized vents. Processes that promote focusing in these systems most likely involve feedbacks among flow, magma rheology, and cooling (Bruce and Huppert, 1989). For example, advection of heat by rapid flow through the widest part of the initial dike will slow, or eventually reverse, rates of chilled margin growth (Holness and Humphreys, 2003); at the same time, lower flow rates through narrower regions will promote cooling and eventual solidification of dike extremities. Viscosity changes caused by degassing and crystallization should produce a similar flow focusing if the rheological changes occur preferentially at the dike margins (for example, in regions of high shear).

The geometry of volcanic conduits can also evolve by mechanical processes. Mechanical erosion is most likely where dikes change orientation, or at shallow levels in explosive vents. Exposures in caldera walls show that dikes are commonly segmented; offsets or jogs between segments are regions of complex brittle deformation, brecciation, and dilation that can localize flow. Xenoliths generated by deformation associated with localization can be removed by flowing magma and transported to the surface (Brown et al., 2007; Kavanagh and Sparks, 2011). Additionally, protracted effusive eruptions may create complex conduit systems. An unusual opportunity to view such a system in a recently active volcanic conduit was provided by the Unzen (Japan) drilling project. Drilling of the conduit system that fed a 1991–1995 dome-building eruption revealed a wide (500 m) conduit zone consisting of numerous individual feeder dikes (e.g., Sakuma et al., 2008).

Explosive eruptions also create conditions that promote mechanical erosion. In particular, cylindrical near-surface conduits develop when early magma is either sufficiently overpressured to excavate a conduit or sufficiently underpressured to cause wall rocks to fail, fall into the conduit, and be transported out of the conduit by high-speed explosive flows (Sparks et al., 2007; Barnett and Lorig, 2007). In powerful explosive eruptions, the level of fragmentation, and thus the depth of the resulting cylindrical conduits, can extend to kilometers. Early phreatic or phreatomagmatic stages of eruptive activity may also form cylindrical near-surface pathways that can then be used by magma fed from a deeper dike.

Synascent Changes in Magma Properties

As magma ascends toward Earth's surface, decompression causes some volatile phases to exsolve and some solid phases to precipitate. These phase transformations affect the density and rheology of the magma and, to a lesser extent, its temperature. The past few decades have seen extensive research on the kinetics of the phase transitions, the rheology of complex (multiphase) suspensions, and the evolution of the gas phase, all of which are important for understanding the highly nonlinear dynamics of conduit flow processes that control eruptions.

Volatiles, Bubbles, and Crystals

Volatiles are more soluble in silicate melts at high pressure than at low pressure (e.g., Newman and Lowenstern, 2002; Papale et al., 2006). For this reason, decompression of volatile-saturated melt causes exsolution of the volatile phase as bubbles (vesiculation). The rate of vesiculation is controlled by the rate of bubble nucleation and growth, which depends not only on the degree of supersaturation caused by the decompression but also on the surface tension and viscosity of the melt phase (e.g., Mangan and Sisson, 2005) and the availability of nucleation sites (e.g., Hurwitz and Navon, 1994). Results from decompression experiments show that in rhyolitic melts, homogeneous nucleation (that is, nucleation within the melt) has to overcome substantial energy barriers and therefore requires very large overpressures (100–150 MPa; Fig. 8). In contrast, the undercooling required for bubble nucleation is much lower if nucleation can occur heterogeneously on crystal surfaces (Hurwitz and Navon, 1994; Gardner et al., 1999).

Bubble number densities preserved in pyroclastic material (pumice) produced by silicic Plinian eruptions suggest that bubble nucleation is commonly homogeneous and controlled by

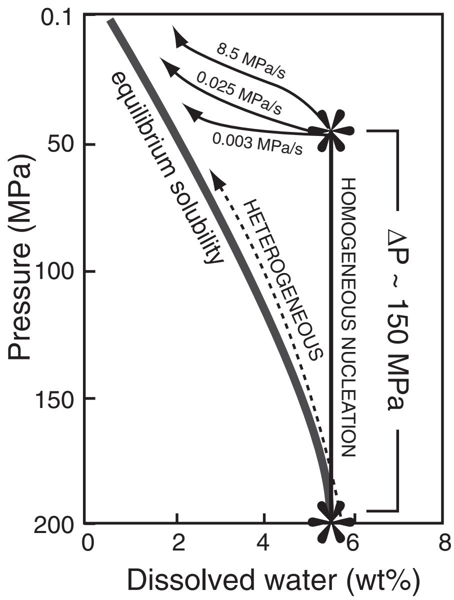

Figure 8. Degassing/vesiculation paths for rhyolite decompression experiments performed at conditions that promote both homogeneous and heterogeneous bubble nucleation. Heterogeneous nucleation permits the melt to maintain equilibrium degassing paths. In contrast, homogeneous nucleation occurs only at large supersaturations (Δ*P*) regardless of magma ascent rates; once nucleation occurs, ascent rate controls the degassing path. Figure is modified from Mangan and Sisson (2000).

exsolution of a mixed (H_2O-CO_2) volatile phase (e.g., Cashman, 2004). This conclusion has important implications for conditions of magma fragmentation in silicic eruptions where delayed nucleation may generate explosive vesiculation bursts at high overpressures (e.g., Mangan et al., 2004; Scandone et al., 2007). Additionally, these data show that the kinetics of bubble and crystal formation are intimately linked and together may control transitions in eruption style. Unfortunately, there are no equivalent data for bubble nucleation in mafic melts because of experimental challenges. Measurement of bubble number densities in the pyroclastic products of low- to moderate-intensity eruptions, however, suggests that there is little to no activation energy barrier for bubble nucleation in mafic melts (e.g., Rust and Cashman, 2011), although textural studies of mafic Plinian deposits show that these systems can attain bubble number densities that approach those of silicic pumice (e.g., Sable et al., 2006; Costantini et al., 2010; Vinkler et al., 2012). Very high bubble number densities may reflect large supersaturations generated by rapid magma decompression, or possibly the effects of rapid (syneruptive) crystallization and associated heterogeneous bubble nucleation.

The number and proportion of crystal phases also provide information on conditions of magma ascent, particularly when the stability of the crystal is controlled by the water content of the melt (e.g., Hammer et al., 2000; Toramaru et al., 2008; Blundy and Cashman, 2008). The time required for crystals to nucleate and grow in response to water exsolution depends on the melt composition and temperature (diffusion rate), the undercooling (driving force) for crystallization, and the presence or absence of phenocryst phases. For a single melt composition, decompression experiments confirm that both the number density and volumetric proportion of plagioclase crystals record the conditions of decompression (reviewed in Blundy and Cashman, 2008; Hammer, 2008). Experiments also confirm observational evidence that decompression-induced crystallization can occur on eruptive time scales (e.g., Geschwind and Rutherford, 1995; Hammer and Rutherford, 2002). The combined effects of vesiculation and crystallization during magma ascent have profound consequences for the rheological evolution of ascending magma, and for the course of volcanic eruptions.

Magma Rheology

Rheology refers to flow behavior (that is, the deformational response to imposed stress). Magma rheology is usually measured by magma viscosity, which varies depending on the melt composition and temperature as well as the bubble and crystal content. The rheological properties of magma govern the dynamics of magma chambers, the wall friction generated by conduits flows, and therefore the rate of eruption, the kinetics of crystal and bubble formation, and the flow of lava on Earth's surface.

Critical constraints on the rheology of silicic melts have been provided by experimentally calibrated models for melt viscosity as a function of composition, temperature, and water content (e.g., Dingwell, 1998; Giordano et al., 2008). Most silicate melts are Newtonian (for details, see Giordano and Dingwell, 2003) and have viscosities that vary from less than 0.1 Pa s to over 10^{12} Pa s. Silicate melts that are either alkalic or hydrous, however, show non-Arrhenian behavior controlled by the effect of alkalis/water on the melt structure. Understanding the effect of water, in particular, is important for modeling the behavior of ascending and degassing magmas. Importantly, the glass transition also varies as a function of melt composition, temperature, and shear rate (e.g., Dingwell and Webb, 1989; Webb and Dingwell, 1990). The glass transition is a kinetic barrier (relaxation time scale) that separates liquid from glassy behavior, which in turn determines the behavior of silicate liquids when strained. One application of these data has been to define magma fragmentation in melt-viscosity shear space (e.g., Gonnermann and Manga, 2003). An important outcome of such an analysis is to demonstrate that viscous rhyolitic glass, in particular, may repeatedly break and re-anneal during slow ascent at shallow levels. Repeated fracture, in turn, may explain the characteristic "hybrid" earthquakes that accompany extrusion of silicic domes (Tuffen et al., 2003; Neuberg et al., 2006).

When the melt contains suspended crystals and bubbles, the magma can develop non-Newtonian rheological properties. The addition of a small volume fraction of crystals causes an increase in magma viscosity; when the crystal content is sufficiently high, crystal interactions generate a yield strength (e.g., Lejeune and Richet, 1995; Mueller et al., 2010; Castruccio et al., 2010; Fig. 9A) and either shear-thickening (shear-dilatancy) or shear-thinning behavior (e.g., Costa et al., 2009; Fig. 9B). The critical crystal volume fraction for particle interactions depends on crystal shape, with higher aspect ratios allowing interaction at lower volume fractions (Saar et al., 2001; Walsh and Saar, 2008). For this reason, crystallization caused by volatile exsolution during rapid decompression, which generates numerous small elongate or platy plagioclase crystals, can cause the apparent viscosity to change by many orders of magnitude as magma ascends from the reservoir to the surface (e.g., Sparks, 1997). The effect of crystals on viscosity is enhanced by the tendency of the remaining melt to become more silicic (more viscous) as crystallization proceeds (e.g., Cashman and Blundy, 2000).

The effect of bubbles on magma rheology depends on both bubble size and shear rate (e.g., Rust and Manga, 2002; Pal, 2003; Llewellin and Manga, 2005). The deformation behavior of bubbles in a shear flow is described by a nondimensional parameter called the capillary number ($Ca = \frac{r\dot{\gamma}\mu}{\Gamma}$, where r is bubble radius, $\dot{\gamma}$ is strain rate, μ is melt viscosity, and Γ is surface tension). In dilute bubble suspensions, the average shear rate and shear stress experienced by a sample can be determined from the dimensions of moderately deformed bubbles (Rust et al., 2003). Suspensions of bubbles in viscous liquids are shear-thinning (Fig. 9C): Addition of bubbles increases the viscosity at low *Ca* (small bubbles, low strain rates) but decreases viscosity at high *Ca* (large bubbles, high strain rates). Bubble suspensions are more strongly shear-thinning at higher bubble volume fractions (ϕ_b). Under these conditions, the relative viscosity (μ_{susp}/μ_{melt}) approaches $1 - \phi_b$ at high *Ca*, because the bubbles are sufficiently deformed that resistance to flow is provided only by the melt fraction ($= 1 - \phi_b$). Shear-thinning behavior means that ascent of bubbly viscous magma through volcanic conduits probably occurs by plug flow, with localization of shear along the conduit margins (e.g., Llewellin and Manga, 2005).

Conduit Controls on Eruption Style

The flow of magma along conduits is driven by pressure gradients between the deep source and the surface, and opposed by both friction

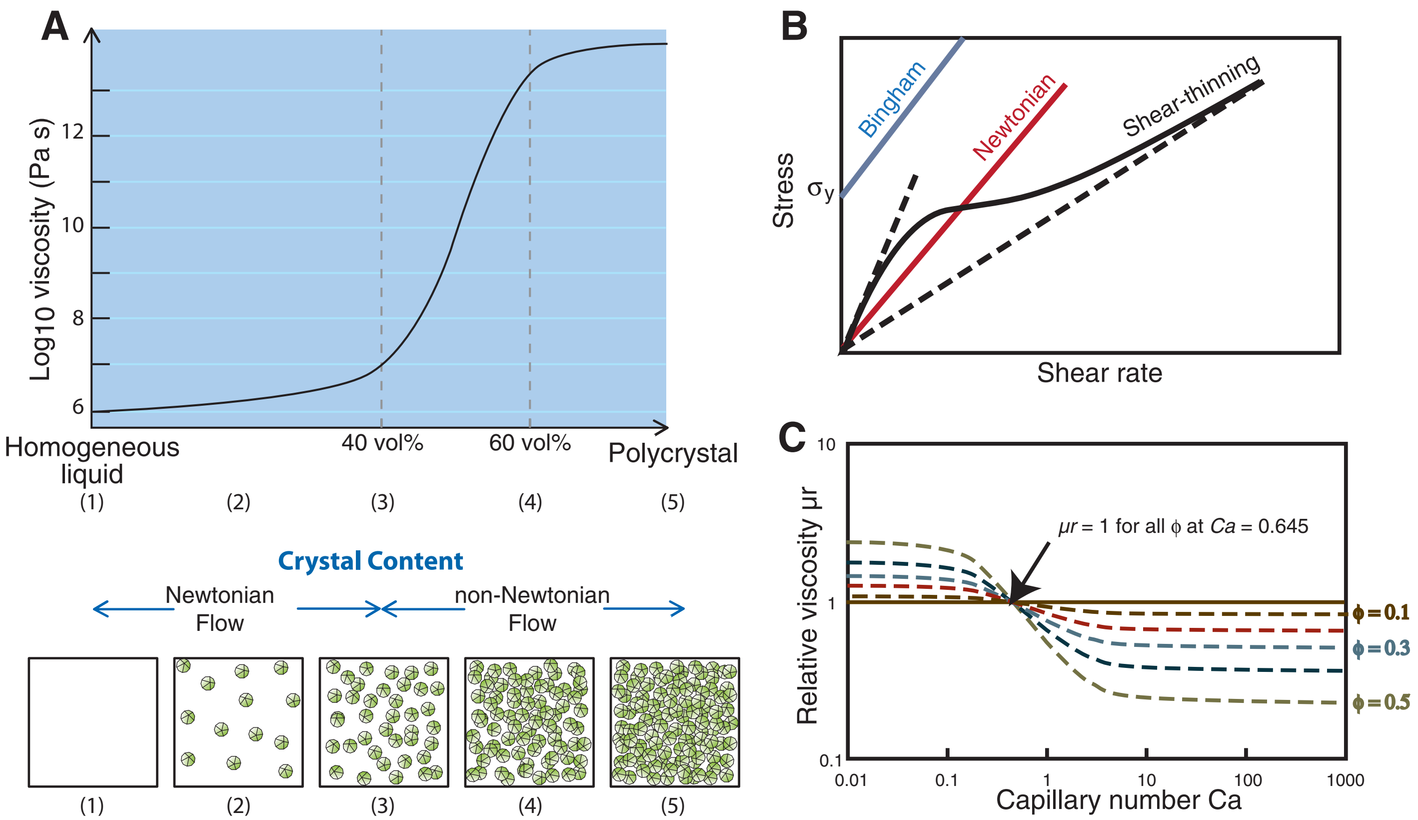

Figure 9. Basics of magma rheology. (A) Effect of adding spherical particles; *y*-axis shows viscosity normalized to reference (melt) viscosity; dashed lines at 40% and 60% particles show locations of rapid viscosity increase and maximum packing, respectively. Diagrams show schematic representation of particle concentrations (modified from Lejeune and Richet, 1995). (B) Schematic stress–shear rate diagram illustrating different rheologies; σ_y is yield strength (minimum stress that must be overcome for fluid deformation). (C) Effect of adding bubbles; viscosity is normalized to bubble-free values and shown as a function of *Ca* for different bubble concentrations (ϕ; modified from Pal, 2003).

along the conduit margins and the tendency of magma to degas and solidify. The rate of magma ascent controls the eruption style (explosive or effusive) by modulating the extent to which exsolving gas is retained within, or lost from, magma during ascent. Gas loss, in turn, is controlled by the relative rates of bubble rise, bubble coalescence, and the development of permeable pathways in magma and surrounding host rocks. As bubble rise is controlled primarily by magma viscosity, the orders-of-magnitude variation in viscosity between mafic and silicic melts means that mechanisms of gas loss are very different in mafic and silicic magmas.

Modeling Conduit Flow

Modeling the flow of magma through volcanic conduits requires coupling equations of mass and momentum with expressions for changes in phase proportions, and resulting changes in rheology. The numerous interacting factors that control flow rates explain the very rich variety of volcano behaviors (reviewed in Melnik et al., 2008). These complex interactions can be illustrated by a simplified reference case for effusive eruption from a pressurized magma chamber with elastic walls. Under these conditions, the flow rate of magma through a cylindrical conduit or parallel-sided fracture is controlled by the pressure gradient and wall friction, which, in turn, reflect both conduit geometry and magma viscosity. If magma viscosity and conduit dimensions are constant, the magma discharge rate will decline exponentially with time as pressure and volume in the chamber decline (e.g., Stasiuk et al., 1993). Deviations from this simple model will occur with (1) the growth of a lava dome, which can increase the column weight; (2) formation of chilled margins, which can reduce conduit width; (3) elastic deformation of the dike itself; (4) viscous dissipation at the flow margins where shear rates are high; and (5) variations of magma composition, temperature, and gas content, which can change viscosity.

Important feedbacks develop during magma ascent because of the competing effects of buoyancy (vesiculation and gas loss), viscosity (which changes with volatile loss and crystal formation), and wall friction. Such feedbacks may explain, for example, three different time scales of episodic behavior that have been identified at Soufriere Hills volcano, Montserrat (e.g., Costa et al., 2006; Wadge et al., 2008). The shortest time scale of several hours to a few days is recorded in deformation and seismic data, and in patterns of dome extrusion and Vulcanian explosions (e.g., Voight et al., 1999). This time scale has been explained by (1) gas pressure cycles that generate either stick-slip dome extrusion or destruction of an impermeable magma plug when overpressure exceeds a threshold (e.g., Wylie et al., 1999; Druitt et al., 2002b), or (2) crystallization coupled with rheological changes (Melnik and Sparks, 1999, 2005). Intermediate time scales are marked by 6–7 wk cycles of earthquakes, tilt, and eruptive activity that may be explained by opening and closing of dikes because of pressure fluctuations (Roman et al., 2006). The longest time scale is represented by 2–3 yr alternating periods of dome growth and quiescence. Long-time-scale behavior can be explained if the magma chamber and conduit act like capacitors, that is, if they store energy because of elastic deformation of the wall rocks and then discharge magma episodically when the pressure exceeds some threshold. The time scale for this process reflects the elastic relaxation of the chamber, with longer periods being the consequence of larger chamber volumes (Barmin et al., 2002). Periodic behavior may occur when magma viscosity increases during magma ascent (because of devolatilization ± crystallization) given an appropriate input flux and input/output viscosity ratio (e.g., Melnik et al., 2008; Fig. 10A). Magma rheology, particularly yield strength, will affect the overpressure threshold that must be exceeded for magma ascent (Fig. 10B).

The reference case described here includes numerous simplifications. For example, in the reference case, the magma chamber pressure changes only with volume, whereas chamber pressure may actually depend on other variables such the presence of bubbles and crystals or the influx of new magma. Bubbles can have a profound effect because gas is highly compressible; for this reason, bubble-bearing magma can sustain much higher chamber pressures during eruption, and therefore erupt much more magma, than a chamber without bubbles (Huppert and Woods, 2002). For this reason, the rise and accumulation of exsolved gas at the top of a magma chamber (a consequence of crystallization of volatile-saturated magma) can generate large pressure increases (Tait et al., 1989), as can influx of new magma.

Gas Behavior during Magma Ascent

Once mobilized, magma ascends because of volatile exsolution; ascent is therefore modulated by conditions of both vesiculation and gas escape, which depend critically on the viscosity of the melt. The low viscosity of basaltic melts allows bubbles to separate from the ascending magma when the rise rate of individual bubbles (the "drift velocity") is rapid relative to the rate of magma ascent (Fig. 11A). As the ratio between drift velocity and ascent velocity increases, the distribution of the gas phase in the liquid changes from distributed bubbles (bubbly flow) to large conduit-filling bubbles (slug flow) to a continuous gas phase concentrated in the center of the conduit (annular flow).

Two-phase flow regimes are well characterized for water-gas systems (e.g., Mudde, 2005). Only recently, however, have volcanologists attempted to scale experiments and develop numerical models to examine two-phase flow

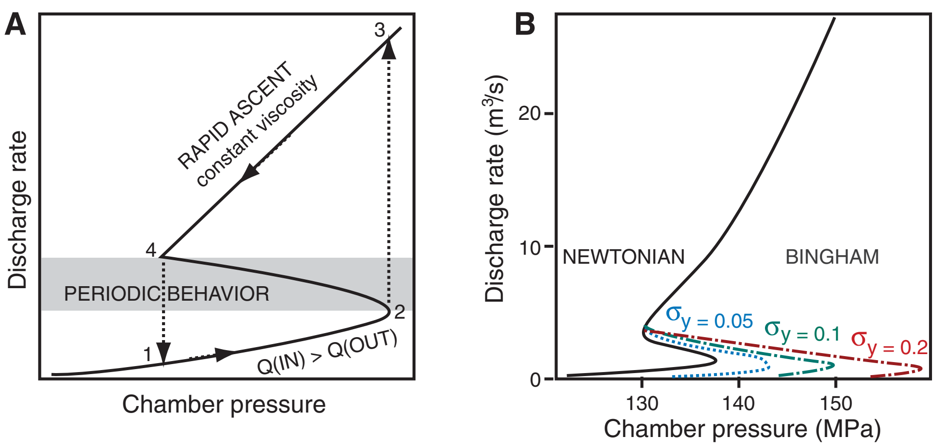

Figure 10. (A) General steady-state solution of feedbacks among magma input, overpressurization, and eruption. When decompression-related changes in magma viscosity are limited, system proceeds as 1–2–3–4; periodic behavior is most likely when magma input lies in gray shaded region. (B) Comparison of steady-state solutions for magmas of Newtonian and Bingham rheology (yield strength σ_y in MPa). Bingham rheology prohibits discharge between eruptions and produces higher chamber pressures prior to renewal of eruptive activity. Figure is modified from Melnik et al. (2008).

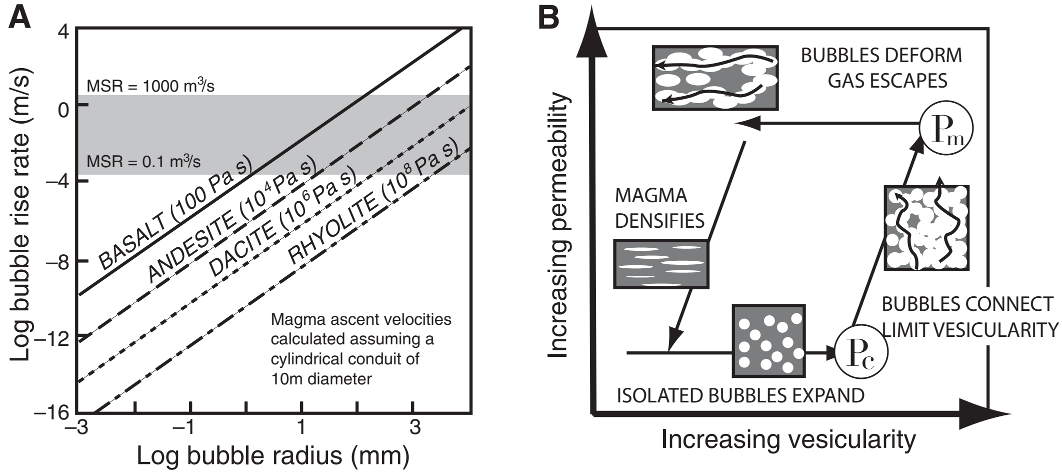

Figure 11. (A) Bubble rise time (drift velocity) as a function of bubble radius and melt viscosity. Shaded area shows magma ascent rates for typical magma supply rates (MSR), calculated assuming a cylindrical conduit of radius = 10 m, and shows that drift velocity is most likely to exceed ascent velocity in low-viscosity (basaltic) magma. (B) Illustration of hysteresis in permeability-porosity data. Initial expansion occurs in isolated bubbles until percolation threshold (P_c) is reached at ~60% vesicularity. Permeability then increases rapidly to a permeability threshold (P_m) that limits further expansion. Deformation of vesicular magma permits gas loss (porosity reduction) without loss of permeability as bubbles deform, until bubble collapse reduces permeability (bubbles again become isolated). Figure is modified from Rust and Cashman (2004).

regimes in viscous fluids and large conduits. When gas is introduced into static liquid columns from below, high-viscosity fluids enhance bubble coalescence by decreasing the drift velocity of individual bubbles, thereby stabilizing slug flow at the expense of bubbly flow (e.g., James et al., 2009; Pioli et al., 2012). Internal vesiculation, the most likely source of distributed bubbles in volcanic systems, has not been studied experimentally from the perspective of two-phase flow regimes. Numerical models suggest that large conduit-filling bubbles may be dynamically unstable during buoyancy-driven ascent (Suckale et al., 2010) and that cyclic patterns of flow developed in two-phase bubbly magmas may explain the strong pulsing of Hawaiian, Strombolian, and violent Strombolian activity (e.g., Manga, 1996; Slezin, 2003). If crystals are present, gas migration may be hindered if bubbles are trapped within the crystal network, or aided by increased bubble coalescence within melt pathways. Either case will affect flow regimes (Belien et al., 2010). Together, these studies suggest that simple two-phase flow interpretations of mafic eruptive activity should be reconsidered.

Bubble rise is sufficiently hindered in viscous magmas that bubbles will remain in the melt from which they formed unless they connect to create permeable networks. Gas escape through a permeable foam may not only allow degassed lavas to form from originally gas-rich magma (Eichelberger et al., 1986), but may also explain sharp transitions between explosive and effusive styles of activity (e.g., Jaupart and Allegre, 1991). Permeability is commonly modeled using percolation theory, which shows that a touching network of spheres (the percolation threshold) will form at volume fractions as low as 30% (Sahimi, 1994). However, evidence from both pumice samples and recent experiments suggests that bubbles in rapidly vesiculating magmas do not always coalesce (become connected) at low vesicularities, and instead attain a connectivity, or percolation, threshold (P_c) at vesicularities of ~60%–70% (Rust and Cashman, 2011). The permeability threshold (P_m) for sufficiently rapid gas escape to prevent continued magma expansion is probably slightly higher than the percolation threshold (Fig. 11B). Available experimental data suggest that the percolation and permeability thresholds may increase with increasing melt viscosity, and decrease with increasing sample crystallinity, although these hypotheses need to be tested by additional experiments.

The high viscosity of silicic melts also promotes bubble deformation (by increasing *Ca*). Evidence for bubble deformation can be found in (1) the prevalence of tube (elongated bubble) pumice in high-intensity silicic eruptions (e.g., Wright et al., 2006); (2) observed bubble flattening; and (3) the common occurrence of pyroclastic obsidian in subplinian eruptions, which probably forms by efficient gas loss along conduit walls (Rust and Cashman, 2007) and may record shear-enhanced permeability development (e.g., Okumura et al., 2009).

Gas escape through the permeable magma leads to some interesting nonlinear dynamics. If bubbles within the magma are sufficiently connected to supply gas to the wall rock, rapid horizontal gas escape can be driven by pressure differences between the magma and low-pressure (wall rock) environments (Jaupart and Allegre, 1991). Gas escape (and collapse of the magma foam) is enhanced when permeability-porosity curves are hysteretic, such that high permeabilities are maintained as bubbles collapse, thereby facilitating gas escape (Fig. 11B). Horizontal gas flow is enhanced at low pressures when fractured wall rocks are at hydrostatic, or atmospheric, pressure. Porosity decrease in the upper parts of the conduit can also occur if vertical gas flow exceeds the ascent rate of host magma (Melnik and Sparks, 1999). In this scenario, hysteretic permeability functions predict rapid formation of compaction waves manifested by alternating regions of high and low porosity (Michaut et al., 2009). Degassing-driven crystallization may further enhance the hysteresis of porosity-permeability relationships in viscous magmas, as shown by the maintenance of high permeabilities to low bulk vesicularities in crystal-rich andesites (Melnik and Sparks, 2002).

Controls on Fragmentation

If gas is retained within magma rather than lost to wall rocks or the atmosphere, then ascending magma will erupt explosively. Rapid vesiculation (and expansion) under closed-system conditions accelerates magma to the surface, as illustrated by the popular Mentos® and Diet Coke® experiments (Coffey, 2008). These two processes—expansion and acceleration—form the core of fragmentation theory. In volcanology, "fragmentation" denotes the transition from a melt (± crystals) with included bubbles to a continuous gas phase with suspended droplets or particles (Fig. 12). Fragmentation may be ductile or brittle; in general, fragmentation is ductile in low-viscosity (basaltic) melts and brittle in high-viscosity (silicic) melts.

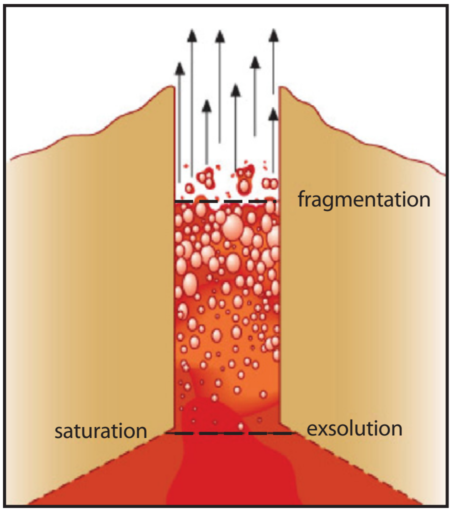

Figure 12. Schematic representation of vesiculation and fragmentation within a volcanic conduit. Saturation level requires saturation with at least one volatile phase; although shown here as top of magma chamber, CO_2-rich magmatic systems may be volatile-saturated throughout the upper-crustal storage region. Exsolution (bubble formation) may occur at any pressure below the saturation level; exsolution pressure depends on vesiculation kinetics. Fragmentation occurs when the exsolved volatile phase reaches one of the criteria discussed in the text.

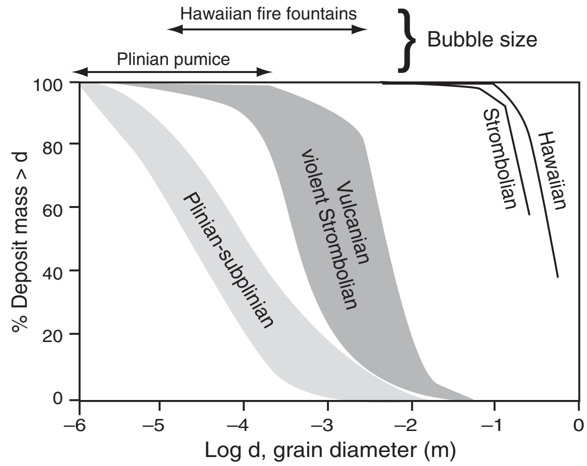

Figure 13. Cumulative total grain-size distributions (TGSDs) for different eruption styles. Steeper curves represent better sorting. Available data suggest a systematic increase in median grain size from Plinian-subplinian to Vulcanian–violent Strombolian to Strombolian-Hawaiian eruption styles, although more data are needed. Also shown is range of bubble sizes observed in individual pyroclasts from Plinian and Hawaiian eruptions. Overlap in bubble size distributions (BSDs) and TGSDs for Plinian eruptions suggests a direct relationship between vesiculation kinetics and fragmentation. Figure is modified from Rust and Cashman (2011).

Ductile fragmentation results from instabilities in the accelerating liquid phase (e.g., Mader et al., 1994; Mangan and Cashman, 1996). Evidence for fragmentation in the fluid, rather than solid, state comes from the fluidal shape of mafic volcanic bombs and commonly associated pyroclasts such as Pele's tears (droplets) and Pele's hair (finely elongated glass strands). Resultant clasts in Hawaiian eruptions are large—tens of centimeters—and substantially larger than constituent bubbles (Fig. 13). This suggests that bubbles accelerate the magma (through expansion) but do not exert a direct control on the fragmentation process (Rust and Cashman, 2011).

Silicic melts, in contrast, are apparently fragmented by brittle processes. Fragmentation may occur when expanding magma exceeds a critical vesicularity, when volatile phases contained within bubbles attain a critical overpressure, and/or when the expanding melt exceeds a critical strain rate. The vesicularity criterion for silicic Plinian eruptions has variously been placed at 60% (Kaminski and Jaupart, 1997), 64% (Gardner et al., 1996), and 75%–83% (Sparks, 1978; Houghton and Wilson, 1989) based on the observed range of vesicularity in preserved pumice clasts. The lower values derive from minimum preserved vesicularities and assume that higher vesicularities record postfragmentation expansion prior to quenching. The critical overpressure criterion accounts for the pressure difference between a growing bubble and the surrounding melt (Melnik, 2000). The strain rate criterion comes from an observed threshold in deformation properties (from ductile to brittle) at high strain rates (Dingwell and Webb, 1989). These criteria are not mutually exclusive, and all require ascending magma to expand until the point of fragmentation. This, in turn, requires that the volume of gas in the component bubbles increases by decompression (expansion) and volatile exsolution faster than it escapes by permeable flow through pathways of interconnected bubbles (Klug and Cashman, 1996). The small grain size of most silicic tephra deposits, and the uniformity of accompanying pumice textures (bubble size and number density; Fig. 13) suggest that fragmentation in silicic explosive eruptions is controlled primarily by bubble-bubble interactions (Rust and Cashman, 2011).

Fragmentation can also occur in highly viscous magma because of unloading by a downward-propagating decompression wave (Alidibirov and Dingwell, 1996; Fowler et al., 2010). Under these conditions, fragmentation may occur by: (1) propagation of an unloading elastic wave, (2) layer-by-layer bubble bursting in response to a pressure difference between the (pressurized) bubbles and the decompression wave, and (3) rapid gas flow through permeable networks (Alidibirov and Dingwell, 2000). In many situations, these mechanisms may act in concert. Experimental investigations of this process describe a minimum pressure differential (fragmentation threshold) that varies with porosity (permeability; Spieler et al., 2004; Koyaguchi et al., 2008; Mueller et al., 2008) and fragmentation efficiency that is controlled by the applied pressure/decompression rate (Kueppers et al., 2006a).

VOLCANIC ERUPTIONS

Eruption styles, and associated volcanic landforms, were introduced descriptively in the previous sections. In this section, we examine ways in which conditions of magma storage and transport combine to generate some of the observed range in eruptive activity. For simplicity, we separate discussions of explosive and effusive eruptions, and then provide an overview of "transitional" eruptions, which show both explosive and effusive behavior.

Explosive Eruptions

Key observable parameters of witnessed explosive eruptions are the plume height (used to infer eruption intensity, or mass eruption rate), the duration of eruptive activity, and the final volume, areal distribution, internal structure, and grain-size characteristics of pyroclastic deposits. Here, we briefly review advances in understanding the dynamics of volcanic plumes and their relationship to the pyroclastic deposits that they produce.

Volcanic Plumes

Volcanic plumes form when fragmented magma and associated gases are ejected into the atmosphere. For ascending hydrous magmas, the pressure at the fragmentation level may be several MPa. At these pressures, the melt retains a substantial amount of water that may be released in the plume, or within density currents. Fragmentation, in turn, decreases the bulk viscosity of mixture by up to 14 orders of magnitude; the change in both bulk viscosity and bulk density causes the gas-particle mixture to accelerate to very high speeds (typically hundreds of meters per second) and to discharge into the atmosphere as a momentum-dominated jet. The exit conditions of the flow can be divided into three cases that are controlled by the flow velocity and vent shape: (1) The flow is able to adjust the atmospheric pressure at the exit; (2) the vent is sufficiently narrow that the mixture exits at above atmosphere pressure (choked flow) and adjusts to ambient pressure in the atmosphere; (3) the mixture reaches supersonic speeds through a diverging vent. The topic of such flows is a complex area of geological fluid mechanics that is far from completely understood (for more details, see Sparks et al., 1997; Ogden et al., 2008; Bercovici and Michaut, 2010).

Once the mixture emerges as a jet into the atmosphere, interaction with the air generates high eruption plumes and/or pyroclastic density currents. The former produce tephra fallout, and the latter form various kinds of pyroclastic surges and flows (and associated ash fall), which are the most destructive and hazardous kinds of volcanic phenomena. In both cases, the fundamental process of interaction is turbulent air entrainment into the high-speed erupting mixture; this has two major consequences. First, entrainment of air decelerates the ascending mixture by momentum transfer (the entrained air has to be accelerated). Second, the entrained air is heated, and the mixture density reduces as the plume rises. As erupting mixtures are almost always denser than air, they typically have enough initial kinetic energy to rise only hundreds of meters to a few kilometers into the atmosphere. Thus, formation of the towering convecting eruption columns commonly seen in Plinian eruptions requires air entrainment and heating of the air by the volcanic particles. This process generates potential energy by converting thermal energy in the magma to mechanical energy through buoyancy of the mixture. Typically, thermal energy is more than an order of magnitude greater than the kinetic energy.

Early model treatment of the erupting mixture of gas and entrained material as a homogeneous "pseudogas" led to the development of two end-member scenarios (Woods, 1995): (1) Heating of entrained air makes the mixture less dense than the surrounding atmosphere, and the jet transforms into a buoyant plume to form a high eruption column in the atmosphere; or (2) air entrainment is not sufficient to reduce the density of the erupting mixture below that of the atmosphere, and the flow runs out of kinetic energy and collapses to feed a pyroclastic density current. More recent models relax the assumption of homogeneity and allow larger particles to separate from the plume. These models show that fallout of dense particles as pyroclastic density currents can increase the rise velocity of the convective plume by decreasing its bulk density (e.g., Clarke et al., 2002). Importantly, these models also explain the common observation of simultaneous production of buoyant plumes and pyroclastic density currents.

Volcanic plumes eventually reach a level of neutral buoyancy (H_B) high in the atmosphere, where they spread laterally (the umbrella region). The tendency of rising plumes to overshoot H_B produces maximum plume heights H_T ~$1.4H_B$. The thermal energy flux determines the final plume height and is proportional to the intensity of the eruption (i.e., the flux of magma through the vent in kg/s; Sparks et al., 1997). During Plinian eruptions, mass fluxes of 10^5 to over 10^9 kg/s feed eruption columns that rise to ≤55 km. As a result, lateral flow within umbrella regions combines with high-level winds to distribute tephra-fall deposits over hundreds to millions of square kilometers. In contrast, weaker explosive eruptions generate small to moderate volcanic plumes with heights that are influenced strongly by wind velocity, particularly because of changes in conditions of air entrainment in bent-over plumes (Bursik, 2001). As a consequence, the mass flux required for weak plumes to reach a specific height increases markedly as wind speed increases.

Pyroclastic Fall Deposits

The characteristics of pyroclastic fall deposits can be related to the nature of the eruption plumes that produced them. For this reason, pyroclastic fall deposits are commonly used to assign both magnitude and intensity to prehistoric eruption deposits, information that is critical for volcanic hazard assessment.

Deposit magnitude is measured by changes in deposit thickness (or, ideally, mass) as a function of distance from the vent. Tephra deposits generally thin exponentially away from the source vent and can be used to estimate the total volume (or mass, if corrected for deposit density) of a fall deposit (Pyle, 1989). Log thickness versus distance (measured as √area) plots for Plinian deposits are thus linear, although they commonly show three or four different linear segments because of variations in fall behavior (e.g., Fierstein and Nathenson, 1992; Fig. 14). The fall behavior (terminal velocity) is controlled by the Reynolds number (*Re*), where $Re = \rho_P U d_p/\mu_a$; here ρ_p is the particle density, U is the fall velocity, d_p is the particle diameter, and μ_a is the viscosity of the air. The *Re*, in turn, controls the drag coefficient, which controls the fall velocity. In subaerial fall deposits, particle size variations exert the primary control on particle *Re*. For this reason, the steep proximal segment shown in Figure 14 can be attributed to fall of large particles (high *Re*) from the outer margin of the rising plume, the middle segment to fall of intermediate-size particles (transitional *Re*) from the umbrella region, and the distal segment to deposition of fine particles in a low-*Re* regime (e.g., Bonadonna et al., 1998; Alfano et al., 2011). The volume of the distal segment is the most difficult to quantify accurately, because fine ash layers are poorly preserved and distributed over vast areas of land and ocean. In submarine environments, density becomes a critical parameter in determining conditions of particle deposition (Cashman and Fiske, 1991); the density difference between pumice and seawater will vary greatly depending on whether the pore spaces within pumice are filled with air, steam, or water (Allen et al., 2008).

Eruption intensity (mass eruption rate) can be inferred from derived relationships among grain size, grain density, column height, and depositional characteristics (e.g., Carey and Sparks, 1986; Ernst et al., 1996; Burden et al., 2011). Although simple in principle, large uncertainties are introduced during the collection of field data (e.g., Biass and Bonadonna, 2011). Perhaps more important is characterization of the total grain-size distribution (TGSD), which is critical input for ash dispersion models (Mastin

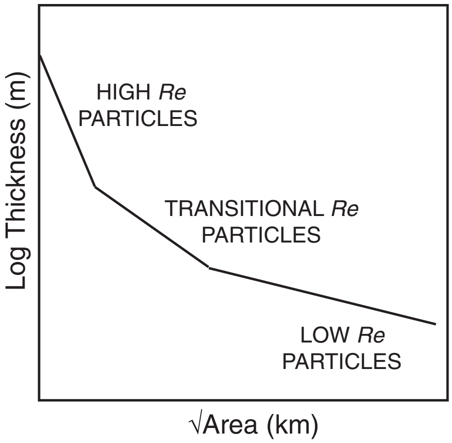

Figure 14. Schematic of deposit thickness as a function of √area covered. Linear segments on a log thickness versus √area plot indicate exponential thinning; individual segments reflect transitions in particle behavior as a function of Reynolds number (see text).

et al., 2009a). TGSDs are notoriously difficult to measure accurately because (1) tephra deposits are widespread, (2) the grain size at a single site often varies up section, thus requiring multiple measurements at individual locations, and (3) fine-grained distal deposits are often poorly preserved and/or limited in accessibility (e.g., deposited within the ocean). For this reason, there are relatively few tephra deposits for which the TGSD is well constrained. A compilation of existing data shows sharp differences among deposits of different types, with Plinian/subplinian deposits typically fine grained and poorly sorted, Vulcanian/violent Strombolian eruptions medium grained and often well sorted (particularly the mafic end members), and Strombolian/Hawaiian deposits coarse grained and well sorted (Fig. 13). Data of this type are critical for developing nominal source input parameters for plume models (e.g., Mastin et al., 2009a).

Pyroclastic Density Currents

Pyroclastic density currents are among the most hazardous of all volcanic phenomena, and yet they are also one of the least understood. Pyroclastic density currents are hot gravity-driven currents that travel at high velocities and inundate (and bury) large areas. They can form by lava dome collapse, by column collapse during Plinian/subplinian eruptions, or accompanying caldera collapse during large-magnitude explosive eruptions. The high velocities, high temperatures, and complex nature of these flows make it impossible to measure either their material properties or their dynamics directly. For this reason, pyroclastic density current studies combine field observations of deposits (ignimbrites) with laboratory experiments and numerical models of flow dynamics.

Detailed studies of individual ignimbrites show that neither the grain size nor the compositional variation of the ignimbrite at any given location can be simply related to the nature of either the eruptive mixture or the parent flow (Wilson, 1985; Branney and Kokelaar, 1992, 2003). Instead, ignimbrites show distinct facies that result from transport and deposition processes. An important factor from a hazards point of view is using the physical attributes of ignimbrites to constrain eruption time scales. For example, in the low-aspect-ratio Taupo ignimbrite, lateral variations in grain-size distribution are similar to vertical variations in a fluidized bed, which suggests that fluidization was critical to flow emplacement and, by extension, that emplacement was rapid and occurred as a discrete event (Wilson, 1985). In contrast, a high-aspect-ratio valley-filling ignimbrite generated by the 1912 eruption of Katmai, Alaska, preserves evidence of multiple discrete flows separated by time breaks of minutes to hours (Fierstein and Wilson, 2005). In the example of the Bishop Tuff, California, a coeval fall deposit has been used to infer an emplacement time of ~90 h for the entire flow-fall sequence (Wilson and Hildreth, 1997).

Field characterization of pyroclastic deposits is often complicated by postemplacement modification of primary ignimbrite textures, particularly those related to welding. Welding refers to the densification (porosity reduction) of pyroclastic flow deposits by a combination of sintering, compaction, and flattening of constituent material. These physical changes reflect the weight of overlying material, the viscosity and porosity of the deposit (controlled by eruption conditions, composition, and temperature), and the time available for deformation (a function of the rates of cooling and gas loss). For the end-member case of no volatile resorption, the degree of compaction is limited by the permeability of the deposit (e.g., Riehle et al., 1995). However, in thick deposits that accumulate rapidly, water vapor can dissolve into glass and facilitate pore-space collapse if pore pressures are sufficiently elevated and permeability is sufficiently low (Sparks et al., 1999). Welding characteristics thus place important constraints on flow emplacement conditions.

From a process perspective, pyroclastic density current deposits can be viewed as either incrementally deposited from the density current (e.g., Branney and Kokelaar, 2003) or deposited rapidly when the flow loses energy (e.g., Wilson, 1985). It is likely that these differences of view reflect the real complexities of these high-temperature multiphase flows. One way to combine these two perspectives is to view pyroclastic density currents as having two components, with overlying dilute turbulent ash-cloud surges and concentrated dense basal flows (e.g., Druitt, 1998). Pyroclastic density currents can then be described as a continuum between these two end members. This conceptual model allows the mass distributed between the two components to vary in space and time, or even to decouple from one another. Such flow transformations (between dilute and dense flows) are often caused by topographic changes and have major hazards implications (e.g., Giordano, 1998; Druitt et al., 2002a). A third component of pyroclastic density currents is the overlying buoyant ash plume that develops in parts of the current that become less dense than the overlying atmosphere (e.g., Calder et al., 1999). Co-flow, or coignimbrite, ash plumes can be generated either continuously during flow or abruptly, if the pyroclastic density current is initially well mixed but suddenly loses mass by deposition and becomes buoyant.

Another important characteristic of many pumiceous pyroclastic flows is their extreme mobility, even on very low slopes (e.g., Druitt, 1998). Recognition of this mobility has led to experimental studies of flow behavior as influenced by fluidization, gas retention, pore-pressure generation, and depositional processes (e.g., Dellino et al., 2010; Roche et al., 2010; Girolami et al., 2010). Fluidization occurs when the weight of a particle is balanced by the vertical drag force exerted by a flowing gas, and is therefore determined by the settling velocity of individual particles (Fig. 15A). A particulate bed expanded by fluidization will collapse when the gas supply is reduced, causing the particles to be deposited (Fig. 15B). When viewed from another perspective, the gas retention (and resultant high pore pressures) within a fluidized flow required for pyroclastic density current mobility will be controlled by time scales for both diffusive outgassing and hindered settling of constituent particles (e.g., Druitt et al., 2007). Also important is the trajectory of particles and gas within the moving flow (e.g., Giordano, 1998).

From a broader perspective, theoretical and experimental studies of multiphase flows show that mixtures of high-temperature solids, liquids, and gases can simultaneously have properties of gas (e.g., compressibility), of solids (through small-scale interactions between particles), and of liquids. Moreover, individual particles can behave like rigid solids or ductile liquids, depending on time scales of deformation. For these reasons, most models use end-member descriptions and treat pyroclastic density currents as either a turbulent suspension (dilute) or a granular flow (dense). Granular flow dynamics, including fluidization by escaping gases, provide a framework for modeling the concentrated parts of pyroclastic density currents (e.g., Titan2D; Patra et al., 2005). Other important factors are interactions with topography that cause the dense basal portion of the flow to decouple from the dilute turbulent cloud (e.g., Andrews and Manga, 2011; Esposti Ongaro et al., 2011). Modeling the dense basal current is critical for predicting maximum runout distances of pyroclastic density currents (Doyle et al., 2008). Limitations of existing models are highlighted by field evidence for a wide range of emplacement temperatures (e.g., McClelland et al., 2004; Gurioli et al., 2005; Lesti et al., 2011), which point to the need to incorporate effects of temperature into existing models. Moreover, although separate models of dilute and dense flow components are useful for understanding individual end members, future models must strive to couple these two different regions to fully describe pyroclastic density current behavior (e.g., Neri et al., 2003).

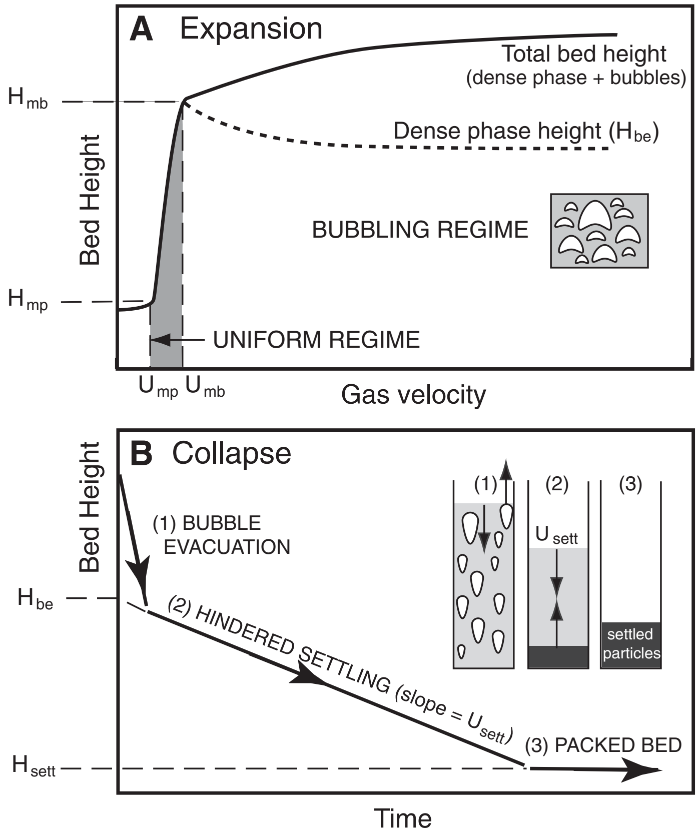

Figure 15. Behavior of fluidized beds. (A) Schematic diagram of the expansion regime, showing the onset of fluidization at U_{mp} (gas velocity that creates maximum pressure drop tolerated by the particle bed) and the onset of the bubbling regime at gas velocity U_{be}. When $U_{mp} < U < U_{be}$, the bed expands uniformly (although the distribution of gas in this regime depends on the particle size, shape, and density distribution). (B) Schematic diagram of the collapse regime, which occurs when the gas flow is reduced. Initially, gas is lost as bubbles rise through the bed. When $H = H_{be}$, all macroscopic bubbles have escaped, and the bed slowly densifies as particles settle. U_{mb} is the gas velocity at which bubbling starts. Figure is modified from Druitt et al. (2007).

Effusive Eruptions

Lava flows form when magma degassing is sufficiently fast relative to the rate of ascent that magma reaches the surface without fragmenting. This may occur by slow ascent of H_2O-rich magma accompanied by gas loss, or more rapid rise of H_2O-poor magma. Alternatively, clastogenic lava flows may form from re-fusion of fragmented material. Individual lava flows may range in volume from a few cubic meters to hundreds (or even a few thousand) cubic kilometers in large flood basalt eruptions. The range of flow emplacement conditions is reflected in the variability of flow morphology, length, thickness, structures, and surface textures. As with explosive eruptions, we consider separately the behavior of mafic and silicic lavas.

Mafic Lava Flows

The two primary laboratories for studies of mafic lava flows over the past two decades have been Hawaii, United States (e.g., Heliker et al., 2003), and Etna, Italy (e.g., Bonaccorso et al., 2004). Both have had frequent (or in the case of Hawaii, continuous) eruptive activity over this time period; as a result, both have contributed extensive observational data sets of lava flow behavior. Moreover, as Hawaii erupts H_2O-poor magma while Etna erupts hydrous magma, comparisons of these two systems allow assessment of the role of water (particularly degassing-induced crystallization) in lava flow emplacement.

In general, Hawaiian lava erupts at near-liquidus temperatures and cools rapidly as it flows. The rates and mechanisms of flow advance are therefore controlled primarily by development of a solid crust on the flow surface (Griffiths, 2000), as well as by cooling-induced crystallization of flow interiors (Cashman et al., 1999). In contrast, lava flows produced by more water-rich magmas, such as those of Mt. Etna, Italy, experience syneruptive crystallization because of volatile loss during magma ascent, and may therefore be highly crystalline on eruption. These flows have higher viscosities, and are shorter and advance more slowly, than Hawaiian lava flows (e.g., Kilburn, 2004). Common to both regions, however, are pahoehoe and ‘a‘ā morphologies, surface textures that reflect both rheological and deformation rate thresholds (Figs. 16A–16C). These morphological differences may also be viewed from the perspective of simple and compound flow forms.

Simple lava flows may have lengths that are limited either by erupted volume or by cooling. When simple flows are cooling-limited, they are generally assumed to have lengths that are proportional to the extrusion rate (Walker et al., 1973; Harris et al., 2007), although this correlation is not always robust for Hawaiian lava flows (e.g., Riker et al., 2009). Also important for hazard assessment is the recognition that higher-effusion-rate flows advance more rapidly than lower-effusion-rate flows (Rowland and Walker, 1990; Kauahikaua et al., 2003), and that flow advance rates diminish with the distance that a flow has traveled. Together, these constraints indicate that lava flow hazards are determined by both initial rates of effusion and proximity to vent regions (e.g., Kauahikaua et al., 2002; Soule et al., 2004).

Another characteristic of simple lava flows is that they form channels by construction of lateral levees. Crystal-rich Etna lavas have a yield strength that promotes channel (and levee) development by inhibiting lateral spreading (Hulme, 1974). In contrast, fluid Hawaiian flows cool rapidly, so that levees develop because spreading is inhibited by solidification at the flow margins (Kerr et al., 2006). An understanding of controls on channel geometries is required for developing fully predictive models of lava flow advance (e.g., Harris and Rowland, 2001). Challenges to modeling include not only the common presence of multiple parallel channels (e.g., Favalli et al., 2010; James et al., 2010) but also the distributary nature of many channelized flows, which split because of topographic barriers and channel overflows produced by temporary increases in lava supply or channel blockages.

Compound lava flows may consist of tens to thousands of individual lava lobes and are most common in large and long-lived tube-fed pahoehoe flow fields, such as the Pu’u ‘Ō’ō-Kūpaianaha flow field that has developed in

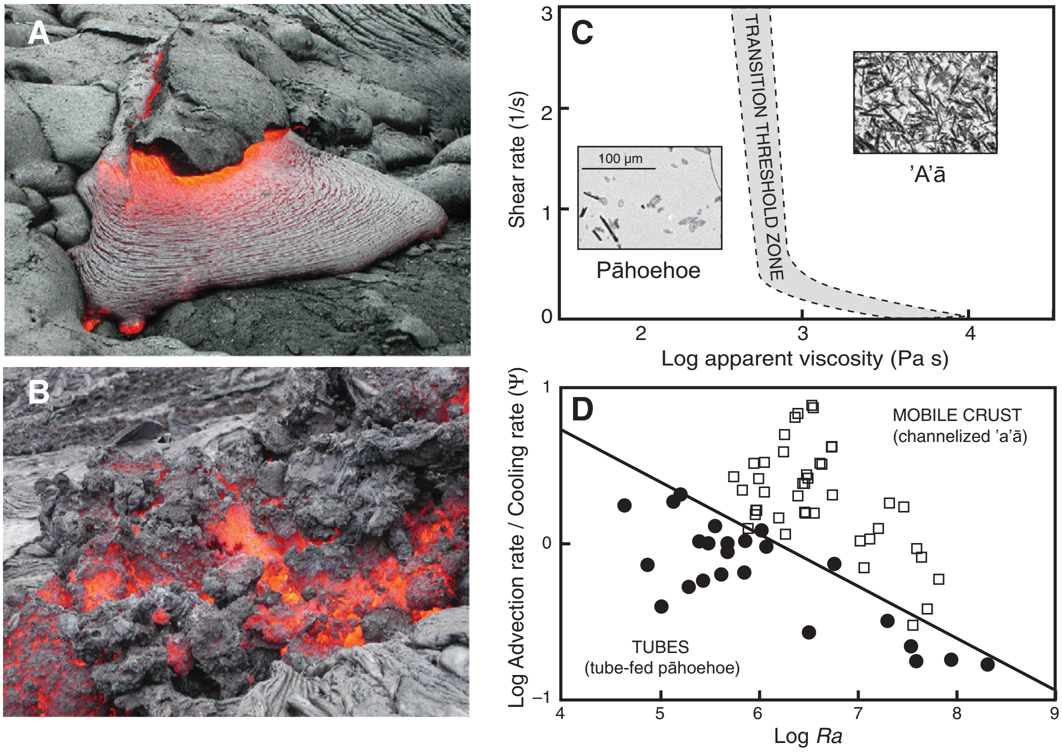

Figure 16. Hawaiian lava flows. (A) Pahoehoe lobe showing rapid cooling, skin formation, and surface deformation during emplacement. (B) ʻAʻā flow with broken crust and exposed lava core. (C) Strain rate–apparent viscosity relationships and estimated transitional threshold zone (TTZ) separating pahoehoe from ʻaʻā (modified from Hon et al., 2003; Soule and Cashman, 2005). Inset photographs are backscattered electron images of quenched pahoehoe and ʻaʻā lavas; dark-gray phase is plagioclase, medium-gray phase is pyroxene, light-gray phase is glass; scale bar is the same for both images. (D) Parameterization from analogue experiments showing threshold in Ψ (advection time scale/cooling time scale)–*Ra* (Rayleigh number measures thermal convection strength) space. Open squares represent experiments in "mobile crust" (open channel) regime; filled circles show experiments in tube regime; line is boundary between regimes (modified from Griffiths et al., 2003).

Hawaii between 1986 and the present (Heliker et al., 2003). Lava tubes form where a solidified roof is created and maintained over a section of the flow (e.g., Peterson et al., 1994; Cashman et al., 2006). Because solidified lava has low thermal conductivity, lava tubes are well insulated and facilitate lava transport over large distances with little cooling (e.g., Helz et al., 1995, 2003; Ho and Cashman, 1997). Two important phenomena in tube-fed compound lavas are flow inflation and lava tube drainage. On low slopes, lava tubes form within spreading sheet flows. The tubes are typically filled with lava, such that continued flow through the tube is accompanied by cooling-induced lava accretion to the tube roof. Under these conditions, maintenance of a constant lava flux through the tubes requires that the flow inflate (Hon et al., 1994). Thus, Hawaiian lava flows with initial heights of only centimeters commonly inflate to several meters during prolonged emplacement. On steeper slopes, lava tubes are not completely filled, and persistent flow in large tubes can lower the tube floor by thermal and mechanical erosion (Kauahikaua et al., 1998; Kerr, 2001). When the lava supply rate diminishes, lava tubes may drain, sometimes creating a series of collapse pits. These features are common in older volcanic landscapes, and have also been recognized on both the Moon and Mars (e.g., Garry and Bleacher, 2011).

A physics-based description of cooling-limited behavior is that the flow has reached a critical Peclet number, which is the ratio of the flow rate to the product of the thermal diffusivity and flow distance (e.g., Pinkerton and Wilson, 1994; Kerr and Lyman, 2007). An extension of this concept shows that flow surface morphology is governed by the balance between flow cooling and flow advection (measured as $\Psi = U_o t_s / H_o$, where U_o is flow velocity, t_s is cooling time, and H_o is flow thickness), and the strength of internal convection within the flow (as measured by the Rayleigh number *Ra*; Fig. 15D). When cooling rates are large relative to flow advance, an insulating surface crust forms to produce lava tubes that feed pāhoehoe flows; when flow advance is rapid, the insulating crust is continually disrupted, the interior lava cools rapidly, and ʻaʻā flows are formed.

The past few decades have seen an explosion of new tools applied to lava flow studies, including global positioning system (GPS), digital topographic data, and satellite-based remote sensing. Appropriate application of these tools requires balancing the spatial and temporal resolution with the areal coverage. Satellite-based thermal images generally have low spatial (1–4 km/pixel) but high temporal resolution, and are therefore used for monitoring entire flow fields (for reviews, see Oppenheimer, 1998; Wright et al., 2004). Satellite-based radar images have the advantages of both seeing through cloud cover and having higher resolution than satellite-based thermal imaging techniques. Radar correlation imaging, in particular, provides image resolution sufficient for monitoring individual lava flows (e.g., Zebker et al., 1996; Dietterich et al., 2012), as well as postemplacement flow volumes (e.g., Stevens et al., 1997; Lu et al., 2003) and cooling-induced subsidence (Stevens et al., 2001). High-resolution thermal imaging data can be obtained using airborne (e.g., Realmuto et al., 1992) and hand-held (e.g., Harris et al., 2005; Ball and Pinkerton, 2006; Spampinato et al., 2011) cameras. Similarly airborne (ALSM) and terrestrial (TLS) laser scanning and ground-based radar provide high-resolution digital topographic data. In all cases, spatial resolution is improved at the expense of the aerial (and often temporal) coverage of satellite-based systems. These data are revolutionizing quantitative analysis of lava flows, as they allow detailed imaging of the thermal and morphological evolution of lava flows that can be related to the dynamics of emplacement (e.g., Harris et al., 2007). Particularly exciting is the advent of multitemporal imaging of active flows (e.g., Favalli et al., 2010; James et al., 2010), which provides detailed information on the development of individual lava flow channels and lobes.

Together, these new measurement capabilities can be used to test proposed models of channel development, lava tube formation, rates of flow advance, and flow conditions within lava channels; they also provide new ways to assess the hazard and risk posed by lava flow inundation.

Viscous Flows and Domes

Well-studied examples of viscous lava flows and domes are provided by recent activity at Mount St. Helens, United States (1980–1986 and 2004–2008; Swanson and Holcomb, 1990; Sherrod et al., 2008), Unzen, Japan (1991–1995; e.g., Nakada and Motomura, 1999), and Soufriere Hills, Montserrat (1995–present; e.g., Voight and Sparks, 2010). In all of these examples, degassing and crystallization during magma ascent cause very large increases in viscosity, and lava dome morphology is controlled by magma ascent rate through the kinetics of the phase changes.

When magma ascent is rapid, volatiles are retained within the melt, and crystallization is limited. In this case, the relatively fluid erupting magma creates either pancake-like domes (e.g., Watts et al., 2002) or obsidian flows. Scaling analysis suggests that eruption rates of ~10–100 m^3/s may be required to produce these flow morphologies (e.g., Lyman et al., 2004). These rates are consistent with strain rates obtained from microlite orientations (Castro et al., 2002) and with recent observations of extrusion rates of 20–100 m^3/s during the first few months of rhyolite lava extrusion during the 2008–2009 eruption of Chaiten volcano, Chile (Carn et al., 2009). The dense and degassed nature of obsidian further requires efficient gas loss via both gas flow through a permeable foam (Eichelberger et al., 1986) and along permeable and fractured conduit walls (e.g., Tuffen et al., 2003; Rust et al., 2004; Cabrera et al., 2011).

When magma ascent is very slow, degassing and crystallization combine to produce magmas with high viscosity and non-Newtonian rheologies. In the extreme, the lava solidifies completely and extrudes as a rigid spine with marginal fault zones (e.g., Cashman et al., 2008; Pallister et al., 2008; Fig. 3D). Thus, a wide spectrum of lava morphologies, from pancake-shaped domes to shear lobes and spines, can be explained simply by variations in effusion rate and resulting changes in bulk rheology (e.g., Nakada and Motomura, 1999; Watts et al., 2002).

Transitional Eruptions

Eruptions may be considered transitional when they include both explosive and effusive activity; transitional activity characterizes eruptions fed by magma supply rates intermediate between those of the explosive and effusive counterparts. Mafic transitional eruptions often show simultaneous Strombolian/violent Strombolian explosions from a central scoria cone and lava effusion from the cone base. A classic example of this type of activity is the 1943–1952 eruption of Paricutin volcano, Mexico (Luhr and Simkin, 1993). Silicic transitional eruptions include alternation between lava dome/plug formation and Vulcanian to subplinian explosions, as seen at Mount St. Helens in 1980 (e.g., Cashman and McConnell, 2005) and at Soufriere Hills, Montserrat in 1996 (e.g., Voight et al., 1999). Although these eruptive patterns do not fit neatly into simple classification schemes, understanding transitions in eruptive behavior is critical for improved hazard assessment during volcanic crises.

Eruptions of low-viscosity mafic magma vary in explosivity with changes in rates of magma ascent. When the magma ascent rate is negligible, rising gas bubbles can coalesce and reach the surface as large bubble bursts, as commonly seen in lava lakes and open vent volcanoes such as Villarica, Chile, Sanguy, Ecuador, and the eponymous Stromboli volcano, Italy. When magma ascent rates are higher, lava flows may emerge from lateral vents (e.g., Ripepe et al., 2005) or initiate simultaneous effusive and explosive activity that characterizes violent Strombolian eruptions (Pioli et al., 2008). At even higher rates of magma ascent, eruptions are subplinian. This progression reflects a decrease in the efficiency of synascent gas segregation (and resulting increase in eruption explosivity and tephra production) with increased rates of magma ascent (Fig. 17).

Intermediate/silicic magmas also have eruptive styles that reflect the rate of magma supply to the vent. In this case, eruptive style changes from Vulcanian to subplinian and finally to sustained Plinian explosive eruptions as the magma supply rate to the vent increases. The change in eruptive style probably reflects the efficiency of both degassing and degassing-induced crystallization relative to the velocity of magma ascent (Cashman, 2004; Mason et al., 2006). Of this spectrum, Vulcanian activity requires the most efficient gas loss from, and densification of, magma residing within shallow conduits (e.g., Fig. 11B). The nature of the resulting plug, and the characteristics of conduit-filling magma between eruptions, can be determined by combining analysis of ejected breadcrust bombs (e.g., Wright et al., 2007) with models that link bomb characteristics to conduit pressure (e.g., Burgisser et al., 2011). Information on the repose interval between events and the volume erupted during each explosion can place important time

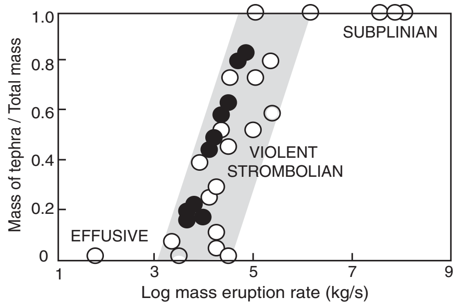

Figure 17. Value of tephra production (mass tephra/ mass$_{[tephra + scoria cone + lava]}$) as a function of mass eruption rate (in kg/s). Filled circles show annual data from the 1943–1952 eruption of Parícutin, Mexico; open circles represent other mafic eruptions. Figure is modified from Pioli et al. (2009).

constraints on the rates of gas loss, densification, and pressure buildup (e.g., Druitt et al., 2002b). Vulcanian activity can trigger subplinian eruptions when the initial downward-propagating decompression wave produced by the Vulcanian event triggers degassing and eruption of gas-rich magma within the conduit. Both Vulcanian and subplinian eruptions are often associated with effusion of lava flows or domes.

Transitional activity at intermediate-composition volcanoes may alternate between Strombolian and Vulcanian explosions depending on the rate of magma supply, which controls the extent of crystallization and, as a result, the composition of the matrix melt (Wright et al., 2012). Examples include ongoing activity at Tungurahua volcano, Ecuador, and Llaima, Chile (http://www.volcano.si.edu). This alternation can be explained by variations in rates of magma ascent, and resulting changes in crystallinity, melt composition, and mode of gas escape (Fig. 11A). Melt composition appears particularly important, as illustrated by a plot of sample crystallinity (phenocryst, microphenocryst, and groundmass) and matrix glass composition (as wt% SiO_2; Fig. 18). This plot shows that the products of volcanoes that exhibit transitional activity are typically crystal-rich, and that the eruptive style (violent Strombolian, Vulcanian, or both) is strongly dependent on the residual melt composition.

Eruptions Involving Water

All of the eruptive behaviors reviewed herein relate to purely magmatic activity, that is, eruptive behavior that is controlled entirely by the physical properties and driving forces of the magma itself. However, rising magma may also encounter either groundwater or surface water/snow/ice

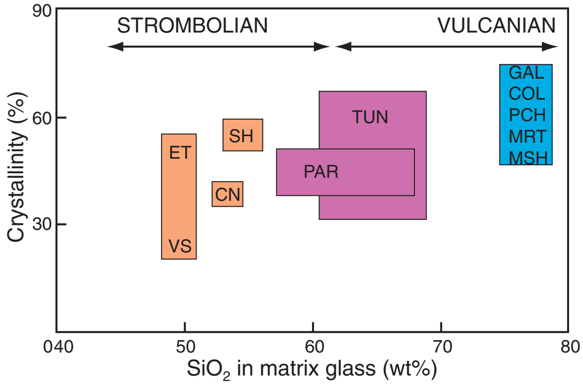

Figure 18. Plot of pyroclast crystallinity (phenocrysts, microphenocrysts, and microlites) as a function of SiO_2 (wt%) in the groundmass glass for products of transitional eruptions; eruptive style is labeled as Strombolian (includes violent Strombolian) and Vulcanian. All eruptive products are highly crystalline; eruption style appears to reflect matrix glass composition (viscosity). Volcanoes that erupt magma with bulk compositions of basaltic andesite to andesite can have different eruptive styles depending on the amount of groundmass crystallization (and resulting evolution of matrix glass). ET—Etna, Italy; VS—Vesuvius, Italy; CN—Cerro Negro, Nicaragua; SH—Shishaldin, United States; PAR—Paricutin, Mexico; TUN—Tungurahua, Ecuador; GAL—Galeras, Colombia; COL—Colima, Mexico; PCH—Pichincha, Ecuador; MRT—Soufriere Hills, Montserrat; MSH—Mount St. Helens, United States. Data are from Santacroce et al. (1993), Calvache and Williams (1997), Roggensack et al. (1997), Cashman and Blundy (2000), Luhr (2001), Stelling et al. (2002), Mora et al. (2002), Harford et al. (2003), Tadduecci et al. (2004), and Wright et al. (2012).

during ascent and eruption. The past few decades have seen numerous advances in field, experimental, and theoretical perspectives on magma-water interactions, as reviewed in Head and Wilson (2003) and White et al. (2003).

In submarine environments, the style of magma-water interaction depends primarily on the height (pressure) of the overlying water column and its effect on vapor formation and expansion (e.g., Kokelaar, 1986; Head and Wilson, 2003). Although the overlying water pressure is unlikely to affect fragmentation of ascending hydrous magmas (which should reach fragmentation conditions well within the conduit), the water column will control the extent to which eruption plumes are suppressed by the weight of the overlying water column. Interaction with seawater can also enhance magmatic fragmentation by rapid quenching.

Observations from many mid-ocean-ridge and ocean-island environments show extensive evidence for fragmentation driven by magmatic gases, including characteristic mafic fluidal pyroclast forms such as Pele's hair (e.g., Davis and Clague, 2006; Clague et al., 2009). In contrast, hydrous mafic magmas that have experienced both degassing and crystallization during ascent appear more susceptible to secondary (quench fragmentation) processes (e.g., Deardorff et al., 2011). Silicic submarine eruptions may be highly explosive, as shown by silicic calderas on the modern seafloor that have produced substantial volumes of highly vesicular pumice deposits (e.g., Fiske et al., 2001; Wright et al., 2003; Tani et al., 2008). Recent review papers on subaqueous eruption-fed density currents (White, 2000), historic submarine pumice eruptions (Kano, 2003), and explosive submarine eruptions (White et al., 2003) discuss eruption and deposition of pumice on the seafloor. A critical factor for understanding pumice deposition is defining conditions under which pumice transforms from being less dense to being more dense than the surrounding seawater (e.g., Cashman and Fiske, 1991; Allen et al., 2008).

Magma-water interactions in subaerial environments include interaction of rising magma with groundwater aquifers, hydrothermal systems, or surface water (including ice and snow). Interaction of magma with external water typically produces abundant fine ash, with the small grain size reflecting the high energy provided by water expansion (e.g., Koyaguchi and Woods, 1996; Mastin, 2007). Introduction of external water may affect the course of magmatic eruptions, as illustrated by the 1875 eruption of Askja volcano, Iceland, where variations in groundwater availability controlled shifts in eruption style (Lupi et al., 2011).

Pyroclasts produced by phreatomagmatic eruptions often have lower vesicularities than pyroclasts from magmatic eruptions, a characteristic that is attributed to premature clast quenching because of water (e.g., Houghton and Wilson, 1989). The angular form of many clasts also points to the importance of quench fragmentation, particularly of rapidly chilled glassy rinds (Mastin et al., 2009b), as does the appearance of quench cracks on particle surfaces (e.g., Büttner et al., 1999; Dellino et al., 2012). Extensive fragmentation requires intimate mixing between magma and water. This is generally most efficient for low-viscosity mafic magmas (e.g., Zimanowski et al., 2003), although recent experiments suggest that shear-induced changes in melt deformation from ductile to brittle may facilitate water interaction in more viscous melts (Austin-Erickson et al., 2011). Both the influence of water on changes in eruption style and the ability of external water to increase the efficiency of magmatic fragmentation are important for evaluating volcanic hazards in regions where there is potential for magma-water interaction, particularly regions of distributed volcanism (such as cinder cone fields). An area of future research is in developing ways to map both the spatial extent of groundwater systems, and the effective permeability of host rocks in active volcanic regions.

CONCLUDING REMARKS

The overview provided here highlights the physical processes responsible for magma ascent, arrest in the upper crust, migration toward Earth's surface, eruption, and emplacement as pyroclastic fall and flow deposits, or as lava flows and domes. Critical factors to most of these processes is the behavior of volatile phases as they exsolve and escape from the transporting magma, the response of the melt phase in terms of phase stability and crystallization, and the resulting changes in rheology. These complex interactions speak to the need for continued advances in our understanding of both physical and chemical aspects of the entire phase space that encompasses mixtures of gases, liquids, and particles. Additionally, because an important goal of volcanological research is improved assessment of the hazards posed by volcanic eruptions and the associated risks to human populations, improved understanding of the underlying processes must be translated to improvements in hazard and risk assessment. For this reason, the past few decades have seen a proliferation of cross-disciplinary research themes and publications related to volcanic activity, including volcano impacts on health (e.g., Hansell and Oppenheimer, 2004; Horwell and Baxter, 2006), culture (e.g., Cashman and Giordano, 2008; Grattan and Torrence, 2010), religion (e.g., Gaillard and Texier, 2010), and societal resilience (e.g., Paton and Johnston, 2006), as well as modeling of ash plumes (e.g., Mastin et al., 2009a) and issues of risk and uncertainty in volcanic hazard assessment (Sparks et al., 2012). Although a thorough review of these themes is outside the scope of this review, we end by placing basic volcanological research within the context of applied research to illustrate the challenges posed by the need for both short- and long-term forecasts of volcanic activity.

The goal of short-term eruption forecasting is to estimate eruption likelihood during periods of obvious volcanic unrest. Challenges relate to the complexity of natural processes and the uncertainties inherent in trying to interpret monitoring signals when the source of those signals lies well below Earth's surface (and is therefore not observable). Forecasting is most accurate when multiple types of monitoring data are available, although detailed predictions of the time, place, and type of eruptive activity are difficult even with accurate data. However, as the number of active volcanoes with good monitoring networks increases, the hope is that patterns of preeruptive activity can be recognized and applied to interpretation of future events. In this regard, there is a push toward developing global databases such as WOVOdata, the World Organization of Volcano Observatories database (http://www.wovodat.org/), and GVM, the Global Volcano Model (http://www.globalvolcanomodel.org/). These databases can be used not only for pattern recognition, but also to provide input for development and testing of predictive models based on eruptive precursors.

Long-term forecasting for the purpose of volcanic hazard and risk assessment requires detailed knowledge of past volcanic activity. Volcanic hazard mapping and risk assessment of individual volcanic centers have evolved considerably over the past 25 yr, aided in large part by the development of new mapping and computer analysis tools (such as geographic information systems [GIS]). Hazard maps now exist for many volcanoes in developed countries, although there is still much work to be done in developing countries (Aspinall et al., 2011). From a global perspective, an important question relates to the frequency of very large eruptions ("supervolcanoes"), that is, eruptions that could threaten global populations. Magnitude-frequency relationships can be assessed using volcano databases, such as that developed by the Global Volcanism Program at the Smithsonian Institution (www.volcano.si.edu/index.cfm). Analysis of this database shows robust magnitude-frequency relationships for Holocene eruptions with a magnitude (M) ≤ 7 according to the Volcano Explosivity Index (Newhall and Self, 1982), which is equivalent to the eruption of ~ 100 km^3 of magma. Larger eruptions lie off the M ≤7 trend, however, which suggests that they are produced by fundamentally different magma accumulation and release mechanisms than smaller eruptions (Deligne et al., 2010). Concern about the potential impacts of a supervolcano eruption continues to spur research in this area.

ACKNOWLEDGMENTS

KVC would like to acknowledge support from the AXA Research Fund; RSJS acknowledges support from the European Research Council. We also thank Guido Giordano and Clive Oppenheimer for helpful feedback on the first draft, and Brendan Murphy for suggesting that we write this paper.

REFERENCES CITED

Acocella, V., 2007, Understanding caldera structure and development: An overview of analogue models compared to natural calderas: Earth-Science Reviews, v. 85, p. 125–160, doi:10.1016/j.earscirev.2007.08.004.

Acocella, V., Cifelli, F., and Funiciello, R., 2000, Analogue models of collapse calderas and resurgent domes: Journal of Volcanology and Geothermal Research, v. 104, p. 81–96, doi:10.1016/S0377-0273(00)00201-8.

Alfano, F., Bonadonna, C., Delmelle, P., and Costantini, L., 2011, Insights on tephra settling velocity from morphological observations: Journal of Volcanology and Geothermal Research, v. 208, p. 86–98, doi:10.1016/j.jvolgeores.2011.09.013.

Alidibirov, M., and Dingwell, D.B., 1996, Magma fragmentation by rapid decompression: Nature, v. 380, p. 146–148, doi:10.1038/380146a0.

Alidibirov, M., and Dingwell, D.B., 2000, Three fragmentation mechanisms for highly viscous magma under rapid decompression: Journal of Volcanology and Geothermal Research, v. 100, p. 413–421, doi:10.1016/S0377-0273(00)00149-9.

Allen, S.R., Fiske, R.S., and Cashman, K.V., 2008, Quenching of steam-charged pumice: Implications for submarine pyroclastic volcanism: Earth and Planetary Science Letters, v. 274, p. 40–49, doi:10.1016/j.epsl.2008.06.050.

Ambrose, S.H., 1998, Late Pleistocene human population bottlenecks, volcanic winter, and differentiation of modern humans: Journal of Human Evolution, v. 34, p. 623–651, doi:10.1006/jhev.1998.0219.

Ambrose, S.H., 2003, Did the super-eruption of Toba cause a human population bottleneck? Reply to Gathorne-Hardy and Harcourt-Smith: Journal of Human Evolution, v. 45, p. 231–237, doi:10.1016/j.jhevol.2003.08.001.

Andrews, B.J., and Manga, M., 2011, Effects of topography on pyroclastic density current runout and formation of coignimbrites: Geology, v. 39, p. 1099–1102, doi:10.1130/G32226.1.

Annen, C., 2009, From plutons to magma chambers: Thermal constraints on the accumulation of eruptible silicic magma in the upper crust: Earth and Planetary Science Letters, v. 284, p. 409–416, doi:10.1016/j.epsl.2009.05.006.

Annen, C., Blundy, J.D., and Sparks, R.S.J., 2006, The genesis of intermediate and silicic magmas in deep crustal hot zones: Journal of Petrology, v. 47, p. 505–539, doi:10.1093/petrology/egi084.

Aspinall, W.P., Auker, M., Hincks, T.K., Mahony, S.H., Pooley, J., Nadim, F., Syre, E., and Sparks, R.S.J., 2011, Volcano Hazard and Exposure in Track II Countries and Risk Mitigation Measures—GFDRR Volcano Risk Study, for The World Bank, NGI Report 20100806.

Atlas, Z.D., Dixon, J.E., Sen, G., Finny, M., and Martin-Del Pozzo, A.L., 2006, Melt inclusions from Volcan Popocatépetl and Volcán de Colima, Mexico: Melt evolution due to vapor-saturated crystallization during ascent: Journal of Volcanology and Geothermal Research, v. 153, p. 221–240, doi:10.1016/j.jvolgeores.2005.06.010.

Austin-Erickson, A., Ort, M.H., and Carrasco-Núñez, G., 2011, Rhyolitic phreatomagmatism explored: Tepexitl tuff ring (Eastern Mexican Volcanic Belt): Journal of Volcanology and Geothermal Research, v. 201, p. 325–341, doi:10.1016/j.jvolgeores.2010.09.007.

Bachmann, O., and Bergantz, G.W., 2006, Gas percolation in upper-crustal silicic crystal mushes as a mechanism for upward heat advection and rejuvenation of near-solidus magma bodies: Journal of Volcanology and Geothermal Research, v. 149, p. 85–102, doi:10.1016/j.jvolgeores.2005.06.002.

Bacon, C.R., 1983, Eruptive history of Mount Mazama and Crater Lake caldera, Cascade Range, U.S.A.: Journal of Volcanology and Geothermal Research, v. 18, p. 57–115, doi:10.1016/0377-0273(83)90004-5.

Bacon, C.R., Gardner, J.V., Mayer, L.A., Buktenica, M.W., Dartnell, P., Ramsey, D.W., and Robinson, J.E., 2002, Morphology, volcanism, and mass wasting in Crater Lake, Oregon: Geological Society of America Bulletin, v. 114, p. 675–692, doi:10.1130/0016-7606(2002)114<0675:MVAMWI>2.0.CO;2.

Ball, M., and Pinkerton, H., 2006, Factors affecting the accuracy of thermal imaging cameras in volcanology: Journal of Geophysical Research, v. 111, B11203, doi:10.1029/2005JB003829.

Barmin, A., Melnik, O., and Sparks, R.S.J., 2002, Periodic behaviour in lava dome eruptions: Earth and Planetary Science Letters, v. 199, p. 173–184, doi:10.1016/S0012-821X(02)00557-5.

Barnett, W.P., and Lorig, L., 2007, A model for stress-controlled pipe growth: Journal of Volcanology and Geothermal Research, v. 159, p. 108–125, doi:10.1016/j.jvolgeores.2006.06.006.

Belien, I.B., Cashman, K.V., and Rempel, A.W., 2010, Gas accumulation in particle-rich suspensions and implications for bubble populations in crystal-rich magma: Earth and Planetary Science Letters, v. 297, p. 133–140, doi:10.1016/j.epsl.2010.06.014.

Bell, A.F., and Kilburn, C.R.J., 2012, Precursors to dyke-fed eruptions at basaltic volcanoes: Insights from patterns of volcano-tectonic seismicity at Kilauea volcano, Hawaii: Bulletin of Volcanology, v. 74, doi:10.1007/s00445-011-0519-3.

Bercovici, D., and Michaut, C., 2010, Two phase dynamics of volcanic eruptions, compaction, compression and the conditions for choking: Geophysical Journal International, v. 182, p. 843–864, doi:10.1111/j.1365-246X.2010.04674.x.

Berlo, K., Blundy, J., Turner, S., Cashman, K., Hawkesworth, C., and Black, S., 2004, Geochemical precursors to volcanic activity at Mount St. Helens, USA: Science, v. 306, p. 1167–1169, doi:10.1126/science.1103869.

Biass, S., and Bonadonna, C., 2011, A quantitative uncertainty assessment of eruptive parameters derived from tephra deposits: The example of two large eruptions of Cotopaxi volcano, Ecuador: Bulletin of Volcanology, v. 73, p. 73–90, doi:10.1007/s00445-010-0404-5.

Bice, D.C., 1985, Quaternary volcanic stratigraphy of Managua, Nicaragua: Correlation and source assignment for multiple overlapping Plinian deposits: Geological Society of America Bulletin, v. 96, no. 4, p. 553–566, doi:10.1130/0016-7606(1985)96<553:QVSOMN>2.0.CO;2.

Biggs, J., Anthony, E.Y., and Ebinger, C.J., 2009, Multiple inflation and deflation events at Kenyan volcanoes, East African Rift: Geology, v. 37, p. 979–982, doi:10.1130/G30133A.1.

Blundy, J., and Cashman, K., 2001, Ascent-driven crystallisation of dacite magmas at Mount St. Helens, 1980–1986: Contributions to Mineralogy and Petrology, v. 140, p. 631–650, doi:10.1007/s004100000219.

Blundy, J., and Cashman, K., 2008, Petrologic reconstruction of magmatic system variables and processes: Reviews in Mineralogy and Geochemistry, v. 69, p. 179–239, doi:10.2138/rmg.2008.69.6.

Blundy, J., Cashman, K.V., and Berlo, K., 2008, Evolving Magma Storage Conditions beneath Mount St. Helens Inferred from Chemical Variations in Melt Inclusions from the 1980–1986 and Current (2004–2006) Eruptions, *in* Sherrod, D.R., Scott, W.E., and Stauffer, P.H., eds., A Volcano Rekindled: The Renewed Eruption of Mount St. Helens, 2004–2006: U.S. Geological Survey Professional Paper 1750, 36 p.

Bonaccorso, A., Calvari, S., Coltelli, M., Del Negro, C., and Falsaperta, S., eds., 2004, Mt. Etna Volcano Laboratory: Geophysical Monograph 143: Washington, D.C., American Geophysical Union, 368 p.

Bonadonna, C., Ernst, G.G.J., and Sparks, R.S.J., 1998, Thickness variations and volume estimates of tephra fall deposits: The importance of particle Reynolds number: Journal of Volcanology and Geothermal Research, v. 81, p. 173–187, doi:10.1016/S0377-0273(98)00007-9.

Branney, M.J., and Kokelaar, P., 1992, A reappraisal of ignimbrite emplacement: Progressive aggradation and changes from particulate to non-particulate flow during emplacement of high-grade ignimbrite: Bulletin of Volcanology, v. 54, p. 504–520, doi:10.1007/BF00301396.

Branney, M.J., and Kokelaar, P., eds., 2003, Pyroclastic Density Currents and the Sedimentation of Ignimbrites: Geological Society of London Memoir 27, 143 p.

Brown, L.D., Zhao, W.J., Nelson, D.K., Hauck, M., Alsdorf, D., and Ross, A., 1996, Bright spots, structure, and magmatism in southern Tibet from INDEPTH seismic reflection profiling: Science, v. 274, p. 1688–1690, doi:10.1126/science.274.5293.1688.

Brown, M., 2007, Crustal melting and melt extraction, ascent and emplacement in orogens: Mechanisms and consequences: Journal of the Geological Society of London, v. 164, p. 709–730, doi:10.1144/0016-76492006-171.

Brown, R.J., Kavanagh, J., Sparks, R.S.J., Tait, M., and Field, M., 2007, Mechanically disrupted and chemically weakened zones in segmented dike systems cause vent localization: Evidence from kimberlite volcanic systems: Geology, v. 35, p. 815–818, doi:10.1130/G23670A.1.

Bruce, P.M., and Huppert, H.E., 1989, Thermal control of basaltic fissure eruptions: Nature, v. 342, p. 665–667, doi:10.1038/342665a0.

Burden, R.E., Phillips, J.C., and Hincks, T.K., 2011, Estimating volcanic plume heights from depositional clast size: Journal of Geophysical Research, v. 116, B11206, doi:10.1029/2011JB008548.

Burgisser, A., Arbaret, L., Druitt, T.H., and Giachetti, T., 2011, Pre-explosive conduit conditions of the 1997 Vulcanian explosions at Soufrière Hills Volcano, Montserrat: II. Overpressure and depth distributions: Journal of Volcanology and Geothermal Research, v. 199, p. 193–205, doi:10.1016/j.jvolgeores.2010.11.014.

Bursik, M., 2001, The effect of wind on the rise height of volcanic plumes: Geophysical Research Letters, v. 28, p. 3621, doi:10.1029/2001GL013393.

Büttner, R., Dellino, P., and Zimanowski, B., 1999, Identifying magma-water interaction from the surface features of ash particles: Nature, v. 401, p. 688–690, doi:10.1038/44364.

Cabrera, A., Weinberg, R.F., Wright, H.M.N., Zlotnik, S., and Cas, R.A.F., 2011, Melt fracturing and healing: A mechanism for degassing and origin of silicic obsidian: Geology, v. 39, p. 67–70, doi:10.1130/G31355.1.

Calder, E.S., Cole, P.D., Dade, W.B., Druitt, T.H., Hoblitt, R.P., Huppert, H.E., Ritchie, L., Sparks, R.S.J., and Young, S.R., 1999, Mobility of pyroclastic flows and surges at the Soufriere Hills volcano, Montserrat: Geophysical Research Letters, v. 26, p. 537–540, doi:10.1029/1999GL900051.

Calvache, M.L., and Williams, S.N., 1997, Emplacement and petrological evolution of the andesitic dome of Galeras volcano, 1990–1992: Journal of Volcanology and Geothermal Research, v. 77, p. 57–69, doi:10.1016/S0377-0273(96)00086-8.

Calvari, S., Inguggiato, S., Puglisi, G., Ripepe, M., and Rosi, M., eds., 2008, The Stromboli Volcano: An integrated study of the 2002–2003 eruption: Geophysical Monograph 182: Washington, D.C., American Geophysical Union, doi:10.1029/GM182, 399 p.

Caress, D.W., Clague, D.A., Paduan, J.B., Martin, J.F., Dreyer, B.M., Chadwick, W.W., Denny, A., and Kelley, D.S., 2012, Repeat bathymetric surveys at 1-metre resolution of lava flows erupted at Axial Seamount in April 2011: Nature Geoscience, v. 5, p. 483–488, doi:10.1038/ngeo1496.

Carey, S., and Sparks, R.S.J., 1986, Quantitative models of the fallout and dispersal of tephra from volcanic eruption columns: Bulletin of Volcanology, v. 48, p. 109–125, doi:10.1007/BF01046546.

Carn, S.A., Pallister, J.S., Lara, L., Ewert, J.W., Watt, S., Prata, A.J., Thomas, R.J., and Villarosa, G., 2009, The unexpected awakening of Chaiten volcano, Chile: Eos (Transactions, American Geophysical Union), v. 90, no. 24, p. 205, doi:10.1029/2009EO240001.

Cas, R.A.F., and Giordano, G., 2006, Explosive mafic volcanism—Preface: Journal of Volcanology and Geothermal Research, v. 155, p. vi, doi:10.1016/j.jvolgeores.2006.02.003.

Cashman, K., and Blundy, J., 2000, Degassing and crystallization of ascending andesite: Philosophical Transactions of the Royal Society of London, v. 358, p. 1487–1513, doi:10.1098/rsta.2000.0600.

Cashman, K., and Cas, R., 2011, Introduction to the special issue of *Bulletin of Volcanology*, "The Cerro Galan ignimbrite and caldera: Characteristics and origins of a very large volume ignimbrite and its magma system": Bulletin of Volcanology, v. 73, no. 10, p. 1425–1426, doi:10.1007/s00445-011-0559-8.

Cashman, K.V., 1992, Groundmass crystallization of Mount St. Helens dacite, 1980–1986—A tool for interpreting shallow magmatic processes: Contributions to Mineralogy and Petrology, v. 109, p. 431–449, doi:10.1007/BF00306547.

Cashman, K.V., 2004, Volatile controls on magma ascent and eruption, *in* Sparks, R.S.J., and Hawkesworth, C.J., The State of the Planet: Frontiers and Challenges in Geophysics: Geophysical Monograph 150: Washington, D.C., American Geophysical Union, p. 109–124, doi:10.1029/150GM10.

Cashman, K.V., and Fiske, R.S., 1991, Fallout of pyroclastic debris from submarine volcanic eruptions: Science, v. 253, p. 275–280, doi:10.1126/science.253.5017.275.

Cashman, K.V., and Giordano, G., 2008, Volcanoes and human history: Journal of Volcanology and Geothermal Research, v. 176, p. 325–329, doi:10.1016/j.jvolgeores.2008.01.036.

Cashman, K.V., and McConnell, S., 2005, Transitions from explosive to effusive activity—The summer 1980 eruptions of Mount St. Helens: Bulletin of Volcanology, v. 68, p. 57–75, doi:10.1007/s00445-005-0422-x.

Cashman, K.V., Thornber, C.R., and Kauahikaua, J.P., 1999, Cooling and crystallization of lava in open channels, and the transition of pahoehoe lava to ʻaʻā: Bulletin of Volcanology, v. 61, p. 306–323, doi:10.1007/s004450050299.

Cashman, K.V., Kerr, R.C., and Griffiths, R.W., 2006, A laboratory model of surface crust formation and disruption on channelized lava flows: Bulletin of Volcanology, v. 68, p. 753–770, doi:10.1007/s00445-005-0048-z.

Cashman, K.V., Thornber, C.R., and Pallister, J.S., 2008, From Dome to Crystallization and Fragmentation of Conduit Magma during the 2004–2006 Dome Extrusion of Mount St. Helens, *in* Sherrod, D.R., Scott, W.E., and Stauffer, P.H., eds., A Volcano Rekindled: The Renewed Eruption of Mount St. Helens, 2004–2006: U.S. Geological Survey Professional Paper 1750, p. 387–413.

Castro, J.M., Manga, M., and Cashman, K.V., 2002, Dynamics of obsidian flows inferred from microstructures: Insights from microlite preferred orientations: Earth and Planetary Science Letters, v. 199, p. 211–226, doi:10.1016/S0012-821X(02)00559-9.

Castruccio, A., Rust, A., and Sparks, R.S.J., 2010, Rheology and flow of crystal-rich bearing lavas: Insights from analogue gravity currents: Earth and Planetary Science Letters, v. 297, p. 471–480, doi:10.1016/j.epsl.2010.06.051.

Chadwick, W.W., Jr., Cashman, K.V., Embley, R.W., Matsumoto, H., Dziak, R.P., de Ronde, C.E.J., Lau, T.K., Deardorff, N.D., and Merle, S.G., 2008, Direct video and hydrophone observations of submarine explosive eruptions at NW Rota-1 volcano, Mariana arc: Journal of Geophysical Research, v. 113, B08S10, doi:10.1029/2007JB005215.

Chadwick, W.W., Jr., Nooner, S.L., Butterfield, D.A., and Lilley, M.D., 2012, Seafloor deformation and forecasts of the April 2011 eruption at Axial Seamount: Nature Geoscience, v. 5, p. 474–477, doi:10.1038/ngeo1464.

Chaput, J.A., Zandomeneghi, D., and Aster, R.C., 2012, Imaging of Erebus volcano using body wave seismic interferometry of Strombolian eruption coda: Geophysical Research Letters, v. 39, L07304, doi:10.1029/2012GL050956.

Charlier, B.L.A., Wilson, C.J.N., Lowenstern, J.B., Blake, S., Van Calsteren, P., and Davidson, J.P., 2005, Magma generation at a large hyperactive silicic volcano (Taupo, New Zealand) revealed by U-Th and U-Pb systematics in zircons: Journal of Petrology, v. 46, p. 3–32, doi:10.1093/petrology/egh060.

Cimarelli, C., Costa, A., Mueller, S., and Mader, H.M., 2011, Rheology of magmas with bimodal crystal size and shape distributions: Insights from analog experiments: Geochemistry, Geophysics, Geosystems, v. 12, Q07024, doi:10.1029/2011GC003606.

Clague, D.A., Paduan, J.B., and Davis, A.S., 2009, Widespread Strombolian eruptions of mid-ocean ridge basalt: Journal of Volcanology and Geothermal Research, v. 180, p. 171–188, doi:10.1016/j.jvolgeores.2008.08.007.

Clarke, A.B., Voight, B., Neri, A., and Macedonio, G., 2002, Transient dynamics of Vulcanian explosions and column collapse: Nature, v. 415, p. 897–901, doi:10.1038/415897a.

Coffey, T.S., 2008, Diet Coke and Mentos: What is really behind this physical reaction?: American Journal of Physics, v. 76, p. 551–557, doi:10.1119/1.2888546.

Coltelli, M., Del Carlo, P., and Vezzoli, L., 1998, The discovery of a Plinian basaltic eruption of Roman age at Etna volcano, Italy: Geology, v. 26, p. 1095–1098, doi:10.1130/0091-7613(1998)026<1095:DOAPBE>2.3.CO;2.

Condomines, M., Gauthier, P.-J., and Sigmarsson, O., 2003, Timescales of magma chamber processes and dating of young volcanic rocks: Reviews in Mineralogy and Geochemistry, v. 52, p. 125–174, doi:10.2113/0520125.

Cooper, K.M., and Reid, M.R., 2008, Uranium-series crystal ages: Reviews in Mineralogy and Geochemistry, v. 69, p. 479–544, doi:10.2138/rmg.2008.69.13.

Costa, A., Melnik, O., Sparks, R.S.J., and Voight, B., 2006, The control of magma flow in dykes on cyclic lava dome extrusion: Geophysical Research Letters, v. 34, L02303, doi:10.1029/2006GL027466.

Costa, A., Caricchi, L., and Bagdassarov, N., 2009, A model for the rheology of particle-bearing suspensions and partially molten rocks: Geochemistry, Geophysics, Geosystems, v. 10, 13 p. doi:10.1029/2008GC002138.

Costa, F., and Morgan, D., 2010, Time constraints from chemical equilibration in magmatic crystals, *in* Dosseto, A., Turner, S., and Van-Orman, J., eds., Timescales of Magmatic Processes: Chichester, UK, John Wiley & Sons, Ltd., p. 125–159.

Costantini, L., Houghton, B.F., and Bonadonna, C., 2010, Constraints on eruption dynamics of basaltic explosive activity derived from chemical and microtextural study: The example of the Fontana Lapilli Plinian eruption, Nicaragua: Journal of Volcanology and Geothermal Research, v. 189, p. 207–224, doi:10.1016/j.jvolgeores.2009.11.008.

Couch, S., Sparks, R.S.J., and Carroll, M.R., 2001, Mineral disequilibrium in lavas explained by convective self-mixing in open magma chambers: Nature, v. 411, p. 1037–1039, doi:10.1038/35082540.

Daniels, K., Kavanagh, J., Menand, T., and Sparks, R.S.J., 2012, The shapes of dykes: Evidence for the influence of cooling and inelastic deformation: Geological Society of America Bulletin, v. 124, p. 1102–1112, doi:10.1130/B30537.1.

Davis, A., and Clague, D., 2006, Volcaniclastic deposits from the North Arch volcanic field, Hawaii: Explosive fragmentation of alkalic lava at abyssal depths: Bulletin of Volcanology, v. 68, p. 294–307, doi:10.1007/s00445-005-0008-7.

Deardorff, N.D., Cashman, K.V., and Chadwick, W.W., Jr., 2011, Observations of eruptive plume dynamics and pyroclastic deposits from submarine explosive eruptions at NW Rota-1, Mariana arc: Journal of Volcanology and Geothermal Research, v. 202, p. 47–59, doi:10.1016/j.jvolgeores.2011.01.003.

Deligne, N.I., Coles, S.G., and Sparks, R.S.J., 2010, Recurrence rates of large explosive volcanic eruptions: Journal of Geophysical Research, v. 115, B06203, doi:10.1016/j.jvolgeores.2008.01.036.

Dellino, P., Dioguardi, F., Zimanowski, B., Buttner, R., Mele, D., La Volpe, L., Sulpizio, R., Doronzo, D.M., Sonder, I., Bonasia, R., Calvari, S., and Marotta, E., 2010, Conduit flow experiments help constrain the regime of explosive eruptions: Journal of Geophysical Research, v. 115, no. B4, B04204, doi:10.1029/2009JB006781.

Dellino, P., Gudmundsson, M.T., Larsen, G., Mele, D., Stevenson, J.A., Thordarson, T., and Zimanowski, B., 2012, Ash from the Eyjafjallajökull eruption (Iceland): Fragmentation processes and aerodynamic behavior: Journal of Geophysical Research, v. 117, B00C04, doi:10.1029/2011JB008726.

De Silva, S., Zandt, G., Trumbull, R., Viramonte, J.G., Salas, G., and Jimenez, N., 2006, Large ignimbrite eruptions and volcano-tectonic depressions in the Central Andes: A thermomechanical perspective, *in* Troise, C., De Natale, G., and Kilburn, C.R.J., eds., Mechanisms of Activity and Unrest at Large Calderas: Geological Society of London Special Publication 269, p. 47–63.

Dietterich, H.R., Poland, M.P., Schmidt, D.A., Cashman, K.V., Sherrod, D.R., and Espinosa, A.T., 2012, Tracking lava flow emplacement on the east rift zone of Kilauea, Hawai'i, with synthetic aperture radar (SAR) coherence: Geochemistry, Geophysics, Geosystems, v. 13, Q05001, doi:10.1029/2011GC004016.

Dingwell, D.B., 1998, The glass transition in hydrous granitic melts: Physics of the Earth and Planetary Interiors, v. 107, p. 1–8, doi:10.1016/S0031-9201(97)00119-2.

Dingwell, D.B., and Webb, S.L., 1989, Structural relaxation in silicate melts and non-Newtonian melt rheology in geologic processes: Physics and Chemistry of Minerals, v. 16, p. 508–516, doi:10.1007/BF00197020.

Dingwell, D.B., Romano, C., and Hess, K.-U., 1996, The effect of water on the viscosity of a haplogranitic melt under *P-T-X* conditions relevant to silicic volcanism: Contributions to Mineralogy and Petrology, v. 124, p. 19–28, doi:10.1007/s004100050170.

Di Stefano, R., and Chiarabba, C., 2002, Active source tomography at Mt. Vesuvius: Constraints for the magmatic system: Journal of Geophysical Research, v. 107, no. B11, p. 2278, doi:10.1029/2001JB000792.

Doyle, E.E., Hogg, A.J., Mader, H.M., and Sparks, R.S.J., 2008, Modeling dense pyroclastic basal flows from collapsing columns: Geophysical Research Letters, v. 35, L04305, doi:10.1029/2007GL032585.

Druitt, T.H., 1992, Emplacement of the 18 May 1980 lateral blast deposit ENE of Mount St. Helens, Washington: Bulletin of Volcanology, v. 54, p. 554–572, doi:10.1007/BF00569940.

Druitt, T.H., 1998, Pyroclastic density currents, *in* Gilbert, J.S., and Sparks, R.S.J., eds., The Physics of Explosive Volcanic Eruptions: Geological Society of London Special Publication 145, p. 145–182, doi:10.1144/GSL.SP.1996.145.01.08.

Druitt, T.H., Mellors, R.A., Pyle, D.M., and Sparks, R.S.J., 1989, Explosive volcanism on Santorini, Greece: Geological Magazine, v. 126, p. 95–126, doi:10.1017/S0016756800006270.

Druitt, T.H., Calder, E.S., Cole, P.D., Hoblitt, R.P., Loughlin, S.C., Norton, G.E., Ritchie, L.J., Sparks, R.S.J., and Voight, B., 2002a, Small-volume, highly mobile pyroclastic flows formed by rapid sedimentation from pyroclastic surges at Soufrière Hills volcano, Montserrat: An important volcanic hazard: Geological Society of London Memoir 21, p. 263–279.

Druitt, T.H., Young, S.R., Baptie, B., Bonadonna, C., Calder, E.S., Clarke, A.B., Cole, P.D., Harford, C.L., Herd, R.A., Luckett, R., Ryan, G., and Voight, B., 2002b, Episodes of cyclic Vulcanian explosive activity with fountain collapse at Soufrière Hills volcano, Montserrat, *in* Druitt, T.H., and Kokellar, B.P., eds., The Eruption of Soufriere Hills Volcano, Montserrat from 1995 to 1999: Geological Society of London Memoir 21, p. 281–306.

Druitt, T.H., Avard, G., Bruni, G., Lettieri, P., and Maez, F., 2007, Gas retention in fine-grained pyroclastic flow materials at high temperatures: Bulletin of Volcanology, v. 69, no. 8, p. 881–901, doi:10.1007/s00445-007-0116-7.

Druitt, T.H., Costa, F., Deloule, E., Dungan, M., and Scaillet, B., 2012, Decadal to monthly timescales of magma transfer and reservoir growth at a caldera volcano: Nature, v. 482, p. 77–80, doi:10.1038/nature10706.

Dziak, R.P., Haxel, J.H., Bohnenstiehl, D.R., Chadwick, W.W., Nooner, S.L., Fowler, M.J., Matsumoto, H., and Butterfield, D.A., 2012, Seismic precursors and magma ascent before the April 2011 eruption at Axial Seamount: Nature Geoscience, v. 5, p. 478–482, doi:10.1038/ngeo1490.

Eichelberger, J.C., Carrigan, C.R., Westrich, H.R., and Price, R.H., 1986, Non-explosive silicic volcanism: Nature, v. 323, p. 598–602, doi:10.1038/323598a0.

Eichelberger, J.C., Chertkoff, D.G., Dreher, S.T., and Nye, C.J., 2000, Magmas in collision: Rethinking chemical zonation in silicic magmas: Geology, v. 28, p. 603–606, doi:10.1130/0091-7613(2000)28<603:MICRCZ>2.0.CO;2.

Embley, R.W., and 16 others, 2006, Long-term eruptive activity at a submarine arc volcano: Nature, v. 441, p. 494–497, doi:10.1038/nature04762.

Ernst, G.G.J., Sparks, R.S.J., Carey, S.N., and Burisk, M.I., 1996, Sedimentation from turbulent jets and plumes: Journal of Geophysical Research, v. 101, no. B3, p. 5575–5589, doi:10.1029/95JB01900.

Favalli, M., Fornaciai, A., Mazzarini, F., Harris, A., Neri, M., Behncke, B., Pareschi, M.T., Tarquini, S., and Boschi, E., 2010, Evolution of an active lava flow field using a multitemporal LIDAR acquisition: Journal of Geophysical Research, v. 115, B11203, doi:10.1029/2010JB007463.

Fedele, F.G., Giaccio, B., and Hajdas, I., 2008, Timescales and cultural process at 40,000 yrs. BP in the light of the Campanian Ignimbrite eruption, western Eurasia: Journal of Human Evolution, v. 55, no. 5, p. 834–857, doi:10.1016/j.jhevol.2008.08.012.

Fialko, Y., 2001, On origin of near-axis volcanism and faulting at fast spreading mid-ocean ridges: Earth and Planetary Science Letters, v. 190, p. 31–39, doi:10.1016/S0012-821X(01)00376-4.

Fierstein, J., and Nathenson, M., 1992, Another look at the calculation of fallout tephra volumes: Bulletin of Volcanology, v. 54, p. 156–167, doi:10.1007/BF00278005.

Fierstein, J., and Wilson, C.J.N., 2005, Assembling an ignimbrite: Compositionally defined eruptive packages in the 1912 Valley of Ten Thousand Smokes ignimbrite, Alaska: Geological Society of America Bulletin, v. 117, p. 1094–1107, doi:10.1130/B25621.1.

Fiske, R.S., Naka, J., Iizasa, K., Yuasa, M., and Klaus, A., 2001, Submarine silicic caldera at the front of the Izu-Bonin Arc, Japan: Voluminous seafloor eruptions of rhyolite pumice: Geological Society of America Bulletin, v. 113, p. 813–824, doi:10.1130/0016-7606(2001)113<0813:SSCATF>2.0.CO;2.

Fiske, R.S., Rose, T.R., Swanson, D.A., Champion, D.E., and McGeehin, J.P., 2009, Kulanaokuaiki Tephra (ca. A.D. 400–1000): Newly recognized evidence for highly explosive eruptions at Kīlauea volcano, Hawai'i: Geological Society of America Bulletin, v. 121, p. 712–728, doi:10.1130/B26327.1.

Fournier, T.J., Pritchard, M.E., and Riddick, S.N., 2010, Duration, magnitude, and frequency of subaerial volcano deformation events: New results from Latin America using InSAR and a global synthesis: Geochemistry, Geophysics, Geosystems, v. 11, no. 1, p. Q01003, doi:10.1029/2009GC002558.

Fowler, A.C., Scheu, B., Lee, W.T., and McGuinness, M.J., 2010, A theoretical model of the explosive fragmentation of vesicular magma: Proceedings of the Royal Society A: Mathematical, Physical and Engineering Science, v. 466, p. 731–752.

Fox, C.G., Chadwick, W.W., and Embley, R.W., 2001, Direct observation of a submarine volcanic eruption from a seafloor instrument caught in a lava flow: Nature, v. 412, p. 727–729, doi:10.1038/35089066.

Francis, P., Glaze, L., and Oppenheimer, C., 1990, Eruption terms: Nature, v. 346, p. 519, doi:10.1038/346519a0.

Frey, H., and Lange, R., 2011, Phenocryst complexity in andesites and dacites from the Tequila volcanic field, Mexico: Resolving the effects of degassing vs. magma mixing: Contributions to Mineralogy and Petrology, v. 162, p. 415–445, doi:10.1007/s00410-010-0604-1.

Funiciello, R., and Giordano, G., eds., 2010, The Colli Albani Volcano: Special Publications of International Association of Volcanology and Chemistry of the Earth's Interior, Volume 3: London, Geological Society of London, 276 p.

Gaillard, J.C., and Texier, P., 2010, Religions, natural hazards, and disasters: An introduction: Religion, v. 40, p. 81–84, doi:10.1016/j.religion.2009.12.001.

Gardner, J.E., Thomas, R.M.E., Jaupart, C., and Tait, S., 1996, Fragmentation of magma during Plinian volcanic eruptions: Bulletin of Volcanology, v. 58, p. 144–162, doi:10.1007/s004450050132

Gardner, J.E., Hilton, M., and Carroll, M.R., 1999, Experimental constraints on degassing of magma: Isothermal bubble growth during continuous decompression from high pressure: Earth and Planetary Science Letters, v. 168, p. 201–218, doi:10.1016/S0012-821X(99)00051-5.

Garry, W.B., and Bleacher, J.E., eds., 2011, Analogs for Planetary Exploration: Geological Society of America Special Paper 483, 567 p.

Geschwind, C.-H., and Rutherford, M.J., 1995, Crystallization of microlites during magma ascent: The fluid mechanics of 1980–1986 eruptions at Mount St Helens: Bulletin of Volcanology, v. 57, p. 356–370.

Giordano, D., and Dingwell, D.B., 2003, Non-Arrhenian muticomponent melt viscosity: Earth and Planetary Science Letters, v. 208, p. 337–349.

Giordano, D., Russell, J.K., and Dingwell, D.B., 2008, Viscosity of magmatic liquids: A model: Earth and Planetary Science Letters, v. 271, p. 123–134, doi:10.1016/j.epsl.2008.03.038.

Giordano, G., 1998, The effect of paleotopography on lithic distribution and facies associations of small volume ignimbrites: The WTT Cupa (Roccamonfina volcano, Italy): Journal of Volcanology and Geothermal Research, v. 87, no. 1–4, p. 255–273, doi:10.1016/S0377-0273(98)00096-1.

Girolami, L., Roche, O., Druitt, T.H., and Corpetti, T., 2010, Particle velocity fields and depositional processes in laboratory ash flows, with implications for the sedimentation of dense pyroclastic flows: Bulletin of Volcanology, v. 72, p. 747–759, doi:10.1007/s00445-010-0356-9.

Gonnermann, H., and Manga, M., 2003, Explosive volcanism may not be an inevitable consequence of magma fragmentation: Nature, v. 426, p. 432–435, doi:10.1038/nature02138.

Grattan, J., and Torrence, R., 2010, Living Under the Shadow: Cultural Impacts of Volcanic Eruptions: Walnut Creek, California, Left Coast Press, 320 p.

Gravley, D.M., Wilson, C.J.N., Leonard, G.S., and Cole, P.W., 2007, Double trouble: Paired ignimbrite eruptions and collateral subsidence in the Taupo volcanic zone, New Zealand: Geological Society of America Bulletin, v. 119, p. 18–30, doi:10.1130/B25924.1.

Griffiths, R.W., 2000, The dynamics of lava flows: Annual Review of Fluid Mechanics, v. 32, p. 477–518, doi:10.1146/annurev.fluid.32.1.477.

Griffiths, R.W., Kerr, R.C., and Cashman, K.V., 2003, Patterns of solidification in channel flows with surface cooling: Journal of Fluid Mechanics, v. 496, p. 33–62, doi:10.1017/S0022112003006517.

Gudmundsson, A., 1987, Lateral magma flow, caldera collapse, and a mechanism of large eruptions in Iceland: Journal of Volcanology and Geothermal Research, v. 34, p. 65–78, doi:10.1016/0377-0273(87)90093-X.

Gudmundsson, A., 1988, Formation of collapse calderas: Geology, v. 16, p. 808–810, doi:10.1130/0091-7613(1988)016<0808:FOCC>2.3.CO;2.

Gurioli, L., Houghton, B.F., Cashman, K.V., and Cioni, R., 2005, Complex changes in eruption dynamics during the 79 AD eruption of Vesuvius: Bulletin of Volcanology, v. 67, p. 144–159, doi:10.1007/s00445-004-0368-4.

Hamada, M., Laporte, D., Cluzel, N., Koga, K., and Kawamoto, T., 2010, Simulating bubble number density of rhyolitic pumices from Plinian eruptions: Constraints from fast decompression experiments: Bulletin of Volcanology, v. 72, p. 735–746, doi:10.1007/s00445-010-0353-z.

Hammer, J.E., 2008, Experimental studies of the kinetics and energetics of magma crystallization: Reviews in Mineralogy and Geochemistry, v. 69, p. 9–59, doi:10.2138/rmg.2008.69.2.

Hammer, J.E., and Rutherford, M.J., 2002, An experimental study of the kinetics of decompression-induced crystallization in silicic melt: Journal of Geophysical Research, v. 107, 2021, doi:10.1029/2001JB000281.

Hammer, J.E., and Rutherford, M.J., 2003, Petrologic indicators of pre-eruption magma dynamics: Geology, v. 31, p. 79–82, doi:10.1130/0091-7613(2003)031<0079:PIOPMD>2.0.CO;2.

Hammer, J.E., Cashman, K.V., and Voight, B., 2000, Magmatic processes revealed by textural and compositional trends in Merapi dome lavas: Journal of Volcanology and Geothermal Research, v. 100, p. 165–192, doi:10.1016/S0377-0273(00)00136-0.

Hansell, A., and Oppenheimer, C., 2004, Health hazards from volcanic gases: A systematic literature review: Archives of Environmental Health: An International Journal (Toronto, Ontario), v. 59, p. 628–639.

Harford, C.L., Sparks, R.S.J., and Fallick, A.E., 2003, Degassing at the Soufrière Hills volcano, Montserrat, recorded in matrix glass compositions: Journal of Petrology, v. 44, p. 1503–1523, doi:10.1093/petrology/44.8.1503.

Harrington, R.M., and Brodsky, E.E., 2007, Volcanic hybrid earthquakes that are brittle-failure events: Geophysical Research Letters, v. 34, L06308, doi:10.1029/2006GL028714.

Harris, A., and Ripepe, M., 2007, Synergy of multiple geophysical approaches to unravel explosive eruption conduit and source dynamics—A case study from Stromboli: Chemie der Erde–Geochemistry, v. 67, p. 1–35.

Harris, A., and Rowland, S.R., 2001, FLOWGO: A kinematic thermo-rheological model for lava flowing in a channel: Bulletin of Volcanology, v. 63, p. 20–44, doi:10.1007/s004450000120.

Harris, A., Dehn, J., Patrick, M., Calvari, S., Ripepe, M., and Lodato, L., 2005, Lava effusion rates from hand-held thermal infrared imagery: An example from the June 2003 effusive activity at Stromboli: Bulletin of Volcanology, v. 68, p. 107–117, doi:10.1007/s00445-005-0425-7.

Harris, A., Dehn, J., and Calvari, S., 2007, Lava effusion rate definition and measurement: A review: Bulletin of Volcanology, v. 70, p. 1–22, doi:10.1007/s00445-007-0120-y.

Hawkesworth, C., George, R., Turner, S., and Zellmer, G., 2004, Time scales of magmatic processes: Earth and Planetary Science Letters, v. 218, p. 1–16, doi:10.1016/S0012-821X(03)00634-4.

Head, J.W., III, and Wilson, L., 2003, Deep submarine pyroclastic eruptions: Theory and predicted landforms and deposits: Journal of Volcanology and Geothermal Research, v. 121, p. 155–193, doi:10.1016/S0377-0273(02)00425-0.

Heliker, C.C., Swanson, D.A., and Takahashi, T.J., eds., 2003, The Puʻu ʻŌʻō-Kūpaianaha Eruption of Kīlauea Volcano, Hawaiʻi: The First 20 Years: U.S. Geological Survey Professional Paper 1676, 215 p.

Helz, R.T., Banks, N.G., Heliker, C., Neal, C.A., and Wolfe, E.W., 1995, Comparative geothermometry of recent Hawaiian eruptions: Journal of Geophysical Research, v. 100, p. 17,637–17,657, doi:10.1029/95JB01309.

Helz, R.T., Heliker, C., Hon, K., and Mangan, M., 2003, Thermal efficiency of lava tubes in the Puʻu ʻŌʻō-Kūpaianaha eruption, *in* Heliker, C.C., Swanson, D.A., and Takahashi, T.J., eds., The Puʻu ʻŌʻō-Kūpaianaha Eruption of Kīlauea Volcano, Hawaiʻi: The First 20 Years: U.S. Geological Survey Professional Paper 1676, p. 105–120.

Hildreth, W.S., 2006, Volcanological perspectives on Long Valley, Mammoth Mountains, and Mono Craters: Several contiguous but discrete systems: Journal of Volcanology and Geothermal Research, v. 13, p. 169–198.

Ho, A.M., and Cashman, K.V., 1997, Temperature constraints on the Ginkgo Flow of the Columbia River Basalt Group: Geology, v. 25, p. 403–406, doi:10.1130/0091-7613(1997)025<0403:TCOTGF>2.3.CO;2.

Hoblitt, R.P., 2000, Was the 18 May 1980 lateral blast at Mt. St. Helens the product of two explosions?: Philosophical Transactions of the Royal Society of London, ser. A, v. 358, p. 1639–1661, doi:10.1098/rsta.2000.0608.

Holness, M.B., and Humphreys, M.C.S., 2003, The Traigh Bhàn na Sgùrra Sill, Isle of Mull: Flow localization in a major magma conduit: Journal of Petrology, v. 44, p. 1961–1976, doi:10.1093/petrology/egg066.

Hon, K., Kauahikaua, J., Denlinger, R., and Mackay, K., 1994, Emplacement and inflation of pahoehoe sheet flows: Observations and measurements of active lava flows on Kilauea volcano, Hawaii: Geological Society of America Bulletin, v. 106, p. 351–370, doi:10.1130/0016-7606(1994)106<0351:EAIOPS>2.3.CO;2.

Hon, K., Gansecki, C., and Kauahikaua, J.P., 2003, The transition from ʻaʻā to pāhoehoe crust on flows emplaced during the Puʻu ʻŌʻō-Kūpaianaha eruption, *in* Heliker, C.C., Swanson, D.A., and Takahashi, T.J., eds., The Puʻu ʻŌʻō-Kūpaianaha Eruption of Kīlauea Volcano, Hawaiʻi: U.S. Geological Survey Professional Paper 1676, p. 89–104.

Horwell, C., and Baxter, P., 2006, The respiratory health hazards of volcanic ash: A review for volcanic risk mitigation: Bulletin of Volcanology, v. 69, p. 1–24, doi:10.1007/s00445-006-0052-y.

Houghton, B.F., and Wilson, C.J.N., 1989, A vesicularity index for pyroclastic deposits: Bulletin of Volcanology, v. 51, no. 6, p. 451–462, doi:10.1007/BF01078811.

Hulme, G., 1974, The interpretation of lava flow morphology: Geophysical Journal of the Royal Astronomical Society, v. 39, p. 361–383, doi:10.1111/j.1365-246X.1974.tb05460.x.

Humphreys, M., Blundy, J.D., and Sparks, R.S.J., 2006, Magma evolution and open-system processes at Shiveluch volcano; insights from phenocryst zoning: Journal of Petrology, v. 47, p. 2303–2334, doi:10.1093/petrology/egl045.

Huppert, H.E., and Woods, A.W., 2002, The role of volatiles in magma chamber dynamics: Nature, v. 420, p. 493–495, doi:10.1038/nature01211.

Hurwitz, S., and Navon, O., 1994, Bubble nucleation in rhyolitic melts: Experiments at high pressure, temperature, and water content: Earth and Planetary Science Letters, v. 122, p. 267–280, doi:10.1016/0012-821X(94)90001-9.

Iizasa, K., Fiske, R.S., Ishizuka, O., Yuasa, M., Hashimoto, J., Ishibashi, J., Naka, J., Horii, Y., Fujiwara, Y., Imai, A., and Koyama, S., 1999, A Kuroko-type polymetallic sulfide deposit in a submarine silicic caldera: Science, v. 283, p. 975–977.

James, M., Lane, S.J., Wilson, L., and Corder, S.D., 2009, Degassing at low magma-viscosity volcanoes: Quantifying the transition between passive bubble-burst and Strombolian eruption: Journal of Volcanology and Geothermal Research, v. 180, p. 81–88, doi:10.1016/j.jvolgeores.2008.09.002.

James, M., Pinkerton, H., and Ripepe, M., 2010, Imaging short period variations in lava flux: Bulletin of Volcanology, v. 72, p. 671–676, doi:10.1007/s00445-010-0354-y.

Jaupart, C., and Allegre, C.J., 1991, Gas content, eruption rate and instabilities of eruption regime in silicic volcanoes: Earth and Planetary Science Letters, v. 102, p. 413–429, doi:10.1016/0012-821X(91)90032-D.

Jellinek, A.M., and DePaolo, D.J., 2003, A model for the origin of large silicic magma chambers: Precursors of caldera-forming eruptions: Bulletin of Volcanology, v. 65, p. 363–381, doi:10.1007/s00445-003-0277-y.

Kaminski, E., and Jaupart, C., 1997, Expansion and quenching of vesicular magma fragments in Plinian eruptions: Journal of Geophysical Research, v. 102, p. 12,187–12,203, doi:10.1029/97JB00622.

Kano, K., 2003, Subaqueous pumice eruptions and their products, *in* White, J.D.L., Smellie, J.L., and Clague, D.A., eds., Explosive Subaqueous Volcanism: Geophysical Monograph 140: Washington, D.C., American Geophysical Union, p. 213–229, doi:10.1029/140GM14.

Katz, M.G., and Cashman, K.V., 2003, Hawaiian lava flows in the third dimension: identification and interpretation of pahoehoe and ʻaʻa distribution in the KP-1 and SOH-4 cores: Geochemistry, Geophysics, Geosystems, v. 4, no. 2, p. 8705, doi:10.1029/2001GC000209.

Kauahikaua, J., Mangan, M., Heliker, C., and Mattox, T., 1996, A quantitative look at the demise of a basaltic vent: The death of Kūpaianaha, Kilauea volcano, Hawaiʻi: Bulletin of Volcanology, v. 57, no. 8, p. 641–648, doi:10.1007/s004450050117.

Kauahikaua, J., Cashman, K.V., Mattox, T.N., Heliker, C.C., Hon, K.A., Mangan, M.T., and Thornber, C.R., 1998, Observations on basaltic lava streams in tubes from Kilauea volcano, Island of Hawaiʻi: Journal of Geophysical Research, v. 103, p. 27303–27323, doi:10.1029/97JB03576.

Kauahikaua, J., Cashman, K.V., Clague, D.A., and Champion, D., 2002, Geology of the most recent eruptions of Hualalai volcano, Hawai`i: Bulletin of Volcanology, v. 64, p. 229–253, doi:10.1007/s00445-001-0196-8.

Kauahikaua, J., Sherrod, D.R., Cashman, K.V., Heliker, C., Hon, K., Mattox, T.N., and Johnson, J.A., 2003, Hawaiian Lava-flow dynamics during the Puʻu ʻŌʻō-Kūpaianaha eruption: A tale of two decades, *in* Heliker, C.C., Swanson, D.A., and Takahashi, T.J., eds., 2003, The Puʻu ʻŌʻō-Kūpaianaha Eruption of Kīlauea Volcano, Hawaiʻi: The First 20 Years: U.S. Geological Survey Professional Paper 1676, p. 63–88.

Kavanagh, J.L., and Sparks, R.S.J., 2011, Insights of dyke emplacement mechanics from detailed 3D dyke thickness datasets: Journal of the Geological Society, v. 168, p. 965–978, doi:10.1144/0016-76492010-137.

Kavanagh, J., Menand, T., and Sparks, R.S.J., 2006, An experimental investigation of sill formation and propagation in layered elastic media: Earth and Planetary Science Letters, v. 245, p. 799–813, doi:10.1016/j.epsl.2006.03.025.

Kent, A.J.R., Darr, C., Koleszar, A.M., Salisbury, M.J., and Cooper, K.M., 2010, Preferential eruption of andesitic magmas through recharge filtering: Nature Geoscience, v. 3, p. 631–636, doi:10.1038/ngeo924.

Kerr, R.C., 2001, Thermal erosion by laminar lava flows: Journal of Geophysical Research, v. 106, p. 26,453–26,465.

Kerr, R.C., and Lister, J.R., 1991, The effects of shape on crystal settling and on the rheology of magmas: The Journal of Geology, v. 99, p. 457–467, doi:10.1086/629506.

Kerr, R.C., and Lyman, A.W., 2007, Importance of surface crust strength during the flow of the 1988–1990 andesite lava of Lonquimay volcano, Chile: Journal of Geophysical Research, v. 112, no. B3, B03209, doi:10.1029/2006JB004522.

Kerr, R.C., Griffiths, R.W., and Cashman, K.V., 2006, Formation of channelized lava flows on an unconfined slope: Journal of Geophysical Research, v. 111, B10206, doi:10.1029/2005JB004225.

Kilburn, C.R.J., 2004, Fracturing as a quantitative indicator of lava flow dynamics: Journal of Volcanology and Geothermal Research, v. 132, p. 209–224, doi:10.1016/S0377-0273(03)00346-9.

Klug, C., and Cashman, K.V., 1996, Permeability relationships in vesiculating magmas: Implications for fragmentation: Bulletin of Volcanology, v. 58, p. 87–100, doi:10.1007/s004450050128.

Kokelaar, P., 1986, Magma-water interactions in subaqueous and emergent basaltic volcanism: Bulletin of Volcanology, v. 48, p. 275–289, doi:10.1007/BF01081756.

Koulakov, I., Gordeev, E.I., Dobretsov, N.L., Vernikovsky, V.A., Senyukov, S., and Jakovlev, A., 2011, Feeding volcanoes of the Kluchevskoy group from the results of local earthquake tomography: Geophysical Research Letters, v. 38, p. L09305, doi:10.1029/2011GL046957.

Koyaguchi, T., and Woods, A.W., 1996, On the formation of eruption columns following explosive mixing of magma and surface-water: Journal of Geophysical Research, v. 101, no. B3, p. 5561–5574, doi:10.1029/95JB01687.

Koyaguchi, T., Scheu, B., Mitani, N.K., and Melnik, O., 2008, A fragmentation criterion for highly viscous bubbly magmas estimated from shock tube experiments: Journal of Volcanology and Geothermal Research, v. 178, p. 58–71, doi:10.1016/j.jvolgeores.2008.02.008.

Kueppers, U., Scheu, B., Spieler, O., and Dingwell, D.B., 2006a, Fragmentation efficiency of explosive volcanic eruptions: A study of experimentally generated pyroclasts: Journal of Volcanology and Geothermal Research, v. 153, p. 125–135, doi:10.1016/j.jvolgeores.2005.08.006.

Kueppers, U., Perugini, D., and Dingwell, D.B., 2006b, Explosive energy during volcanic eruptions from fractal analysis of pyroclasts: Earth and Planetary Science Letters, v. 248, p. 800–807, doi:10.1016/j.epsl.2006.06.033.

Lees, J.M., 1992, The magma system of Mount St. Helens: Non-linear high-resolution P-wave tomography: Journal of Volcanology and Geothermal Research, v. 53, p. 103–116, doi:10.1016/0377-0273(92)90077-Q.

Lejeune, A.M., and Richet, P., 1995, Rheology of crystal-bearing silicate melts: An experimental study at high viscosities: Journal of Geophysical Research, v. 100, p. 4215–4229, doi:10.1029/94JB02985.

Lesti, C., Porreca, M., Giordano, G., Mattei, M., Cas, R., Wright, H., Folkes, C., and Viramonte, J., 2011, High-temperature emplacement of the Cerro Galán and Toconquis Group ignimbrites (Puna Plateau, NW Argentina) determined by TRM analyses: Bulletin of Volcanology, v. 73, no. 10, p. 1535–1565, doi:10.1007/s00445-011-0536-2.

Linde, A.T., Agustsson, K., Sacks, I.S., and Stefansson, S., 1993, Mechanism of the 1991 eruption of Hekla from continuous borehole strain monitoring: Nature, v. 365, p. 737–740, doi:10.1038/365737a0.

Lipman, P.W., 1997, Subsidence of ash-flow calderas: Relation to caldera size and magma-chamber geometry: Bulletin of Volcanology, v. 59, p. 198–218, doi:10.1007/s004450050186.
Lipman, P.W., and Mullineaux, D.R., 1981, The 1980 Eruptions of Mount St. Helens: U.S. Geological Survey Professional Paper 1250, 850 p.
Lister, J.R., and Kerr, R.C., 1991, Fluid-mechanical models of crack propagation and their application to magma transport in dykes: Journal of Geophysical Research, v. 96, no. B6, p. 10,049–10,077, doi:10.1029/91JB00600.
Liu, Y., Anderson, A.T., Wilson, C.J.N., Davis, A.M., and Steele, I.M., 2006, Mixing and differentiation in the Oruanui rhyolitic magma, Taupo, New Zealand: Evidence from volatiles and trace elements in melt inclusions: Contributions to Mineralogy and Petrology, v. 151, p. 71–87, doi:10.1007/s00410-005-0046-3.
Llewellin, E., and Manga, M., 2005, Bubble suspension rheology and implications for conduit flow: Journal of Volcanology and Geothermal Research, v. 143, p. 205–217, doi:10.1016/j.jvolgeores.2004.09.018.
Lu, Z., Fielding, E., Patrick, M.R., and Trautwein, C.M., 2003, Estimating lava volume by precision combination of multiple baseline spaceborne and airborne interferometric synthetic aperture radar: The 1997 eruption of Okmok volcano, Alaska: Geoscience and Remote Sensing: IEEE Transactions, v. 41, p. 1428–1436.
Luhr, J., 2001, Glass inclusions and melt volatile contents at Parícutin volcano, Mexico: Contributions to Mineralogy and Petrology, v. 142, p. 261–283, doi:10.1007/s004100100293.
Luhr, J.F., and Simkin, T., 1993, Paricutín: The Volcano Born in a Mexican Cornfield: Phoenix, Arizona, Geoscience Press, Inc., 427 p.
Lupi, M., Geiger, S., Carey, R.J., Thordarson, T., and Houghton, B.F., 2011, A model for syn-eruptive groundwater flow during the phreatoplinian phase of the 28–29 March 1875 Askja volcano eruption, Iceland: Journal of Volcanology and Geothermal Research, v. 203, p. 146–157, doi:10.1016/j.jvolgeores.2011.04.009.
Lyman, A.W., Koenig, E., and Fink, J.H., 2004, Predicting yield strengths and effusion rates of lava domes from morphology and underlying topography: Journal of Volcanology and Geothermal Research, v. 129, p. 125–138, doi:10.1016/S0377-0273(03)00236-1.
Mader, H.M., Zhang, Y., Phillips, J.C., Sparks, R.S.J., Sturtevant, B., and Stolper, E., 1994, Experimental simulations of explosive degassing of magma: Nature, v. 372, p. 85–88, doi:10.1038/372085a0.
Manga, M., 1996, Waves of bubbles in basaltic magmas and lavas: Journal of Geophysical Research, v. 101, p. 17,457–17,465, doi:10.1029/96JB01504.
Mangan, M., and Sisson, T., 2000, Delayed, disequilibrium degassing in rhyolite magma: Decompression experiments and implications for explosive volcanism: Earth and Planetary Science Letters, v. 183, p. 441–455, doi:10.1016/S0012-821X(00)00299-5.
Mangan, M., and Sisson, T., 2005, Evolution of melt-vapor surface tension in silicic volcanic systems: Experiments with hydrous melts: Journal of Geophysical Research, v. 110, B01202, doi:10.1029/2004JB003215.
Mangan, M., Mastin, L., and Sisson, T., 2004, Gas evolution in eruptive conduits: Combining insights from high temperature and pressure decompression experiments with steady-state flow modeling: Journal of Volcanology and Geothermal Research, v. 129, p. 23–36, doi:10.1016/S0377-0273(03)00230-0.
Mangan, M.T., and Cashman, K.V., 1996, The structure of basaltic scoria and reticulite and inferences for vesiculation, foam formation, and fragmentation in lava fountains: Journal of Volcanology and Geothermal Research, v. 73, p. 1–18, doi:10.1016/0377-0273(96)00018-2.
Mason, B.G., Pyle, D.M., and Oppenheimer, C., 2004, The size and frequency of the largest explosive eruptions: Bulletin of Volcanology, v. 66, p. 735–748, doi:10.1007/s00445-004-0355-9.
Mason, R.M., Starostin, A.B., Melnik, O.E., and Sparks, R.S.J., 2006, From Vulcanian explosions to sustained explosive eruptions: The role of diffusive mass transfer in conduit flow dynamics: Journal of Volcanology and Geothermal Research, v. 153, p. 148–165, doi:10.1016/j.jvolgeores.2005.08.011.
Mastin, L.G., 2007, A user-friendly one-dimensional model for wet volcanic plumes: Geochemistry, Geophysics, Geosystems, v. 8, no. 3, Q03014, doi:10.1029/2006GC001455.
Mastin, L.G., and Pollard, D.D., 1988, Surface deformation and shallow dyke intrusion processes at Inyo Craters, Long Valley, California: Journal of Geophysical Research, v. 93, p. 13,221–13,235, doi:10.1029/JB093iB11p13221.
Mastin, L.G., and 16 others, 2009a, A multidisciplinary effort to assign realistic source parameters to models of volcanic ash-cloud transport and dispersion during eruptions: Journal of Volcanology and Geothermal Research, v. 186, p. 10–21, doi:10.1016/j.jvolgeores.2009.01.008.
Mastin, L.G., Spieler, O., and Downey, W.S., 2009b, An experimental study of hydromagmatic fragmentation through energetic, non-explosive magma–water mixing: Journal of Volcanology and Geothermal Research, v. 180, p. 161–170.
Melnik, O., 2000, Dynamics of two-phase conduit flow of high-viscosity gas-saturated magma: Large variations of sustained explosive eruption intensity: Bulletin of Volcanology, v. 62, no. 3, p. 153–170, doi:10.1007/s004450000072.
Melnik, O., and Sparks, R.S.J., 1999, Nonlinear dynamics of lava extrusion: Nature, v. 402, p. 37–41, doi:10.1038/46950.
Melnik, O., and Sparks, R.S.J., 2002, Dynamics of magma ascent and lava extrusion at Soufriere Hills volcano, Montserrat, *in* Druitt, T.H., and Kokelaar, B.P., eds., The Eruption of Soufriere Hills Volcano, Montserrat, from 1995 to 1999: Geological Society of London Memoir 21, p. 153–171.
Melnik, O., and Sparks, R.S.J., 2005, Controls on conduit magma flow dynamics lava-extrusion building eruptions: Journal of Geophysical Research, v. 110, B02209, doi:10.1029/2004JB003183.
Melnik, O., Sparks, R.S.J., Costa, A., and Barmin, A., 2008, Volcanic eruptions: Cyclicity during lava dome growth, *in* Meyers, R.A., ed., Encyclopedia of Complexity and Systems Science: Springer, p. 1–22.
Menand, T., 2011, Physical controls and depth of emplacement of igneous bodies: A review: Tectonophysics, v. 500, p. 11–19, doi:10.1016/j.tecto.2009.10.016.
Métrich, N., and Wallace, P.J., 2008, Volatile abundances in basaltic magmas and their degassing paths tracked by melt inclusions: Reviews in Mineralogy and Geochemistry, v. 69, p. 363–402, doi:10.2138/rmg.2008.69.10.
Michaut, M., Bercovici, D., and Sparks, R.S.J., 2009, Ascent and compaction of gas rich magma and the effects of hysteretic permeability: Earth and Planetary Science Letters, v. 282, p. 258–267, doi:10.1016/j.epsl.2009.03.026.
Mitchell, N., 2012, Submarine volcanism: Hot, cracking rocks deep down: Nature Geoscience, v. 5, p. 444–445, doi:10.1038/ngeo1505.
Mora, J., Macias, J., Saucedo, R., Orlando, A., Manetti, P., and Vaselli, O., 2002, Petrology of the 1998–2000 products of Volcán de Colima, México: Journal of Volcanology and Geothermal Research, v. 117, p. 195–212, doi:10.1016/S0377-0273(02)00244-5.
Moran, S., Malone, S., Qamar, A.I., Thelen, W., Wright, A.K., and Caplan-Auerbach, J., 2008, Seismicity associated with the renewed dome-building eruption of Mount St. Helens, 2004–2005, *in* Sherrod, D.R., Scott, W.E., and Stauffer, P.H., eds., A Volcano Rekindled: The Renewed Eruption of Mount St. Helens, 2004–2006: U.S. Geological Survey Professional Paper 1750, p. 27–60.
Moran, S., Newhall, C., and Roman, D., 2011, Failed magmatic eruptions: Late-stage cessation of magma ascent: Bulletin of Volcanology, v. 73, p. 115–122, doi:10.1007/s00445-010-0444-x.
Mudde, R.F., 2005, Gravity-driven bubbly flows: Annual Review of Fluid Mechanics, v. 37, p. 393–423, doi:10.1146/annurev.fluid.37.061903.175803.
Mueller, S., Scheu, B., Spieler, O., and Dingwell, D., 2008, Permeability control on magma fragmentation: Geology, v. 36, p. 399–402, doi:10.1130/G24605A.1.
Mueller, S., Llewellin, E.W., and Mader, H.M., 2010, The rheology of suspensions of solid particles: Proceedings of the Royal Society A: Mathematical, Physical and Engineering Science, v. 466, p. 1201–1228.
Murphy, M.D., Sparks, R.S.J., Barclay, J., Carroll, M.R., and Brewer, T.S., 2000, Remobilization of andesite magma by intrusion of mafic magma at the Soufriere Hills volcano, Montserrat, West Indies: Journal of Petrology, v. 41, p. 21–42, doi:10.1093/petrology/41.1.21.
Nakada, S., and Motomura, Y., 1999, Petrology of the 1991–1995 eruption at Unzen: Effusion pulsation and groundmass crystallization: Journal of Volcanology and Geothermal Research, v. 89, p. 173–196, doi:10.1016/S0377-0273(98)00131-0.
Nakada, S., Shimizu, H., and Ohta, K., 1999, Overview of the 1990–1995 eruption at Unzen Volcano: Journal of Volcanology and Geothermal Research, v. 89, p. 1–22, doi:10.1016/S0377-0273(98)00118-8.
Neri, A., Esposti Ongaro, T., Macedonio, G., and Gidaspow, D., 2003, Multiparticle simulation of collapsing volcanic columns and pyroclastic flow: Journal of Geophysical Research, v. 108, no. B4, p. 2202, doi:10.1029/2001JB000508.
Neuberg, J.W., Tuffen, H., Collier, H., Green, D., Powell, T., and Dingwell, D.B., 2006, The trigger mechanism of low-frequency earthquakes on Montserrat: Journal of Volcanology and Geothermal Research, v. 153, p. 37–50, doi:10.1016/j.jvolgeores.2005.08.008.
Newhall, C.G., and Dzurisin, D., 1989, Historical unrest at large calderas of the world: Journal of Geology, v. 97, 650 p.
Newhall, C.G., and Punongbayan, R.S., eds., 1996, Fire and Mud—Eruptions and Lahars of Mount Pinatubo, Philippines: Seattle, University of Washington Press, 1126 p.
Newhall, C.G., and Self, S., 1982, The volcanic explosivity index (VEI) An estimate of explosive magnitude for historical volcanism: Journal of Geophysical Research, v. 87, p. 1231–1238, doi:10.1029/JC087iC02p01231.
Newman, S., and Lowenstern, J.B., 2002, VolatileCalc: A silicate melt–H_2O–CO_2 solution model written in Visual Basic for excel: Computers & Geosciences, v. 28, p. 597–604, doi:10.1016/S0098-3004(01)00081-4.
Nooner, S.L., and Chadwick, W.W., Jr., 2009, Volcanic inflation measured in the caldera of Axial Seamount: Implications for magma supply and future eruptions: Geochemistry, Geophysics, Geosystems, v. 10, no. 2, Q02002, doi:10.1029/2008GC002315.
Ofeigsson, B.G., Hooper, A., Sigmundsson, F., Sturkell, E., and Grapenthin, R., 2011, Deep magma storage at Hekla volcano, Iceland, revealed by InSAR time series analysis: Journal of Geophysical Research, v. 116, no. B5, B05401, doi:10.1029/2010JB007576.
Ogden, D., Glatzmeier, G., and Wohletz, K., 2008, Effects of vent overpressure on buoyant eruption columns; implications for plume stability: Earth and Planetary Science Letters, v. 268, p. 283–292, doi:10.1016/j.epsl.2008.01.014.
Okumura, S., and Nakamura, M., et al., 2009, Magma deformation may induce non-explosive volcanism via degassing through bubble networks: Earth and Planetary Science Letters, v. 281, p. 267–274, doi:10.1016/j.epsl.2009.02.036.
Ongaro, T.E., Widiwijayanti, C., Clarke, A.B., Voight, B., and Neri, A., 2011, Multiphase-flow numerical modeling of the 18 May 1980 lateral blast at Mount St. Helens, USA: Geology, v. 39, no. 6, p. 535–538, doi:10.1130/G31865.1.
Oppenheimer, C., 1998, Volcanological applications of meteorological satellites: International Journal of Remote Sensing, v. 19, p. 2829–2864, doi:10.1080/014311698214307.
Oppenheimer, C., 2003, Climatic, environmental and human consequences of the largest known historic eruption: Tambora volcano (Indonesia) 1815: Progress in Physical Geography, v. 27, p. 230–259, doi:10.1191/0309133303pp379ra.
Pal, R., 2003, Rheological behavior of bubble-bearing magmas: Earth and Planetary Science Letters, v. 207, p. 165–179, doi:10.1016/S0012-821X(02)01104-4.
Pallister, J.S., Thornber, C.R., Cashman, K.V., Clynne, M.A., Lowers, H.A., Brownfield, I.K., and Meeker, G.P., 2008, Petrology of the 2004–2006 Mount St. Helens lava dome—Implications for magmatic plumbing, explosivity and eruption triggering, *in* Sherrod, D.R., Scott, W.E., and Stauffer, P.H., eds., A Volcano

Rekindled: The Renewed Eruption of Mount St. Helens, 2004–2006: U.S. Geological Survey Professional Paper 1750, p. 647–702.

Papale, P., Moretti, R., and Barbato, D., 2006, The compositional dependence of the saturation surface of H_2O-CO_2 fluids in silicate melts: Chemical Geology, v. 229, p. 78–95, doi:10.1016/j.chemgeo.2006.01.013.

Paton, D., and Johnston, D.M., 2006, Disaster Resilience: An Integrated Approach: Springfield, Illinois, Charles C. Thomas, 320 p.

Patra, A.K., Bauer, A.C., Nichita, C.C., Pitman, E.B., Sheridan, M.F., Bursik, M., Rupp, B., Webber, A., Stinton, A.J., Namikawa, L.M., and Renschler, C.S., 2005, Parallel adaptive numerical simulation of dry avalanches over natural terrain: Journal of Volcanology and Geothermal Research, v. 139, p. 1–21, doi:10.1016/j.jvolgeores.2004.06.014.

Paulatto, M., Annen, C., Henstock, T.J., Kiddle, E., Minshull, T.A., Sparks, R.S.J., and Voight, B., 2012, Magma chamber properties from integrated seismic tomography and thermal modeling at Montserrat: Geochemistry, Geophysics, Geosystems, v. 13, Q01014, doi:10.1029/2011GC003892.

Pearse, J., and Fialko, Y., 2010, Mechanics of active magmatic intraplating in the Rio Grande Rift near Socorro, New Mexico: Journal of Geophysical Research, v. 115, B07413, doi:10.1029/2009JB006592.

Pérez, W., and Freundt, A., 2006, The youngest highly explosive basaltic eruptions from Masaya caldera (Nicaragua), *in* Rose, W.I., Bluth, G.J.S., Carr, M.J., Ewert, J.W., Patino, L.C., and Vallance, J.W., eds., Volcanic Hazards in Central America: Geological Society of America Special Paper 412, p. 189–207.

Peterson, D.W., Holcomb, R.T., Tilling, R.I., and Christiansen, R.L., 1994, Development of lava tubes in the light of observations at Mauna Ulu, Kilauea volcano, Hawaii: Bulletin of Volcanology, v. 56, p. 343–360.

Pichavant, M., Costa, F., Burgisser, A., Scaillet, B., Martel, C., and Poussineau, S., 2007, Equilibration scales in silicic to intermediate magmas—Implications for experimental studies: Journal of Petrology, v. 48, p. 1955–1972, doi:10.1093/petrology/egm045.

Pinel, V., and Jaupart, C., 2004, Magma storage and horizontal dyke injection beneath a volcanic edifice: Earth and Planetary Science Letters, v. 221, p. 245–262, doi:10.1016/S0012-821X(04)00076-7.

Pinkerton, H., and Wilson, L., 1994, Factors controlling the lengths of channel-fed lava flows: Bulletin of Volcanology, v. 56, p. 108–120.

Pioli, L., Erlund, E., Johnson, E., Cashman, K.V., Wallace, P., Rosi, M., and Delgado Granados, H., 2008, Explosive dynamics of violent Strombolian eruptions: The eruption of Parícutin volcano 1943–1952 (Mexico): Earth and Planetary Science Letters, v. 271, p. 359–368, doi:10.1016/j.epsl.2008.04.026.

Pioli, L., Azzopardi, B.J., and Cashman, K.V., 2009, Controls on the explosivity of scoria cone eruptions: Magma segregation at conduit junctions: Journal of Volcanology and Geothermal Research, v. 186, p. 407–415, doi:10.1016/j.jvolgeores.2009.07.014.

Pioli, L., Bonadonna, C., Azzopardi, B.J., Phillips, J.C., and Ripepe, M., 2012, Experimental constraints on the outgassing dynamics of basaltic magmas: Journal of Geophysical Research, v. 117, B03204, doi:10.1029/2011JB008392.

Pritchard, M.E., and Simons, M., 2004, An InSAR-based survey of volcanic deformation in the central Andes: Geochemistry, Geophysics, Geosystems, v. 5, no. 2, Q02002, doi:10.1029/2003GC000610.

Putirka, K.D., 2008, Thermometers and barometers for volcanic systems: Reviews in Mineralogy and Geochemistry, v. 69, no. 1, p. 61–120, doi:10.2138/rmg.2008.69.3.

Pyle, D.M., 1989, The thickness, volume and grainsize of tephra fall deposits: Bulletin of Volcanology, v. 51, p. 1–15, doi:10.1007/BF01086757.

Realmuto, V.J., Hon, K., Kahle, A.B., Abbott, E.A., and Pieri, D.C., 1992, Multispectral thermal infrared mapping of the 1 October 1988 Kupaianaha flow field, Kilauea volcano, Hawaii: Bulletin of Volcanology, v. 55, p. 33–44, doi:10.1007/BF00301118.

Riddick, S.N., and Schmidt, D.A., 2011, Time-dependent changes in volcanic inflation rate near Three Sisters, Oregon, revealed by InSAR: Geochemistry, Geophysics, Geosystems, v. 12, Q12005, doi:10.1029/2011GC003826.

Riehle, J.R., Miller, T.F., and Bailey, R.A., 1995, Cooling, degassing and compaction of rhyolitic ash flow tuffs: A computational model: Bulletin of Volcanology, v. 57, no. 5, p. 319–336.

Riker, J.M., Cashman, K.V., and Kauahikaua, J.P., 2009, The length of channelized lava flows: Insight from the 1859 eruption of Mauna Loa volcano, Hawaii: Journal of Volcanology and Geothermal Research, v. 183, p. 139–156, doi:10.1016/j.jvolgeores.2009.03.002.

Ripepe, M., Marchetti, E., Ulivieri, G., Harris, A., Dehn, J., Burton, M., Caltabiano, T., and Salerno, G., 2005, Effusive to explosive transition during the 2003 eruption of Stromboli volcano: Geology, v. 33, p. 341–344, doi:10.1130/G21173.1.

Roche, O., Montserrat, S., Nio, Y., and Tamburrino, A., 2010, Pore fluid pressure and internal kinematics of gravitational laboratory air-particle flows: Insights into the emplacement dynamics of pyroclastic flows: Journal of Geophysical Research, v. 115, B09206, doi:10.1029/2009JB007133.

Roggensack, K., Hervig, R.L., McKnight, S.B., and Williams, S.N., 1997, Explosive basaltic volcanism from Cerro Negro volcano: Influence of volatiles on eruptive style: Science, v. 277, p. 1639–1642, doi:10.1126/science.277.5332.1639.

Roman, D.C., and Cashman, K.V., 2006, The origin of volcanotectonic earthquake swarms: Geology, v. 34, p. 457–460, doi:10.1130/G22269.1.

Roman, D.C., Neuberg, J., and Luckett, R.R., 2006, Assessing the likelihood of volcanic eruption through analysis of volcanotectonic earthquake fault-plane solutions: Earth and Planetary Science Letters, v. 248, p. 244–252, doi:10.1016/j.epsl.2006.05.029.

Rowland, S.K., and Walker, G.P.L., 1990, Pahoehoe and aa in Hawaii: Volumetric flow rate controls the lava structure: Bulletin of Volcanology, v. 52, p. 631–641, doi:10.1007/BF00301212.

Rubin, K.H., Soule, S.A., Chadwick, W.W.J., Fornari, D.J., Clague, D.A., Embley, R.W., Baker, E.T., Perfit, M.R., Caress, D.W., and Dziak, R.P., 2012, Volcanic eruptions in the deep sea: Oceanography, v. 25, p. 142–157.

Ruprecht, P., and Cooper, K.M., 2012, Integrating the uranium-series and elemental diffusion geochronometers in mixed magmas from Volcán Quizapu, Central Chile: Journal of Petrology, v. 53, p. 801–840, doi:10.1093/petrology/egs001.

Rust, A.C., and Cashman, K.V., 2004, Permeability and degassing of vesicular silicic magma: Earth and Planetary Science Letters, v. 228, p. 93–107, doi:10.1016/j.epsl.2004.09.025.

Rust, A.C., and Cashman, K.V., 2007, Multiple origins of obsidian pyroclasts and implications for changes in the dynamics of the 1300 B.P. eruption of Newberry volcano, USA: Bulletin of Volcanology, v. 69, p. 825–845, doi:10.1007/s00445-006-0111-4.

Rust, A.C., and Cashman, K.V., 2011, Permeability controls on expansion and size distributions of pyroclasts: Journal of Geophysical Research, v. 116, B11202, doi:10.1029/2011JB008494.

Rust, A.C., and Manga, M., 2002, Bubble shapes and orientations in low Re simple shear flow: Journal of Colloid and Interface Science, v. 249, p. 476–480, doi:10.1006/jcis.2002.8292.

Rust, A.C., Manga, M., and Cashman, K.V., 2003, Determining flow type, shear rate and shear stress in magmas from bubble shapes and orientations: Journal of Volcanology and Geothermal Research, v. 122, no. 1–2, p. 111–132, doi:10.1016/S0377-0273(02)00487-0.

Rust, A.C., Cashman, K.V., and Wallace, P.J., 2004, Magma degassing buffered by vapor flow through brecciated conduit margins: Geology, v. 32, p. 349–352, doi:10.1130/G20388.2

Ryan, M., 1987, Neutral buoyancy and the mechanical evolution of magmatic systems, *in* Mysen, B.O., ed., Magmatic Processes: Physiochemical Principles, A Volume in Honor of Hatten S. Yoder, Jr.: The Geochemical Society, p. 259–288.

Saar, M.O., Manga, M., Cashman, K.V., and Fremouw, S., 2001, Numerical models of the onset of yield strength in crystal-melt suspensions: Earth and Planetary Science Letters, v. 187, p. 367–379, doi:10.1016/S0012-821X(01)00289-8.

Sable, J.E., Houghton, B.F., Del Carlo, P., and Coltelli, M., 2006, Changing conditions of magma ascent and fragmentation during the Etna 122 BC basaltic Plinian eruption: Evidence from clast microtextures: Journal of Volcanology and Geothermal Research, v. 158, p. 333–354, doi:10.1016/j.jvolgeores.2006.07.006.

Sahimi, M., 1994, Applications of Percolation Theory: London, Taylor & Francis, 276 p.

Sakuma, S., Kajiwara, T., Nakada, S., Uto, K., and Shimizu, H., 2008, Drilling and logging results of USDP-4—Penetration into the volcanic conduit of Unzen volcano, Japan: Journal of Volcanology and Geothermal Research, v. 175, no. 1–2, p. 1–12, doi:10.1016/j.jvolgeores.2008.03.039.

Santacroce, R., Bertagnini, A., Civetta, L., Landi, P., and Sbrana, A., 1993, Eruptive dynamics and petrogenetic processes in a very shallow magma reservoir: The 1906 eruption of Vesuvius: Journal of Petrology, v. 34, p. 383–425.

Saunders, K., Blundy, J., Dohmen, R., and Cashman, K., 2012, Linking petrology and seismology at an active volcano: Science, v. 336, p. 1023–1027, doi:10.1126/science.1220066.

Scandone, R., and Malone, S.D., 1985, Magma supply, magma discharge and readjustment of the feeding system of Mount St. Helens during 1980: Journal of Volcanology and Geothermal Research, v. 23, p. 239–262, doi:10.1016/0377-0273(85)90036-8.

Scandone, R., Cashman, K.V., and Malone, S.D., 2007, Magma supply, magma ascent and the style of volcanic eruptions: Earth and Planetary Science Letters, v. 253, p. 513–529, doi:10.1016/j.epsl.2006.11.016.

Scandone, R., Barberi, F., and Rosi, M., 2009, The 2007 eruption of Stromboli: Preface: Journal of Volcanology and Geothermal Research, v. 182, p. 3–4, doi:10.1016/j.jvolgeores.2008.12.019.

Self, S., 1992, Krakatau revisited: The course of events and interpretation of the 1883 eruption: GeoJournal, v. 28, p. 109–121, doi:10.1007/BF00177223.

Sherrod, D.R., Scott, W.E., and Stauffer, P.H., eds., 2008, A Volcano Rekindled; the Renewed Eruption of Mount St. Helens, 2004–2006: U.S. Geological Survey Professional Paper 1750, 856 p. and DVD-ROM, http://pubs.usgs.gov/pp/1750/.

Sigmundsson, F., and 15 others, 2010, Intrusion triggering of the 2010 Eyjafjallajökull explosive eruption: Nature, v. 468, p. 426–430, doi:10.1038/nature09558.

Sigurdsson, H., Houghton, B., Rymer, H., and Stix, J., eds., 2000, Encyclopedia of Volcanoes: New York, Academic Press, 1389 p.

Simkin, T., and Fiske, R.S., 1983, Krakatau 1883: The Volcanic Eruption and its Effects: Washington, D.C., Smithsonian Institution Press.

Singh, S.C., Harding, A.J., Kent, G.M., Sinha, M.C., Combier, V., Bazin, S., Tong, C.H., Pye, J.W., Barton, P.J., Hobbs, R.W., White, R.S., and Orcutt, J.A., 2006, Seismic reflection images of the Moho underlying melt sills at the East Pacific Rise: Nature, v. 442, p. 287–290, doi:10.1038/nature04939.

Slack, P.D., Fox, C.G., and Dziak, R.P., 1999, P wave detection thresholds, Pn velocity estimates, and T wave location uncertainty from oceanic hydrophones: Journal of Geophysical Research, v. 104, no. B6, p. 13,061–13,072, doi:10.1029/1999JB900112.

Slezin, Y.B., 2003, The mechanism of volcanic eruption (steady state approach): Journal of Volcanology and Geothermal Research, v. 122, p. 7–50, doi:10.1016/S0377-0273(02)00464-X.

Smith, V.C., Blundy, J.D., and Arce, J.L., 2009, A temporal record of magma accumulation and evolution beneath Nevado de Toluca, Mexico, preserved in plagioclase phenocrysts: Journal of Petrology, v. 50, p. 405–426, doi:10.1093/petrology/egp005.

Soule, S.A., and Cashman, K.V., 2005, The shear rate dependence of the pahoehoe-to-a'a transition: Analog experiments: Geology, v. 33, p. 361–364, doi:10.1130/G21269.1.

Soule, S.A., Cashman, K.V., and Kauahikaua, J.P., 2004, Examining flow emplacement through the surface

morphology of three rapidly emplaced, solidified lava flows, Kilauea volcano, Hawai'i: Bulletin of Volcanology, v. 66, p. 1–14, doi:10.1007/s00445-003-0291-0.
Spampinato, L., Calvari, S., Oppenheimer, C., and Boschi, E., 2011, Volcano surveillance using infrared cameras: Earth-Science Reviews, v. 106, p. 63–91.
Sparks, R.S.J., 1978, The dynamics of bubble formation and growth in magmas: A review and analysis: Journal of Volcanology and Geothermal Research, v. 3, p. 1–37, doi:10.1016/0377-0273(78)90002-1.
Sparks, R.S.J., 1997, Causes and consequences of pressurisation in lava dome eruptions: Earth and Planetary Science Letters, v. 150, p. 177–189, doi:10.1016/S0012-821X(97)00109-X.
Sparks, R.S.J., and Young, S.R., 2002, The eruption of Soufrière Hills volcano, Montserrat: Overview of scientific results, *in* Druitt, T.H., and Kokelaar, B.P., eds., The Eruption of Soufrière Hills Volcano, Montserrat, from 1995 to 1999: Geological Society of London Memoir 21, p. 45–69.
Sparks, R.S.J., Bursik, M.I., Carey, S.N., Gilbert, J.S., Glaze, L., Sigurdsson, H., and Woods, A.W., 1997, Volcanic Plumes: John Wiley and Sons, 557 p.
Sparks, R.S.J., Tait, S.R., and Yanev, Y., 1999, Dense welding caused by volatile resorption: Journal of the Geological Society of London, v. 156, p. 217–225, doi:10.1144/gsjgs.156.2.0217.
Sparks, R.S.J., Brown, R.J., Field, M., and Gilbertson, M., 2007, Kimberlite ascent and eruption: Nature, v. 450, p. E21–E21, doi:10.1038/nature06435.
Sparks, R.S.J., Aspinall, W.P., Crosweller, H.S. and Hincks, T.K., 2012, Risk and uncertainty assessment of volcanic hazards, *in* Hill, L., Rougier, J., and Sparks, R.S.J., eds., Assessment of Risk and Uncertainty for Natural Hazards: Cambridge, Cambridge University Press (in press).
Spieler, O., Kennedy, B., Kueppers, U., Dingwell, D.B., Scheu, B., and Taddeucci, J., 2004, The fragmentation threshold of pyroclastic rocks: Earth and Planetary Science Letters, v. 226, no. 1–2, p. 139–148, doi:10.1016/j.epsl.2004.07.016.
Stasiuk, M.V., Jaupart, C., and Sparks, R.S.J., 1993, Variations of flow rate and volume during eruption of lava: Earth and Planetary Science Letters, v. 114, p. 505–516, doi:10.1016/0012-821X(93)90079-O.
Stelling, P.S., Beget, J.B., Nye, C.N., Gardner, J.G., Devine, J.D., and George, R.G., 2002, Geology and petrology of ejecta from the 1999 eruption of Shishaldin volcano, Alaska: Bulletin of Volcanology, v. 64, p. 548–561, doi:10.1007/s00445-002-0229-y.
Stevens, N.F., Murray, J.B., and Wadge, G., 1997, The volume and shape of the 1991–1993 lava flow field at Mount Etna, Sicily: Bulletin of Volcanology, v. 58, p. 449–454, doi:10.1007/s004450050153.
Stevens, N.F., Wadge, G., and Williams, C.A., 2001, Post-emplacement lava subsidence and the accuracy of ERS InSAR digital elevation models of volcanoes: International Journal of Remote Sensing, v. 22, p. 819–828, doi:10.1080/01431160051060246.
Stolper, E.M., DePaolo, D.J., and Thomas, D.M., 2009, Deep drilling into a mantle plume volcano: The Hawaii Scientific Drilling Project: Scientific Drilling, v. 7, p. 4–14.
Suckale, J., Hager, B.H., Elkins-Tanton, L.T., and Nave, J.-C., 2010, It takes three to tango: 2. Bubble dynamics in basaltic volcanoes and ramifications for modeling normal Strombolian activity: Journal of Geophysical Research, v. 115, B07410, doi:10.1029/2009JB006917.
Swanson, D.A., 2008, Hawaiian oral tradition describes 400 years of volcanic activity at Kīlauea: Journal of Volcanology and Geothermal Research, v. 176, no. 3, p. 427–431, doi:10.1016/j.jvolgeores.2008.01.033.
Swanson, D.A., and Holcomb, R.T., 1990, Regularities in the growth of the Mount St. Helens dacite dome, 1980–1986, *in* Fink, J., eds., Lava Flows and Domes. International Association of Volcanology and Chemistry of the Earth's Interior Proceedings in Volcanology: Heidelberg, Germany, Springer-Verlag, p. 3–24.
Swanson, D.A., Rose, T.R., Fiske, R.S., and McGeehin, J.P., 2012, Keanakākoʻi Tephra produced by 300 years of explosive eruptions following collapse of Kīlauea's caldera in about 1500 CE: Journal of Volcanology and Geothermal Research, v. 215–216, p. 8–25, doi:10.1016/j.jvolgeores.2011.11.009.
Taddeucci, J., Pompilio, M., and Scarlato, P., 2004, Conduit processes during the July–August 2001 explosive activity of Mt. Etna (Italy): Inferences from glass chemistry and crystal size distribution of ash particles: Journal of Volcanology and Geothermal Research, v. 137, p. 33–54, doi:10.1016/j.jvolgeores.2004.05.011.
Taisne, B., and Jaupart, C., 2009, Dike propagation through layered rocks: Journal of Geophysical Research, v. 114, B09203, doi:10.1029/2008JB006228.
Taisne, B., and Tait, S., 2009, Eruption versus intrusion? Arrest of propagation of constant volume, buoyant, liquid-filled cracks in an elastic, brittle host: Journal of Geophysical Research, v. 114, B06202, doi:10.1029/2009JB006297.
Taisne, B., and Tait, S., 2011, Effect of solidification on a propagating dike: Journal of Geophysical Research, v. 116, B01206, doi:10.1029/2009JB007058.
Tait, S., Jaupart, C., and Vergniolle, S., 1989, Pressure, gas content and eruption periodicity of a shallow crystallizing magma chamber: Earth and Planetary Science Letters, v. 92, p. 107–123, doi:10.1016/0012-821X(89)90025-3.
Tani, K., Fiske, R., Tamura, Y., Kido, Y., Naka, J., Shukuno, H., and Takeuchi, R., 2008, Sumisu volcano, Izu-Bonin arc, Japan: Site of a silicic caldera-forming eruption from a small open-ocean island: Bulletin of Volcanology, v. 70, p. 547–562, doi:10.1007/s00445-007-0153-2.
Tarasewicz, J., Brandsdottir, B., White, R.S., Hensch, M., and Thorbjarnardottir, B., 2012, Using microearthquakes to track repeated magma intrusions beneath the Eyjafjallajökull stratovolcano, Iceland: Journal of Geophysical Research, v. 117, B00C06, doi:10.1029/2011JB008751.
Toramaru, A., Noguchia, S., Oyoshiharab, S., and Tsunea, A., 2008, MND (microlite number density) water exsolution rate meter: Journal of Volcanology and Geothermal Research, v. 175, no. 1–2, p. 156–167, doi:10.1016/j.jvolgeores.2008.03.035.
Tuffen, H., Dingwell, D.B., and Pinkerton, H., 2003, Repeated fracture and healing of silicic magma generate flow banding and earthquakes?: Geology, v. 31, no. 12, p. 1089–1092, doi:10.1130/G19777.1.
Vergniolle, S., and Jaupart, C., 1986, Separated two-phase flow and basaltic eruptions: Journal of Geophysical Research, v. 91, p. 12,842–12,860.
Vinkler, A.P., Cashman, K., Giordano, G., and Groppelli, G., 2012, Evolution of the mafic Villa Senni caldera-forming eruption at Colli Albani volcano, Italy, indicated by textural analysis of juvenile fragments: Journal of Volcanology and Geothermal Research, v. 235–236, p. 37–54, doi:10.1016/j.jvolgeores.2012.03.006.
Voight, B., and Sparks, R.S.J., 2010, Introduction to special section on the "Eruption of Soufriere Hills Volcano, Montserrat, the CALIPSO Project, and the SEA-CALIPSO Arc-Crust Imaging Experiment": Geophysical Research Letters, v. 37, L00E23, doi:10.1029/2010GL044254.
Voight, B., and 24 others, 1999, Magma flow instability and cyclic activity at Soufriere Hills volcano, Montserrat, B.W.I.: Science, v. 283, p. 1138–1142, doi:10.1126/science.283.5405.1138.
Voight, B., Komorowski, J.-C., Norton, G.E., Belousov, A.B., Belousova, M., Boudon, G., Francis, P.W., Franz, W., Heinrich, P., Sparks, R.S.J., and Young, S.R., 2002, The 26 December (Boxing Day) 1997 sector collapse and debris avalanche at Soufrière Hills volcano, Montserrat, *in* Druitt, T.H., and Kokellar, B.P., eds., The eruption of Soufriere Hills Volcano, Montserrat from 1995 to 1999: Geological Society of London Memoir 21, p. 363–407.
Wadge, G., Macfarlane, D.G., Odbert, H.M., James, M.R., Hole, J.K., Ryan, G., and Bass, V., 2008, Time series radar observations of a growing lava dome: Journal of Geophysical Research, v. 113, B08210, doi:10.1029/2007JB005466.
Waite, G.P., and Moran, S.C., 2009, VP structure of Mount St. Helens, Washington, USA, imaged with local earthquake tomography: Journal of Volcanology and Geothermal Research, v. 182, no. 1–2, p. 113–122, doi:10.1016/j.jvolgeores.2009.02.009.
Waite, G.P., Chouet, B.A., and Dawson, P.B., 2008, Eruption dynamics at Mount St. Helens imaged from broadband seismic waveforms: Interaction of the shallow magmatic and hydrothermal systems: Journal of Geophysical Research, v. 113, B02305, doi:10.1029/2007JB005259.
Walker, G.P.L., Huntingdon, A.T., Sanders, A.T., and Dinsdale, J.L., 1973, Lengths of lava flows: Philosophical Transactions of the Royal Society of London, ser. A, Mathematical and Physical Sciences, v. 274, no. 1238, p. 107–118, doi:10.1098/rsta.1973.0030.
Wallace, P.J., Anderson, A.T., Jr., and Davis, A.M., 1999, Gradients in H_2O, CO_2, and exsolved gas in a large-volume silicic magma system: Interpreting the record preserved in melt inclusions from the Bishop Tuff: Journal of Geophysical Research, v. 104, p. 20097–20122, doi:10.1029/1999JB900207.
Walsh, S.D.C., and Saar, M.O., 2008, Numerical models of stiffness and yield stress growth in crystal-melt suspensions: Earth and Planetary Science Letters, v. 267, p. 32–44, doi:10.1016/j.epsl.2007.11.028.
Watts, R.B., Herd, R.A., Sparks, R.S.J., and Young, S.R., 2002, Growth patterns and emplacement of the andesite lava dome at the Soufriere Hills volcano, Montserrat, *in* Druitt, T.H., and Kokelaar, B.P., eds., The Eruption of the Soufrière Hills Volcano, Montserrat 1995 to 1999: Geological Society of London Memoir 21, p. 115–152.
Webb, S.L., and Dingwell, D.B., 1990, The onset of non-Newtonian rheology of silicate melts: Physics and Chemistry of Minerals, v. 17, p. 125–132, doi:10.1007/BF00199663.
White, J.D.L., 2000, Subaqueous eruption-fed density currents and their deposits: Precambrian Research, v. 101, p. 87–109, doi:10.1016/S0301-9268(99)00096-0.
White, J.D.L., and Ross, P.S., 2011, Maar-diatreme volcanoes: A review: Journal of Volcanology and Geothermal Research, v. 201, p. 1–29, doi:10.1016/j.jvolgeores.2011.01.010.
White, J.D.L., Smellie, J.L., and Clague, D.A., eds., 2003, Explosive Subaqueous Volcanism: Geophysical Monograph 140: Washington, D.C., American Geophysical Union, 379 p.
White, S.M., Crisp, J.A., and Spera, F.J., 2006, Long-term volumetric eruption rates and magma budgets: Geochemistry, Geophysics, Geosystems, v. 7, no. 3, Q03010, doi:10.1029/2005GC001002.
Williams, S.N., 1983, Plinian airfall deposits of basaltic composition: Geology, v. 11, p. 211–214, doi:10.1130/0091-7613(1983)11<211:PADOBC>2.0.CO;2.
Wilson, C., and Hildreth, W., 1997, The Bishop Tuff: New insights from eruptive stratigraphy: The Journal of Geology, v. 105, p. 407–440, doi:10.1086/515937.
Wilson, C.J.N., 1985, The Taupo eruption, New Zealand: II. The Taupo ignimbrite: Philosophical Transactions of the Royal Society of London, ser. A, v. 314, p. 229–310, doi:10.1098/rsta.1985.0020.
Wilson, C.J.N., and Charlier, B.L.A., 2009, Rapid rates of magma generation at contemporaneous magma systems, Taupo volcano, New Zealand: Insights from U-Th model-age spectra in zircons: Journal of Petrology, v. 50, p. 875–907, doi:10.1093/petrology/egp023.
Woods, A.W., 1995, The dynamics of explosive volcanic eruptions: Reviews of Geophysics, v. 33, no. 4, p. 495–530, doi:10.1029/95RG02096.
Wright, H.M.N., Roberts, J.J., and Cashman, K.V., 2006, Permeability of anisotropic tube pumice: Model calculations and measurements: Geophysical Research Letters, v. 33, no. 17, doi:10.1029/2006GL027224.
Wright, H.M.N., Cashman, K.V., Rosi, M., and Cioni, R., 2007, Breadcrust bombs as indicators of Vulcanian eruption dynamics at Guagua Pichincha volcano, Ecuador: Bulletin of Volcanology, v. 69, no. 3, p. 281–300, doi:10.1007/s00445-006-0073-6.
Wright, H.M.N., Folkes, C.B., Cas, R.A.F., and Cashman, K.V., 2011, Heterogeneous pumice populations in the 2.56 Ma Cerro Galan ignimbrite: Implications for magma recharge and ascent preceding a large volume silicic eruption: Bulletin of Volcanology, doi:10.1007/s00445-011-0525-5.
Wright, H.M.N., Cashman, K.V., Mothes, P.A., Hall, M.L., Ruiz, A.G., and Le Pennec, J.-L., 2012, Estimating rates of decompression from textures of erupted ash particles produced by 1999–2006 eruptions of

Tungurahua volcano, Ecuador: Geology, v. 40, p. 619–622, doi:10.1130/G32948.1.

Wright, I., and Gamble, J.A., 1999, Southern Kermadec submarine caldera arc volcanoes (SW Pacific): Caldera formation by effusive and pyroclastic eruption: Marine Geology, v. 161, p. 207–227, doi:10.1016/S0025-3227(99)00040-7.

Wright, I., Gamble, J., and Shane, P., 2003, Submarine silicic volcanism of the Healy caldera, southern Kermadec arc (SW Pacific): I—Volcanology and eruption mechanisms: Bulletin of Volcanology, v. 65, no. 1, p. 15–29.

Wright, R., Flynn, L.P., Garbeil, H., Harris, A.J.L., and Pilger, E., 2004, MODVOLC: Near-real-time thermal monitoring of global volcanism: Journal of Volcanology and Geothermal Research, v. 135, p. 29–49, doi:10.1016/j.jvolgeores.2003.12.008.

Wylie, J.J., Voight, B., and Whitehead, J.A., 1999, Instability of magma flow from volatile-dependent viscosity: Science, v. 285, p. 1883–1885, doi:10.1126/science.285.5435.1883.

Zandt, G., Leidig, M., Chmielowski, J., Baumont, D., and Yuan, X., 2003, Seismic detection and characterization of the Altiplano-Puna magma body, central Andes: Pure and Applied Geophysics, v. 160, p. 789–807, doi:10.1007/PL00012557.

Zebker, H.A., Rosen, P., Hensley, S., and Mouginis-Mark, P.J., 1996, Analysis of active lava flows on Kilauea volcano, Hawaii, using SIR-C radar correlation measurements: Geology, v. 24, p. 495–498, doi:10.1130/0091-7613(1996)024<0495:AOALFO>2.3.CO;2.

Zellmer, G.F., Sparks, R.S.J., Hawksworth, C.J., and Wiedenbeck, M., 2003, Magma emplacement and remobilization timescales beneath Montserrat: Insights from Sr and Ba zonation in plagioclase phenocrysts: Journal of Petrology, v. 44, no. 8, p. 1413–1431, doi:10.1093/petrology/44.8.1413.

Zimanowski, B., Wohletz, K., Dellino, P., and Büttner, R., 2003, The volcanic ash problem: Journal of Volcanology and Geothermal Research, v. 122, p. 1–5, doi:10.1016/S0377-0273(02)00471-7

Science Editor: Brendan Murphy

Manuscript Received 30 April 2012
Revised Manuscript Received 10 August 2012
Manuscript Accepted 27 August 2012

Printed in the USA